DRUMMOND 1966

Mineralogical and Chemical Study of Craigmont Mine, Merritt, British Columbia

By

Arthur Darryl Drummond

B.A.Sc. (University of British Columbia) 1959
M.A.Sc. (University of British Columbia) 1961

DISSERTATION

Submitted in partial satisfaction of the requirements for the degree of

DOCTOR OF PHILOSOPHY

in

Geology

in the

GRADUATE DIVISION

of the

UNIVERSITY OF CALIFORNIA, BERKELEY

Approved:

Sigurd H. Curtis .....

.....

.....

Committee in Charge

Degree conferred.....
Date

66-8305

DRUMMOND, Arthur Darryl, 1936-
MINERALOGICAL AND CHEMICAL STUDY OF CRAIGMONT MINE, MERRITT, BRITISH COLUMBIA.

University of California, Berkeley, Ph.D., 1966
Geology

University Microfilms, Inc., Ann Arbor, Michigan

CONTENTS

FIGURES

PLATES

TABLES

ABSTRACT

The Craigmont orebody lies along an east-west, steeply south dipping, zone in Upper Triassic Nicola group rocks within the 1,000 feet wide metamorphic aureole of the Lower Jurassic Guichon batholith. Within this zone, an incompetent calcareous bed has been deformed into a drag fold which plunges about 40 degrees east.

Sedimentary and volcanic rocks in the Nicola group were made into hornfelses. Fe-Mg-Si metasomatism in the calcareous bed formed skarn assemblages. Hornfels and skarn rocks are consistent with the hornblende-hornfels facies and are possibly transitional to the albite-epidote-hornfels facies.

A detailed study of (1) silicate and metallic phases in the skarn rocks, (2) the compositional variation of coexisting phases, and (3) the distribution of specific mineral associations indicates the following: (1) garnet-epidote and actinolite-epidote are associated with specularite and magnetite respectively; (2) garnet-epidote-actinolite rocks have both magnetite and specularite; (3) actinolite and epidote composition are constant throughout the skarn; (4) garnet composition changes depending on associated phases; (5) chlorite composition shows variation; (6) the skarn distribution is not a simple outward zoning from the diorite contact.

Importance of oxygen in controlling the mineralogy of the skarn rocks is suggested by the following reaction:

$$2Ca_3(Al,Fe)Si_3O_{12} + 4Fe_2O_3 + Ca_2(Al_2Fe)Si_3O_{12}(OH) + 3H_2O +$$
(garnet) (hematite) (epidote)

$$21SiO_2 + 2CaO + 9MgO =$$

$$3Ca_2(Mg_3Fe_2)Si_8O_{22}(OH)_2 + Fe_3O_4 + 2Ca_2(Al_2Fe)Si_3O_{12}(OH) + \tfrac{3}{2} O_2.$$
(actinolite) (magnetite) (epidote)

The reaction suggests a mechanism for dehydration by increasing P_{O_2} at constant temperature and P_{total}.

The P_{S_2} and P_{O_2} in the vapor phase in equilibrium with the skarn rocks would control the deposition of sulphides. In an environment of relatively high iron in the Cu-Fe-S-O system, ferrous iron could be present in excess of that which may be accommodated by actinolite. Excess ferrous iron would be taken up by magnetite and chalcopyrite which explains the simultaneous precipitation of sulphide and iron oxide with silicates.

Actinolite-epidote skarn has been altered adjacent to veins by the introduction of potassium. Changes in the activity of hydrogen (pH) in the vein system were caused by this reaction with the wall rocks. The reaction is illustrated as follows:

$$2Ca_2(Al_2Fe)Si_3O_{12}(OH) + 6SiO_2 + 4CO_2 + H_2O + 4K^+ =$$
(epidote)

$$4KAiSi_3O_8 + Fe_2O_3 + 4CaCO_3 + 4H^+.$$
(K-feldspar)

The association of K-feldspar and platy magnetite (pseudomorphous after specularite) in veins may be explained by a reaction of the type: $8Fe^{+++} + S^{=} + 4H_2O = 8Fe^{++} + SO_4^{=} + 8H^+$.

Polished sections of euhedral and platy magnetite show anisotropism which is correlated to a high temperature of formation.

Veining and brecciation of skarn and hornfels rocks and deposition of specularite-chalcopyrite with or without K-feldspar has produced a second type of economic rock in which chalcopyrite is a stable phase under high P_{O_2} pressures.

Introduction

The chalcopyrite-magnetite-specularite orebody of Craigmont Mines lies within a garnet-epidote-actinolite skarn in steeply south dipping Triassic Nicola rocks which parallel the southern end of the Jurassic Guichon batholith. The orebody extends 2000 feet along strike and from 4400 to 2400 feet elevation. Cretaceous Kingsvale volcanic rocks and a thin layer of glacial debris overlie the orebody. Outcrop area in the mine vicinity is about 10 percent.

Moderate local relief ranges from an elevation of 1850 feet at the Nicola River, 4200 feet at the west end of the open pit, to 5600 feet at the top of Promontory Hill. Vegetation and climate are characteristic of the semi-arid 'dry belt' of British Columbia. Rainfall is about 16 inches per year. Lower slopes are open and covered by sagebrush. Upper slopes receive more rainfall and are covered by forest growth.

A mineralogical study of the contact metasomatic silicates and metallic minerals was undertaken to determine the presence or absence of consistent mineral associations. This study discusses the chemical aspects of the mineral associations and the genesis of the Craigmont skarn deposit.

Acknowledgements

The writer gratefully acknowledges the financial

support of Craigmont Mines Ltd., Merritt, British Columbia who made this study possible. The writer also wishes to thank the geological staff at the mine for its cooperation.

Selection of Geological Sections

Craigmont Mine maintains a set of geological sections 100 feet apart which are perpendicular to the east-west strike of the mine structure. Sections are numbered from east to west and start at section 10,000. For the present study, the following sections were selected as best illustrating the distribution of rocks, mineral associations, and structure: 9715, 9315, 8915, 8515, 8115, 7715, and 7415. Phase associations and rock distribution on these sections is based on a detailed study of diamond drill cores. The information obtained is supplemented by mapping in the open pit and in the underground workings. In cases of widely spaced drill holes, the company's mine geology sections were used to aid correlation.

Location of Area

Craigmont Mine is situated in southern British Columbis on the eastern slope of Promontory Hill about 10 miles northwest of Merritt and about 240 miles northeast of Vancouver. Latitude and longitude are 50° 12' 28" N and 120° 54' 48" W (Figure 1). The property is accessible by paved road and is within 4 miles of the Canadian Pacific Railway.

History and Development.

Two copper showings are known within one and one half miles of the present mine. The Eric claims, known since 1939, showed chalcopyrite-magnetite-specularite with epidote and tourmaline in a N 70 E/ 65 NW fault zone in diorite (Cockfield (1948) p. 124).

The company was incorporated in 1946. In 1954, Craigmont acquired 14 mineral claims which form the core of the present property. First discovery of the Craigmont orebody occurred in 1957. Renshaw and Price (1958) described the soil sample and magnetometer surveys used to outline the ore zone. An adit to check continuity and grade was developed on the 3500 level (levels are numbered according to their elevation above sea level). By 1959, the ore zone was known to occur "to the south of the north fork of Birkett Creek at surface elevations between 3800 and 4200 feet" (Carr (1959) B. C. Minister of Mines Report, p. 31). Since then, the steeply south dipping ore zone has been followed downward to 2400 elevation. An open pit operation was developed in 1960-1961 to mine the ore above the 3500 level. During 1960-1963, underground levels were established at 2400, 2560, 2700, 2850, 3008, and 3060. An internal shaft connects all levels except the 3500. Stope development is currently underway. The present property consists of ninety mineral claims. The mine was officially opened in September 1961. Geology and structure of the mine as known to 1961 is summarized by Rennie, Pentland,

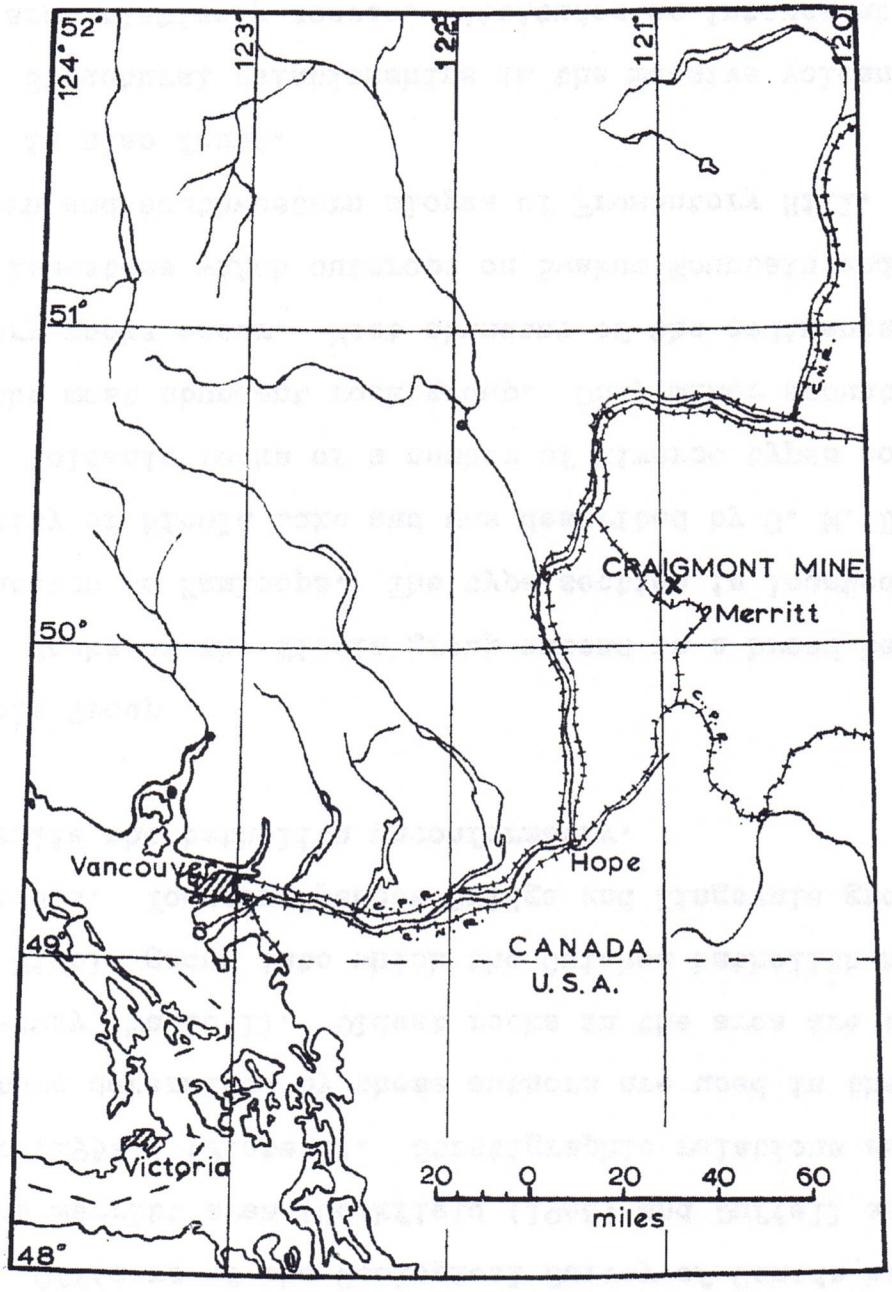

Figure 1: Map showing location of Craigmont Mine in southwest British Columbia.

and Sheng (1961). Ore reserves at the end of 1964 were reported as 23,071,000 tons averaging 1.76 percent copper (Vancouver Sun, January 25, 1965).

Regional Geology

Officers of the Geological Survey of Canada have mapped the Merritt area (Cockfield (1948) and Duffell and McTaggart (1952)) (Plate 1). Stratigraphic relations and nomenclature determined by these authors are used in the present study (Table 1). Oldest rocks in the area are the Triassic Nicola group into which the Guichon batholith has been intruded. Younger Spences Bridge and Kingsvale group rocks overlie the batholith unconformably.

Nicola Group

Rocks of the Nicola group extend in a broad belt from Princeton to Kamloops. The type section is located in the vicinity of Nicola Lake and was described by G. M. Dawson in 1896. Volcanic rocks of a number of diverse types constitute the most abundant rock group. Only minor amounts of sedimentary rocks occur. Most abundant of the sedimentary rocks is limestone which outcrops on Swakum Mountain and on the western and southwestern slopes of Promontory Hill. Minor argillite is also found.

Structural relationships in the massive volcanic portions are relatively scarce. Attitudes on intercalated

GEOLOGY OF THE MERRITT AREA
BRITISH COLUMBIA

LEGEND

TERTIARY

Miocene or Later

7 Valley Basalt

Miocene or Earlier

6 Kamloops Group

5 Coldwater Beds

CRETACEOUS

Lower Cretaceous

4 Kingsvale Group

3 Spences Bridge Group

JURASSIC

Lower Jurassic

2 Guichon Batholith

TRIASSIC

Upper Triassic

1 Nicola Group

Bedding — Mineral locality x
Fault ~~~ Glacial striae →
Fossil locality (F) Road — Trail ---

Contour Interval = 500 feet

Scale: 1 inch = 4 miles

(Compiled from Cockfield (1948) and Duffell and McTaggart (1952))

Plate 1

sediments indicate the presence of north-south trending synclinal and anti-clinal forms. Cockfield (1948) studied the limestone on Swakum Mountain and reported: (p. 14)

> If these limestone occurrences can be assumed to represent a general horizon in the volcanic rocks, the structure is that of an asymmetrical anticline with a southerly plunging, north-trending axis.

Interpretation elsewhere is made difficult by the lack of understanding of the Upper Triassic stratigraphy.

The age of the Nicola rocks is based on fossil determinations from widely scattered localities. Most of the fossils are poorly preserved and consist of crinoid columns, corals, bryozoa, and gastropods. Monotis subcircularis and a Pecten have been identified at Stump Lake, 24 miles northwest of Merritt. At Lookout Point, atop Promontory Hill, 2 miles west of the mine, W. R. Danner identified the pelecypod Halobia which suggests that these rocks belong to the Karnian stage of the Upper Triassic (Carr (1960) p. 29). The writer collected a poorly preserved coral in a limestone lense about 2 miles west of the mine and south of the Halobia locality. These corals were identified by J. W. Durham, Department of Paleontology, University of California (oral communication, 1964) as Thecosmilia but a species name could not be determined. This coral lived during the Upper Triassic. Gastropod parts and crinoid stems are also present.

Coast Intrusions

Within the Merritt area, the Coast Intrusions are

Table 1

Table of Formations in the Merritt Area

Period	Epoch	Formation	Lithology
Quaternary	Pleistocene and Recent		Stream alluvium and deposits; glacial drift and glacio-fluvial deposits
		Unconformity	
Tertiary	Miocene or earlier	Kamloops group	Rhyolite, andesite, basalt; associated tuffs, breccias and agglomerates
			Unconformity
		(Coldwater beds)	Conglomerate, sandstone, shale, and coal
		Not in Contact	
Cretaceous	Lower Cretaceous	Kingsvale group	Rhyolite, andesite, basalt; tuff, breccia, agglomerate arkose, and conglomerate
		Unconformity	
		Spences Bridge group	Andesite, dacite, basalt, rhyolite; tuff, breccia, agglomerate; conglomerate, sandstone, greywacke, and arkose
		Erosional Contact	
Jurassic	Lower Jurassic	Coast Intrusions	Granite, granodiorite, quartz diorite, and diorite
		Intrusive Contact	
Triassic	Upper Triassic	Nicola group	Greenstone, andesite, basalt; tuff, breccia, agglomerate; limestone, quartzite, argillite, arkose and greywacke

After Cockfield (1948) and Duffell and McTaggart (1952).

represented by the composite Guichon batholity which consists of granodiorite, quartz diorite, and diorite. White, et al, (1957) described intrusive phases in the Highland Valley area. Diorite outcrops along the southern margin and is intrusive into rocks of the Nicola group. Duffell and McTaggart (1952) p. 31, report that Middle to Upper Jurassic sandstones and conglomerates unconformably overlie the Guichon batholith near Ashcroft. The batholith is accordingly dated as probably Lower Jurassic and is one of the oldest of the numerous Coast Intrusions in western Canada.

Baadsgaard et al (1961) give a potassium-argon date on biotite from the Guichon batholith of 186±10 m.y.

Spences Bridge Group

Volcanic breccias, pyroclastics and flows of the Spences Bridge group outcrop along the western side of the Guichon batholith. They overlie the Guichon and are deformed into open folds. Fossil plant remains within interbedded tuffs indicate an age of Aptian or early upper Lower Cretaceous (Duffell and McTaggart (1952) p. 55). South of Merritt, Spences Bridge group rocks rest unconformably on rocks of the Nicola group (Rice (1947) p. 25).

Kingsvale Group

Diverse light colored volcanic rocks compose the Kingsvale group which outcrops west of Merritt along the

Nicola river. These rocks overlie the Spences Bridge group and the Nicola group unconformably. The latter relation is well exposed in the Craigmont pit.

The age of the Kingsvale group is based on fossil plants from a locality 14 miles south of Merritt and is considered to be Albian or lower Cretaceous (Rice (1947) p. 26). Potassium-argon analysis of biotite by the Geological Survey of Canada from an "argillized vitrophyric biotite andesite lava", which was collected near the forks of Birkett Creek at about 4,230 feet elevation gave an age of 80 m. y. (Lowden (1963) p. 19). This suggests that the Kingsvale group volcanic rocks are of Upper Cretaceous age.

Kamloops Group

Sequences of volcanic and sedimentary rocks are included in the Kamloops group which has been used to designate most of the recognizable Tertiary rocks of the region. In the Merritt area, nearly horizontal volcanic rocks unconformably overly moderately dipping sedimentary rocks which are recognized as Coldwater beds (Cockfield (1948) p. 38). Fossil leaves in the Coldwater beds "suggest very strongly a Tertiary age not younger than the Miocene" (Duffell and McTaggart (1952) p. 68).

Pleistocene and Recent Deposits

Pleistocene and Recent deposits cover much of the

bedrock of the entire area. They include gracial drift, deposits of glacial streams and lakes, and deposits of Recent streams. Ice covered the Merritt area during Pleistocene time as glacial striae are found on the surfounding high summits. When the ice receded, glacial debris mantled most of the upper slopes and formed thick deposits in the valleys. As a consequence, the outcrop area was reduced to its present state.

Geology of The Mine

The Craigmont orebody lies in an east-west striking, steeply south dipping zone within thermally and metasomatically altered rocks of the Nicola group adjacent to the Guichon diorite contact. Nicola group sedimentary and volcanic rocks within 1,000 feet of the diorite contact have been hornfelsed. On Promontory Hill, two miles west of the mine, Nicola rocks are virtually unmetamorphosed. Fossiliferous limestones show very little evidence of recrystallization except where locally deformed into minor folds. Rocks in the mine area occur only in the thermal aureole of the Guichon diorite.

Hornfelses

Hornfelsed sedimentary rocks of the Nicola group are predominantly poorly sorted quartz-plagioclase wackes. Quartzofeldspathic sediments with biotite, chlorite, or

hornblende are poorly sorted while quartzofeldspathic sediments without appreciable mafic content are relatively well sorted. Grain size variation in poorly sorted rocks is gradational, that is, all sizes are present from about 4 mm. maximum to 0.01 mm. Determination of percentage matrix in these rocks is difficult. If the matrix constitutes greater than 10 percent, the rocks are classified as hornfelsed wackes; if the matrix is less than 10 percent, rocks are hornfelsed sandstones (Williams, Turner, and Gilbert (1954) p. 292). During hornfelsing the finer matrix has been recrystallized, thereby adding to the difficulty of determining the amount of matrix.

Petrography of the Hornfelsed Wackes

The most abundant hornfelsed wackes are those with chlorite and biotite. Hornblende-bearing hornfelses are relatively minor.

Chlorite- and Biotite-Bearing Hornfels

These rocks are hornfelsed chlorite and biotite-bearing quartzofeldspathic wackes. Grains of quartz with twinned and/or untwinned plagioclase constitute most of the rock. Biotite, chlorite, and muscovite occur in the finer grained portion of these poorly sorted rocks. Acicular crystals of tremolitic hornblende (colorless, $Z' \wedge c = 18$) may be developed with the biotite-bearing rocks. Modes of several typical rocks are given in Table 2.

Table 2

Modes of Hornfelsed Rocks

(visual estimate in volume percent)

Mineral	A	B	C	D	E	F	G
Quartz	20	10	30	24	25	10	12
Plagioclase	70	75	60	40	56	57	41
	(An_{39})	(An_{25})	(An_{15})	(An_{23})	(An_{10}?)	(An_{20}?)	(An_{25})
K-feldspar	-	-	-	20	-	-	-
Chlorite	-	1-2	10	5	2	5	1
Biotite	8	14	-	-	1	-	-
Muscovite	-	-	tr.	1	-	-	-
Hornblende	1-2	-	-	-	5	15	6
Tremolite/ Actinolite	tr.	-	-	-	-	-	-
Epidote	-	-	tr.	-	-	2	-
Calcite	-	-	tr.	tr.	-	-	-
Sphene	tr.	tr.	tr.	tr.	tr.	tr.	tr.
Apatite	tr.	tr.	tr.	tr.	tr.	tr.	tr.
Magnetite	tr.	-	-	tr.	1	-	-
Pyrite	-1	1	tr.	-	-	-	-
Fragments	-	-	-	-	10	10	40

A. Biotite-bearing hornfels (663-56).
B. Biotite-bearing hornfels (663-58).
C. Chlorite-bearing hornfels (663-61).
D. Chlorite-bearing hornfels (663-69).
E. Hornblende-bearing hornfels (663-66).
F. Hornblende-bearing hornfels (663-65).
G. Hornfelsed lithic wacke (663-75).

Biotite-bearing hornfelses have a greater range of texture than mineralogy. One hand specimen may have a distinct schistosity while another may have a non-directional texture.

Light colored lenses resemble tuffaceous or volcanic rock with euhedral plagioclase crystals in an aphanitic matrix. Thin mosaic quartz lenses lie parallel to this banding. Biotite, clastic plagioclase and some quartz constitute the majority of the rock in which these other bands occur.

Chlorite and muscovite-bearing wacke hornfelses are similar to those with biotite. Typical modes are listed on Table 2, C and D.

Grains of bluish quartz are locally present in some coarse-grained wacke rocks (663-68).

Hornblende-Bearing Hornfelses

Hornblende-bearing wacke hornfelses are scarce in the mine workings. Modes of a few typical rocks are listed on Table 2, E and F. Superficially these may be confused with the metamorphosed andesite which is more homogeneous both in texture and composition. As with the biotite-bearing wacke hornfelses, hornblende-bearing examples may have a hornfelsic to a schistose texture. Specimen 663-66 which contains many lithic fragments does not show a preferred orientation in the hornblende grains (Z' dark green).

Other Hornfelses

When the percentage of lithic fragments is greater than about 25 percent, the rock is termed a lithic wacke hornfels. Granular quartz-rich sedimentary and porphyritic volcanic fragments may constitute up to 40 percent of the rock (663-75, 76) (Table 2, G).

A fine-grained quartz-rich light grey 'sandstone' hornfels is common on the north side of the mineralized zone. This type contains abundant granoblastic quartz and plagioclase with minor biotite which locally is altered to chlorite. These rocks are distinct in that there is an absence of recognizable matrix (663-72, 71).

A whitish dense hornfelsic rock with 1 mm. rounded quartz grains in a matrix of quartz-diopside-muscovite is present west of the main mine area (663-77).

Petrography of Argillaceous Rocks

Dense, dark, finely laminated argillite and interlayered, lighter colored, very fine-grained sandstone are grouped under this heading. Argillaceous bands are composed of grains which are uniformly about 0.01 mm. A few feldspar grains (0.05 mm.) are scattered throughout. Sandy layers have a higher percentage of quartz and feldspar grains (up to 1 mm. diameter) in a groundmass of < 0.1 mm. grains.

Both rocks contain the same mineralogy. Quartz, feldspar (plagioclase, minor potash feldspar) compose about

90% of the rock with the remainder being chlorite, biotite and/or white mica (muscovite ?), calcite, magnetite and pyrite, (663-48 to 51). Pyrite clubes have developed across the foliation (663-51). In one specimen (663-49), prismatic crystals of colorless prehnite have developed across the foliation. This specimen also contains quartz-calcite-prehnite veings. Barren late calcite veins are common.

The groundmass is granoblastic. Minute grains of magnetite are aligned through the recrystallized matrix. Micaceous minerals are approximately parallel to this direction which is also parallel to the contact of the variation in rock-type.

A dark, greenish grey, dense, irregularly laminated 'argillite' hornfels is a source of confusion during mapping (663-52). Without the aid of a thin section, this rock-type may resemble very fine-grained hornfelsed andesite. Small lenses of slightly coarser grained quartz-feldspar may impart a slight porphyritic appearance in hand specimen. Grain sizes range between 0.5 to 0.1 mm. Some hornblende and magnetite grains are 0.5 mm. in longest dimension. The hornfelsed 'argillite' is composed of 65% quartz and untwinned plagioclase (oligoclase) (An_{25}), 25% hornblende (Z' dark green), 5% chlorite (anomalous blue and brown), 5% lithic fragments, and 2% magnetite. Strongly foliated, the hornblende, chlorite, strings of magnetite grains, and dust sweep around mosaic lenses of quartz and feldspar. Within these lenses, small hornblende needles have developed.

Petrography of Cherty Rocks

Cherty appearing rocks are included under this classification. Two specimens, one grey with a pink caste, the other grey with a greenish caste are composed of coarse silt-very fine sand size grains of quartz, untwinned plagioclase (about An_5), chlorite, sphene, apatite, magnetite. Slightly larger feldspar grains occur in an interlocking mosaic groundmass. The pink specimen showed no potash feldspar peaks on an X-ray diffractometer pattern (663-53). The pink color must be caused by iron stain. In thin section, the feldspar is uniformly cloudy in both specimens. Greenish color is caused by about 5% chlorite in 663-54. Both specimens are veined by quartz-calcite-epidote (Z' yellow). These cherty rocks are hornfelsed very fine-grained quartzofeldspathic sandstones.

Petrography of Marbles

Rocks classified as marbles are those which contain greater than 50% recrystallized calcite and which do not contain abundant garnet, epidote, or actinolite. Rocks which contain appreciable amounts of these minerals will be discussed under the heading of skarn.

Typical marbles are fine-grained, dense, and whitish grey with locally a greenish caste. Calcite constitutes about 92% of the rock (specimens 663-41 to 45). Interstitial quartz (2 - 3%) and feldspar (?) (1%) are always present. The greenish

color is imparted by chlorite (normal birefringence, optically negative) (1 - 2%), tremolite-actinolite (colorless to weakly greenish prismatic crystals with Z' c 18) (1%), and clinozoisite-epidote (colorless to pleochroic yellow grains) (1 - 2%). Minor disseminated pyrite is common (1 - 2%).

One specimen contains about 25% colorless diopside as fine granules either in patches or disseminated in calcite (663-40). Another specimen contains trace amounts of scapolite (meionite, colorless, uniaxial negative) (663-41).

Banded marbles in the 30-783 Service Drift West show several colors. A grey green layer contains scattered weakly pleochroic clinozoisite-epidote grains in strongly oriented recrystallized calcite (663-36). Where greenish coloration is most distinct the rock contains about 5% greenish tremolite-actinolite (663-37). A second parallel layer is white and contains only quartz and 2-3% colorless tremolite. This white band grades into a grey-white layer which contains minor amounts of tremolite (663-38).

A grey white marble in the 30-783 cross-cut shows granular chalcopyrite aligned parallel to the foliation in the marble (663-39). Locally in the cross-cut, very coarse white marble is present with individual calcite grains more than two inches in diameter. Chalcopyrite is found around the edges of these areas and interstitially scattered throughout. Blocks up to five feet long and three feet wide of relatively fine-grained banded marble are surrounded by the coarse calcite.

The characteristic marble mosaic texture is present in all cases. Under crossed nicols, a strong preferred orientation can be observed in the calcite grains. All other constituents are either interstitial or randomly distributed in the calcite. Recrystallization of calcite took place either simultaneous with or prior to the growth of tremolite-actinolite, as acicular actinolite grains lie across the boundary between adjacent calcite crystals. Some post-recrystallization movements have occurred, as calcite cleavage planes are bent and chlorite may be developed on late granulated planes through the marble.

Promontory Hill Limestone

Dark grey fossil-bearing limestones from Promontory Hill (two miles west of the mine) are composed entirely of very fine-grained calcite (663-33,-34). An X-ray diffractometer pattern on another fossiliferous limestone (663-47) indicates the presence of some dolomite within the fossil shells. One sandy, dark grey, non fossil-bearing limestone contains fragments or grains of volcanic rock, plagioclase feldspar, and quartz (663-35). The volcanic rock and feldspar grains are partially replaced by calcite. Coarse calcite only develops as pseudomorphs and late veins. The lack of recrystallization of the calcite matrix indicates that these Nicola group limestones were not affected by the contact metamorphism which affected the mine area.

Contact Metamorphic Facies

Wacke and sandstone hornfels in the thermal aureole are characterized by the following assemblages:

1. Quartz-plagioclase-biotite-(muscovite) (663-55, 58, 60)
2. Quartz-plagioclase-biotite-hornblende (663-56, 66)
3. Quartz-plagioclase-hornblende-chlorite (663-65)
4. Quartz-plagioclase-chlorite-muscovite (663-61, 62)
5. Quartz-plagioclase-orthoclase-muscovite-chlorite (663-69)

The above assemblages are plotted on an ACF diagram for the hornblende-hornfels facies (Figure 2). The numbers on the diagram correspond to those assemblages above. Biotite and chlorite are used in the diagram. Chlorite is found along cleavage planes and around the edges of some biotite grains which indicates alteration of some biotite (663-66). All assemblages plot close together and indicate a quartzo-feldspathic bulk composition.

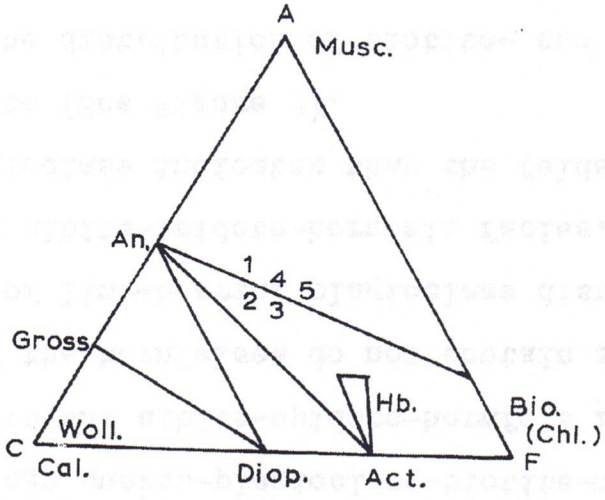

Figure 2: ACF diagram of hornblende-hornfels facies showing plot of wacke hornfelses. Assemblages with excess SiO_2 and K_2O. Quartz and microcline are possible phases. After Fyfe, Turner, Verhoogen (1958) Figure 85, p. 206.

The above quartzofeldspathic rocks were metamorphosed under conditions of the hornblende-hornfels facies of contact metamorphism (Turner and Verhoogen (1960) p. 511-520). The assemblage quartz-plagioclase-biotite-muscovite could also apply to the albite-epidote-hornfels facies, because the majority of the hornfelses do not contain amphibole. Presence or absence of lime-bearing plagioclase distinguishes the hornblende- and albite-epidote-hornfels facies. The Ca-content of the plagioclase indicates that the feldspar in these rocks is not albite (See Figure 3).

The distribution of biotite- and hornblende-bearing hornfelses appears to bear no relation to the nearby diorite contact. Figure 3 compares the Ca-content of the plagioclase with biotite, chlorite, or hornblende and the distance to the nearest diorite body. All assemblages are those of the hornblende-hornfels facies. They do not occur in any zonal arrangement within the contact aureole as observed in the mine workings.

In the very fine-grained hornfelsic argillite rocks, there are two distinct assemblages. Quartz-plagioclase-chlorite-biotite-muscovite is found in one group (663-48 to 51). As these rocks contain minor amounts of potash feldspar, andalusite and cordierite would not be expected (Turner and Verhoogen (1960) p. 515). Quartz-plagioclase-hornblende-chlorite is the second assemblage (663-52). The two associations suggest that argillite has been metamorphosed under

conditions of the hornblende-hornfels facies of contact metamorphism.

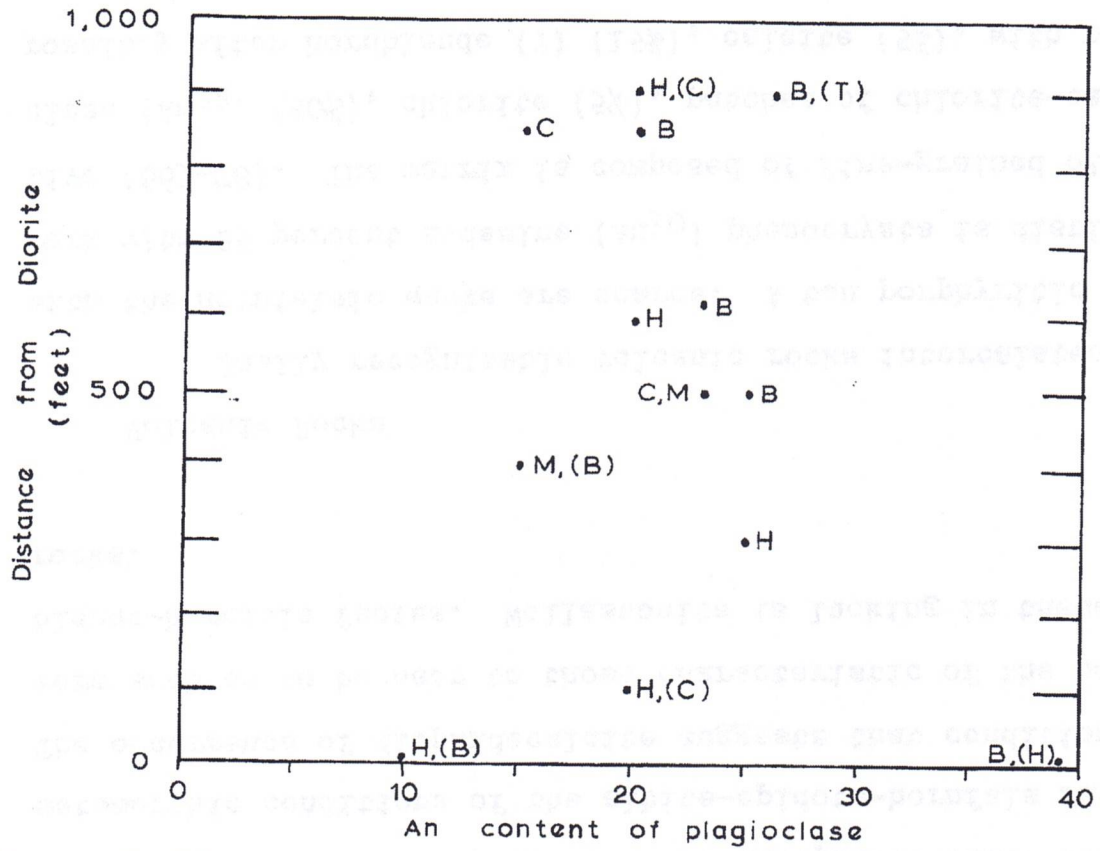

Figure 3: Diagram comparing plagioclase composition in biotite, chlorite, and hornblende hornfelses with distance from diorite. (H - hornblende, B - biotite, C - chlorite, M - muscovite, T - tremolite, brackets indicate minor amounts of that mineral)

The majority of the marbles examined indicate the following assemblages:

1. Calcite-chlorite (scapolite) (pyrite) (663041)
2. Calcite-quartz-tremolite-sphene (pyrite) (663-42)
3. Calcite-quartz-chlorite-tremolite/actinolite-epidote (pyrite) (663-44)
4. Calcite-prehnite-quartz-tremolite/actinolite (pyrite) (663-43)
5. Calcite-clinozoisite/epidote (pyrite) (663-46).

The presence of magnesium bearing minerals indicates that magnesium has been introduced, as the nearest limestone (that on Promontory Hill) contains only minor amounts of constituents which could carry magnesium. However, the amount of magnesium added must be small and it is conceivable that the magnesium seen in the tremolite and chlorite could have been present in the limestone prior to metamorphism. The scattered distribution of the epidote--clinozoisite suggests that alumina was probably present originally. With the lack of evidence that the constituent elements of the marbles were externally introduced, it is concluded that the assemblages represent calcareous rocks metamorphosed under contact metamorphic conditions of the albite-epidote-hornfels facies. The occurrence of diopsidecalcite suggests that conditions were such as to be near to those characteristic of the hornblende-hornfels facies. Wollastonite is lacking in these rocks.

Volcanic Rocks

Easily recognizable volcanic rocks intercalated with the hornfelsic wacke are scarce. A tan porphyritic rock with 25 percent andesine (An_{30}) phenocrysts is distinctive (663-78). The matrix is composed of fine-grained oligoclase (An_{22}) (50%), chlorite (5%), patches of chlorite-calcite, possibly after hornblende (?) (15%), calcite (5%), with minor amounts of quartz, muscovite, and trace amounts of disseminated

magnetite. Phenocrysts are cloudy and altered to sericite (?) but may have a clear rim of plagioclase in optical continuity. The rim has a slight negative relief with respect to Canada balsam. This suggests either late stage zoning in the rock or development of an albitic rim during thermal metamorphism. Grains in the matrix are arranged in a subparallel manner which could be the result of flowage.

A dense dark porphyritic andesite outcrops along the south side of the open pit. White euhedral andesine (An_{25-30}) phenocrysts constitute about 10% of the rock. Phenocryst size ranges from 2 mm. to 0.5 mm. The black matrix is a granoblastic mosaic of untwinned plagioclase (80%), aligned and/or irregular grains of green biotite and chlorite (10%), hornplenae (5%), quartz (2%), magnetite (2%) with accessories of apatite, sphene, epidote and calcite. Broken phenocrysts have been annealed by untwinned potassium feldspar and quartz. Minute grains of chlorite and tremolitic hornblende (?) have been developed in some phenocrysts. Pyroxene is absent. (Specimens 663-31, 32)

This andesite is texturally distinct when compared with the intruded and hornfelsic hornblende andesite. It occurs only on the south wall of the open pit and in Hole 35-59 at 435 feet (section 8515). It is unconformably overlain by the Kingsvale group and is considered as part of the Nicola group.

Coarse-Grained Intrusive Rocks

Guichon Diorite

Guichon diorite is a light grey, hypidiomorphic-granular, fine- to fine- to medium-grained rock. Modes of dioritic rocks are given and compared with that from the nearby Eric claims and with the granodiorite which outcrops inwards from the southern margin of the batholith (Table 3).

Plagioclase, the most abundant mineral in these rocks, is commonly altered to a colorless white mica. In cases where feldspar was too clouded for optical determination, the x-ray methods of Smith (1956) ($2\theta(111) - 2\theta(1\bar{1}1)$) or of Smith and Yoder (1956) ($2\theta(131) - 2\theta(1\bar{3}1)$) were used. Some plagioclase grains have a sharply bounded intensely sericitic core which is surrounded by a lightly clouded rim. This may represent normal zoning in which the more calcic core has been most intensely affected.

Hornblende is generally in dark green prismatic crystals (Z' dark green, X' pale brown). In a few specimens, uralitic hornblende rims a colorless diopsidic pyroxene of which usually only small grains may remain. Alteration of hornblende is to either an anomalous blue (optically negative) or an anomalous brown (optically positive) chlorite. Both varieties may occur in the same altered hornblende.

Quartz, in variable quantities, is interstitial.

Table 3

Modes of Guichon Diorite

(visual estimate in volume percent)

Mineral	A	B	C	D	E
Quartz	5.0	0.7	15.0	14.0	25.0
Microcline	-	-	5.0	-	25.0
Plagioclase	65.0 (An_{45}) unzoned	67.2 (An_{35}) unzoned	45.0 (An_{25})	60.0 (An_{30}) zoned	40.0 (An_{30}) unzoned
Hornblende	15.0	24.1	30.0	6.4	-
Diopside	5.0	0.8	-	0.5	-
Biotite	7.0	-	3.0	10.2	9.0
Chlorite	2.0	3.1	-	3.5	1.0
Epidote	tr	0.3	-	2.1	tr
Sphene	tr	0.7	*	0.5	tr
Apatite	tr	1.0	*	0.3	tr
Calcite	-	0.3	-	0.7	-
Magnetite	1.0	1.3	*	1.6	tr
Pyrite	-	0.5	-	0.2	-
K-spar/total feldspar	0	0	0.10	0	0.40

* 2% accessory minerals
A. Diorite from Eric claims (663-1)
B. Averaged diorite (663-3, -5, -6)
C. Granodiorite, after M. Carr, (1960) p. 33
D. Averaged quartz diorite (663-5, -7)
E. Quartz monzonite (663-18).

Brown biotite is commonly altered to pale green chlorite which under crossed nicols, can be either anomalous blue or brown. There is no apparent difference between this chlorite and the chlorite with altered hornblende. Epidote is present in minor amounts either within plagioclase grains or as minute lenses in altered biotite. This epidote is strongly pleochroic (Z' bright yellow, X' nearly colorless).

Accessory minerals are apatite, sphene which is in part altered to leucoxene, pyrite and magnetite. Pyrite/magnetite ratio appears to increase locally in proximity to the diorite contact.

Variations in Diorite

The rocks of the batholith range in quartz and potassium feldspar content so that diorite grades locally into quartz diorite, granodiorite, and quartz monzonite. Average mode of two quartz diorites is compared with the average mode of three diorites and a quartz monzonite in Table 3. The major difference among these rocks is the predominance of biotite over hornblende with increasing quartz content. Quartz monzonite is lighter colored than the others because of the abundance of quartz and white microcline. Grain size is uniformly 1 - 3 mm. in these rocks.

Relation of Diorite to Other Rocks

Diorite includes fragments of hornfelsic hornblende

andesite (663-29, 30) and is cut by granite and pyroxene andesite dykes. Nicola group rocks are intruded by both diorite and hornblende andesite but definite cross-cutting relationships between these two rocks are lacking.

Alteration of Diorite

All specimens of diorite show clouded feldspar and chloritization of hornblende. Presence of minor amounts of epidote and calcite also indicate breakdown of the original minerals. Diorite is noticeably altered adjacent to some chalcopyrite-bearing epidote veins. Not all epidote veinlets show an alteration envelope. A well developed example is outline in Table 4.

Propylitized diorite is locally developed. Minute epidote and chlorite grains are seen within plagioclase and hornblende. Epidote becomes more abundant in the diorite adjacent to fractured zones which are now mostly epidote. Within regular diorite textured rock, clouded plagioclase An_{45} (75%), hornblende (Z' dark green) with actinolitic rims (Z' pale blue green) (20%) can change within one millimeter into a similar textured rock composed of epidote (Z' yellow, X' colorless) (90%) and 'hornblende' (mostly Z' dark green, some Z' blue green) (10%). Just at the 'contact' on the diorite side, epidote patches and cores replace plagioclase (663-11). Within the epidote area, thin chalcopyrite veinlets occur.

Table 4

Alteration in Diorite Adjacent to Epidote Vein

(visual estimate in volume percent)

Mineral	Vein 3 mm. wide	Diorite 7 mm.	(distance from vein) 15 mm.
Plagioclase	-	75	75 (An_{45})
Sericite	-	intense	less intense
Hornblende	-	-	20 (Z' dk gn)
Tremolite Actinolite	-	20 (Z' pale bl gn to colorless)	-
Chlorite	-	1 - 2	5
Epidote	88	-	-
Quartz	1 - 2	<1	-
Calcite	5	2	-
Sphene	-	2 - 3	<1
Magnetite	<1	trace	1
Chalcopyrite	5	-	-

Late prehnite-calcite veins are common in diorite. These veins cut epidote-bearing veins and hence, are later than the epidote veins (Specimen 663-7).

Pale pink laumonite occurs on late fractures in diorite. X-ray diffractometer patterns agree with ASTM 11-93 (663-8).

Granite

Granite is fine-grained (1 - 2 mm.) pink hypidiomorphic granular rock. Modes of several specimens are listed in Table 5. Subhedral to anhedral quartz is interstitial. Euhedral potassium feldspar is perthitic with string-like untwinned albite in sporadically pericline twinned microcline. Twinned oligoclase ($\perp$ a, X' $\wedge$ 010 = 13, An_{27}) (663-15) or albite form scattered interstitial euhedral grains. Both feldspars are cloudy under plain light. Accessory minerals are sphene, leucoxene, clinozoisite, calcite, magnetite, and pyrite.

Subgraphic textured granite dykes have the same mineralogy as that described above (Table 5). The difference between these two granite dykes is only textural.

Relation of Granite to Other Rocks

Fine-grained regular and subgraphic dykes have a common origin. Both cut grey Guichon diorite and both cut the hornfelses and skarn rocks of the Nicola group. Subgraphic granite may occur separately as sharply bordered dykes or may show gradational contacts when found within granite. One specimen (663-17) shows an abrupt grain size change between the coarse and fine-grained rocks. The subgraphic veins are probably the expression of a slightly later stage of the regular fine-grained granite.

The Coyle stock, about two miles south of the mine,

Table 5

Modes of Granite

(visual estimate in volume percent)

Mineral	A	B	C	D	E
Quartz	40.0	40.0	10.0	35.0	40.0
Microperthite	55.0	55.00	80.0	55.0*	40.0
Microcline/ albite	50/5	53/2	70/10	50/5	36/4
Plagioclase (interstitial)	3 - 4 (An_0)	3 - 4 (An_0)	8.0 (An_5)	8.0 (An_{28})	20.0 (An_{28})
Muscovite	tr	tr	-	-	<1
Chlorite	1 - 2	-	1 - 2	1 - 2	-
Biotite	-	tr(?)	-	-	-
Sphene	tr	tr	tr	tr	tr
Apatite	-	tr	tr	tr	tr
Clinozoisite	-	tr	tr	tr	-
Calcite	-	tr	-	tr**	-
Magnetite	tr	-	tr	-	tr
K-spar/total	0.93	0.93	0.91	0.87	0.66

* One extremely pink grain shows limonite stain throughout.
** One grain of hornblende(?) or biotite(?) has been altered to a fine-grained mixture of chlorite and calcite.
A. Subgraphic granite dyke, Open Pit (663-12)
B. Subgraphic granite dyke (663-13)
C. Massive pink K-spar, 2850 level (663-14)
D. Granite, 2850 level (663-15)
E. Coyle Stock granite (663-16).

is composed of "mainly quartz diorite and discordant bodies of granite or quartz monzonite" (Carr (1960) p. 34). Granite described by Carr closely resembles that found on the 2850 level (663-15). The Coyle stock is considered by Cockfield (1948) to be part of the Guichon batholith.

Fine-Grained Intrusive Rocks

Hornblende Andesite (Hornfels)

Dark greenish grey dense, very fine-grained rock with about 5 percent clouded plagioclase phenocrysts (length about 1.5 mm.) in a flow-texture matrix (size range, 0.4 to < 0.05 mm.). Averaged mode for eleven rocks is given as follows: andesine plagioclase (An_{35}) (55.4%), hornblende (35.6%), quartz (1.6%), chlorite (4.5%), biotite (1.4%), magnetite (2.0%), and trace amounts of epidote, sphene, apatite, calcite, and pyrite. (Specimens 663-20 to 27). Plagioclase in phenocrysts and in matrix have the same andesine composition. All are clouded, and twinning is locally absent. Hornblende occurs in fresh, irregular grains (Z' dark green). Reddish brown biotite is present in minor amounts. Chlorite is present either as anomalous blue or brown and is an alteration product of biotite and/or hornblende. Magnetite occurs as finely disseminated grains in the matrix.

Evidence of Hornfelsing

Evidence of hornfels formation is seen in the development of minute hornblende crystals within and along cracks in the relict euhedral plagioclase phenocrysts (Plate 2). The preferred orientation of the plagioclase laths in the matrix is still preserved in most specimens. Minute dark green hornblende needles are found within and across grain boundaries of the matrix plagioclase which suggests that hornblende developed after the plagioclase laths. Other specimens show a more granoblastic matrix with irregular seive-like hornblende. In these rocks, preferred orientation is only weakly observed.

Presence of interstitial biotite and quartz further suggests recrystallization. Williams, Turner, and Gilbert (1954) p. 195 state that the basic hornfelses in the hornblende-hornfels facies which contain biotite and quartz were likely derived from andesitic parent rock.

Thin vein-like stringers of coarser grained rock (1 mm.) appear to intrude the andesite. These are composed of clouded plagioclase (35%), quartz (40%), tremolite-actinolite (25%) (Z' very pale green to bluish green), magnetite (2%), and pyrite (tr.). Quartz content is far in excess of any diorite or quartz diorite at the mine. The discontinuous and branching nature suggests that the coarser grained material, rather than intruding the andesite, has been developed as a consequence of the recrystallization during thermal metamorphism.

Contact Metamorphic Facies

Absence of pyroxene and the presence of hornblende and plagioclase with minor interstitial biotite and quartz indicates that these rocks were metamorphosed under conditions of the hornblende-hornfels facies.

Relation of Andesite to Other Rocks

Hornblende andesite intrudes the Nicola group rocks. It has been observed to intrude the diorite. Andesitic fragments which are found within diorite indicate that the andesite was pre-diorite.

Pyroxene Andesite

A black aphanitic dyke cuts the Guichon diorite near the Eric claims. Microscopically, the rock is slightly porphyritic with 1 to 1½ mm. fresh unzoned plagioclase phenocrysts ($\perp$ a, $X' \wedge 010 = 29$, An_{44}). Phenocrysts tend to be an aggregate of several 1 mm. crystals rather than one large crystal. Matrix comprises about 95% of the rock and is composed of a granular mixture of colorless diopsidic augite, hypersthene (optically negative), hornblende (Z' dark green), magnetite and fresh unzoned plagioclase which has the same composition as the slightly larger phenocrysts. Mode is listed as follows: plagioclase (An_{46}) (73%), diopsidic augite (15%), hypersthene (5%), hornblende (1 - 2%), magnetite (5%), chlorite (tr.). Matrix grain size ranges from 0.7 to < 0.2 mm. Alignment of the

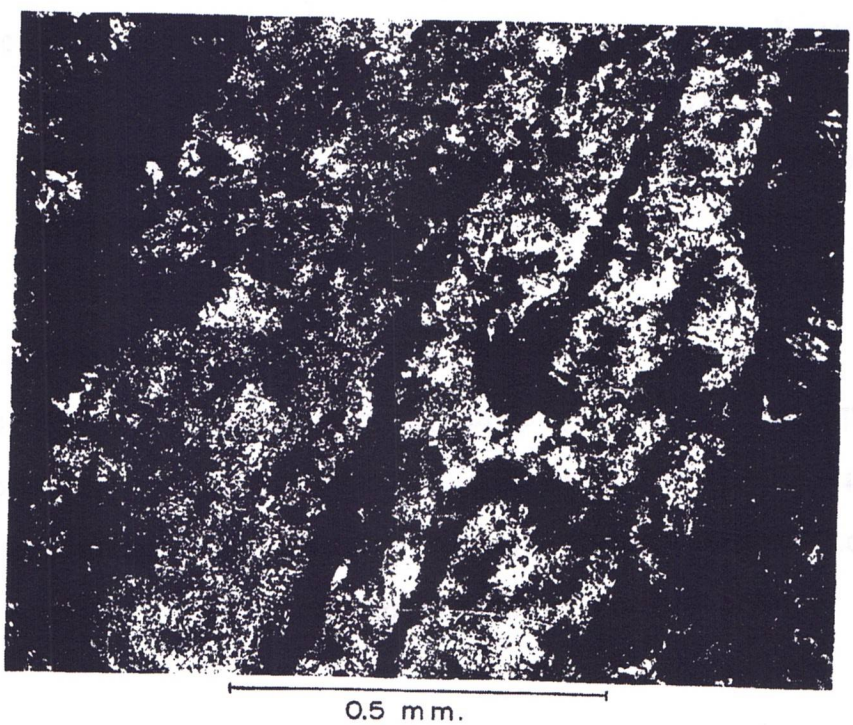

Plate 2 Photomicrograph showing hornblende within and along cleavage of plagioclase. Plain light. (Specimen 663-21).

composition plane in the twinned plagioclase imparts a preferred orientation in thin section.

This fresh andesite intrudes diorite and is considered post diorite. Pyroxene andesite has not been observed in the mine workings.

Basalt

Porphyritic, dense, dark basalt intrudes the Nicola group. Microscopically, greenish tinged optically positive rounded crystals of diopsidic augite (0.5 mm.) constitute the phenocrysts (about 5%). Flow aligned labradorite microlites (40%) and small rounded serpentine(?) areas (10%) occurs in a clouded greenish matrix (45%) which includes magnetite dust(2%). Serpentine areas may have been olivine(?) originally. (Specimen 663-19).

The basalt is post Triassic Nicola group and is probably related to Tertiary volcanism.

Petrography of The Skarn Rocks

Mineralogy of the Craigmont skarn rocks is simple. Principal lime silicates are actinolite, epidote, grossularite-andradite garnet, and minor diopside. Calcite and quartz are present in all assemblages. Apatite and sphene are usually present as accessory minerals. Compositional variations in the constituent silicates with each other and with associated iron oxide and sulphide phases are investigated.

Actinolite

Dark green actinolite is optically negative with $2V_x = 68° \pm 3$ as determined on the Universal stage. Refractive indices are: $n_z = 1.655 \pm 0.002$; $n_y = 1.644 \pm 0.002$; $n_x = 1.634 \pm 0.002$; $n_z - n_x = 0.021$. $Z \wedge c$ is $14\frac{1}{2}°$. Pleochroism is Z blue green, Y pale green, X nearly colorless with a pale greenish tinge ($Z > Y > X$). Variation in optical properties between actinolite and hornblende in a suite of metamorphic rocks is given by Shido and Miyashiro (1959) in Figure 4. Craigmont actinolite plotted well within the actinolite field which indicates very small alumina content. Differential thermal analysis of two actinolites (663-91, 92) produced endothermic peaks at 1010 and 1015 degrees Centigrade respectively (Figure 5). Vermaas (1952) noted only one endothermic peak at 1061 - 1122 degrees Centigrade in actinolite but noted two peaks in tremolite (one exothermic peak at 815 - 824 C and one endothermic peak at 930 - 988 C).

Preliminary investigation of homogeneity of the actinolite for possible electron microprobe analysis indicated that it was inhomogeneous and not suitable for analysis. Specimen 663-114 indicated that the variation in counts per 10 second interval for Al, Fe, and Ca was in the order of 100%, 25 - 30%, and 2% respectively. As a consequence, the average composition of actinolite was determined by using the optical data of Deer, Howie, and Zussman (1962) volume 2, page 257 and Figure 6. Though variable within individual crystals, the range of

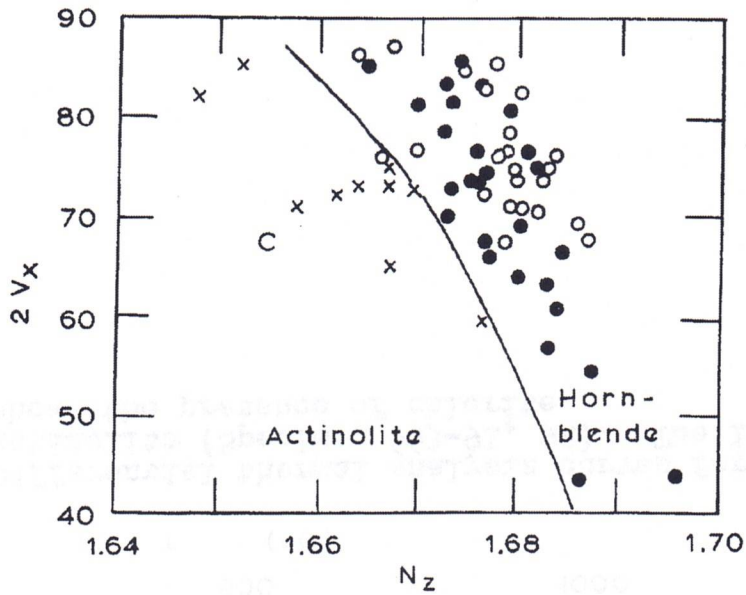

Figure 4: Diagram showing relation of $2V_x$ and n_z of amphiboles from metamorphic rocks. (crosses - actinolite; solid circles - blue green hornblende with about 12 wt.% alumina; open circles - hornblende with 8.87 to 12.56 wt.% alumina; C - Craigmont actinolite). After Shido and Miyashiro (1959).

composition does not change appreciably within the geographical limits of the mine. Figure 6 shows the range and average n_z of actinolite for various mine sections. Actinolite composition averages 37 mole percent $Ca_2Fe_5Si_8O_{22}(OH)_2$ with a range of 27 to 44 mole percent. All compositions are 2% assuming that the refractive index is 0.002. As alumina content is small, the average composition is as follows: $Ca_2(Mg_3Fe_2)Si_8O_{22}(OH)_2$.

Association with other silicate phases shows only minor effect of the actinolite composition. Figure 7 compares the refractive index of actinolite with that of epidote and

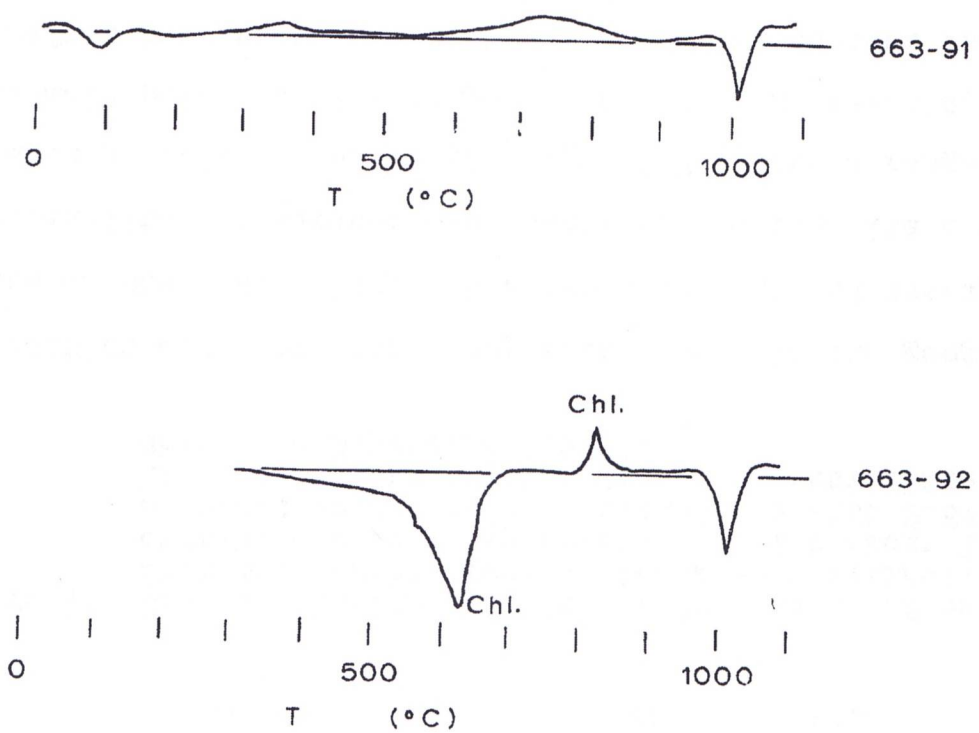

Figure 5: Differential thermal analysis curves for Craigmont actinolite (Specimen 663-91, 92). The lower curve shows the presence of chlorite.

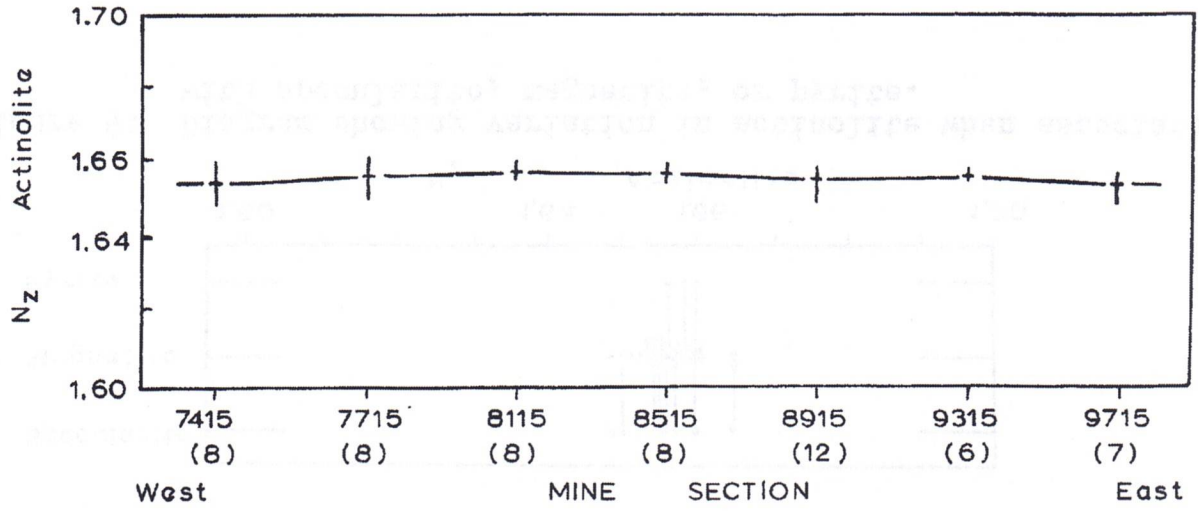

Figure 6: Diagram showing the range and average n_z of actinolite along the length of the mine.

shows no significant pattern. Figure 8 compares refractive index of actinolite and garnet. This shows that there is little effect on the actinolite while ferric iron in the grossularite-andradite garnet increases.

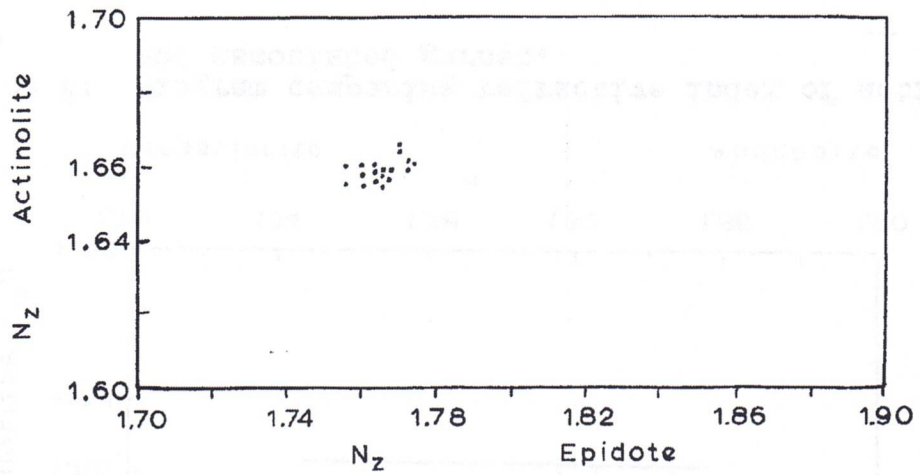

Figure 7: Diagram comparing the refractive index of actinolite associated with epidote.

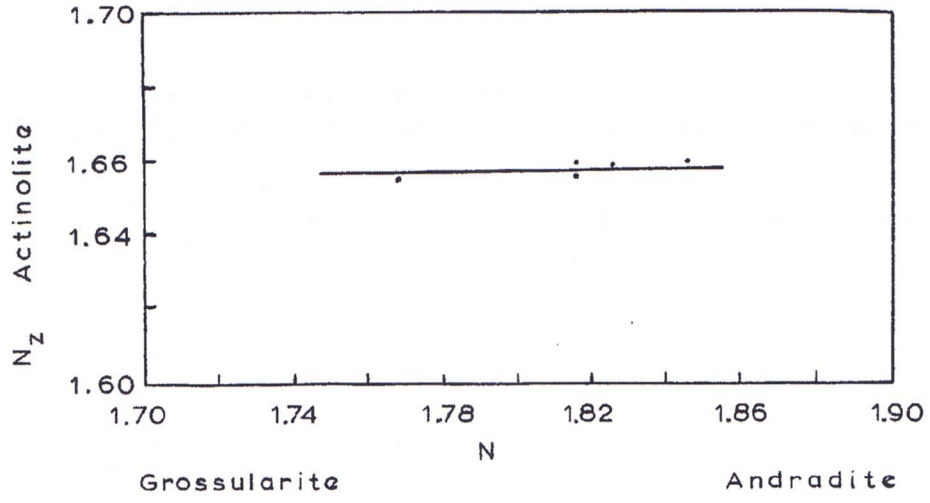

Figure 8: Diagram comparing refractive index of actinolite and associated garnet.

Actinolite composition is also independent of association with magnetite, specularite, chalcopyrite, and pyrite. The refractive index of actinolite associated with either magnetite, specularite and/or pyrite is compared in Figure 9. Chalcopyrite occurs with these minerals and could not be separated. Lines which connect magnetite, specularite, and/or pyrite indicate that more than one metallic phase is associated with the actinolite.

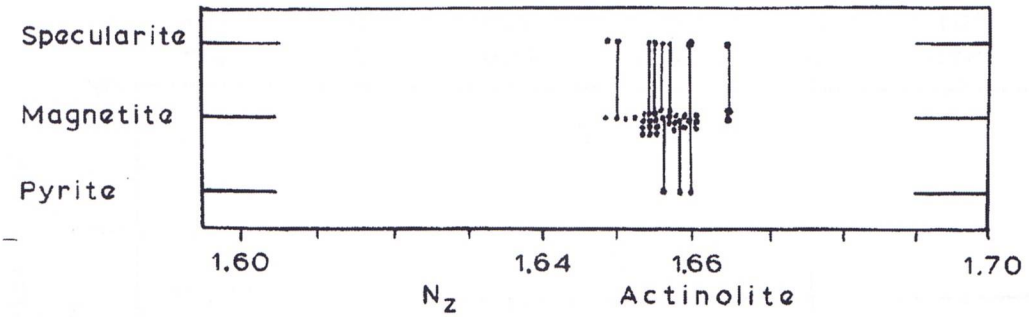

Figure 9: Diagram showing variation in actinolite when associated with specularite, magnetite, or pyrite.

Epidote

Pistachio green epidote occurs throughout the mine. A typical epidote has $n_z = 1.765 \pm 0.003$ and $n_x = 1.732 \pm 0.003$; $n_z - n_x = 0.033$; strong dispersion with 'r' less than 'v' about X; and strong pleochroism with Z bright yellow, Y pale yellow, and X very pale yellow to colorless ($Z > Y > X$). Universal stage determination of 2V gave $2V_x = 70, 76, 78 \pm 3$.

Epidote was determined to be inhomogeneous and not suitable for electron microprobe analysis. Aluminum, iron, and calcium counts per 10 second interval ranged 10%, 6%, and 3%. An inverse relationship was noted between Al and Fe (higher Al, lower Fe; lower Al, higher Fe) which suggests that Fe substitutes for Al (specimen 663-115).

Only minor variation in the composition of epidote is indicated by Figure 10 which shows the range and average n_z for the section listed. Using the optical curves of Deer, Howie, and Zussman (1962) volume 1, page 203, average epidote contains 27 mole percent $Ca_2Fe_3(SiO_4)_3(OH)$ with a range of 26 to 32 mole percent. Average composition is about $Ca_2(Al_2Fe^{+++}_1)\ (SiO_4)\ (OH)$.

Epidote composition does not change with associated silicate phase. No significant relationship is seen between epidote and associated actinolite (Figure 7, page 40). Composition of grossularite-andradite garnet associated with epidote is shown in Figure 11. Figure 11 suggests that very little change in the Al/Fe^{+++} ratio occurs in epidote while there is appreciable change in the Al/Fe^{+++} ratio of garnet.

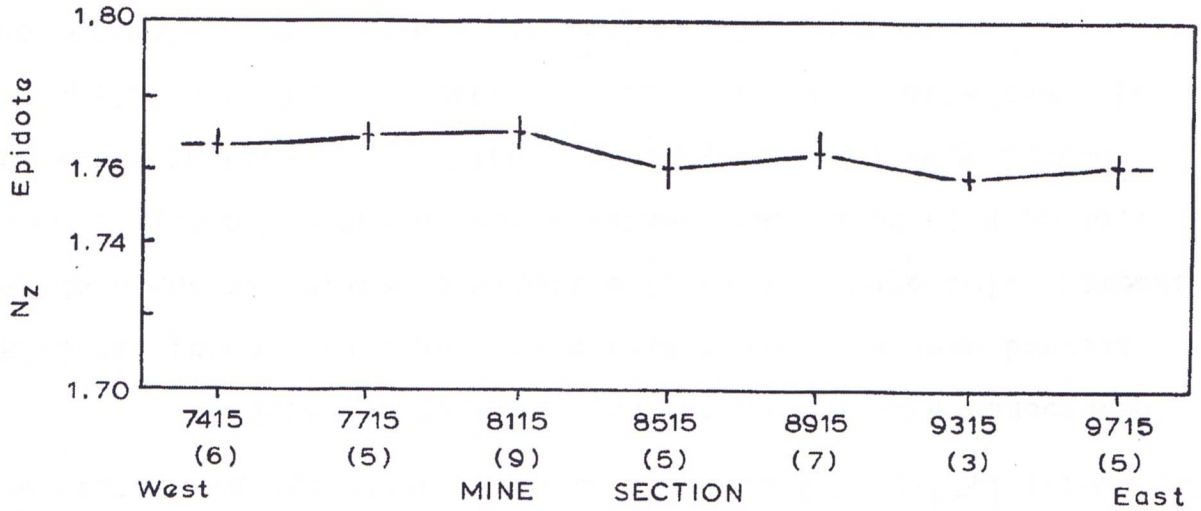

Figure 10: Diagram showing range and average n_z epidote for various mine sections. Number in brackets refers to number of determinations.

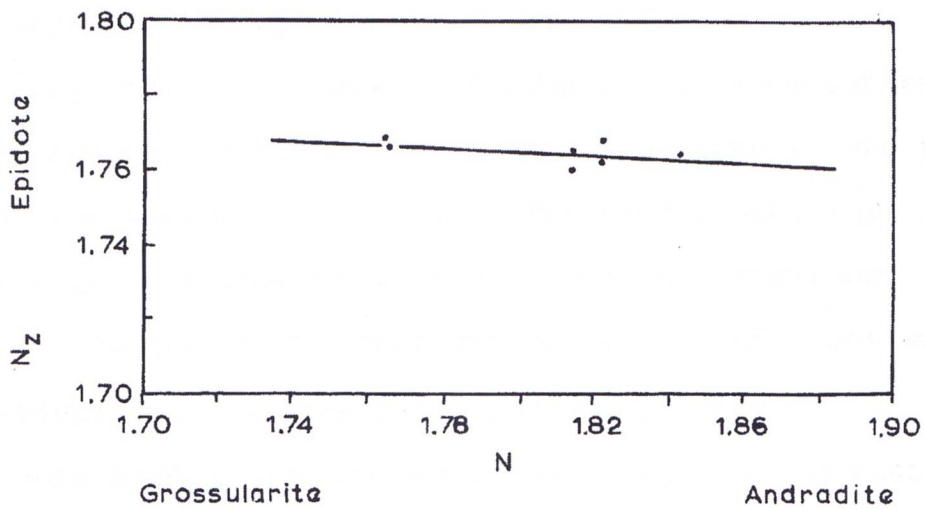

Figure 11: Diagram showing variation in garnet with associated epidote.

Epidote composition does not vary with associated metallic phases. Figure 12 indicates that composition is independent of association with magnetite, specularite, or pyrite. Join-lines in Figure 12 indicate rocks in which magnetite, specularite and/or pyrite are associated with epidote. Chalcopyrite is present throughout, and consequently is not considered separately.

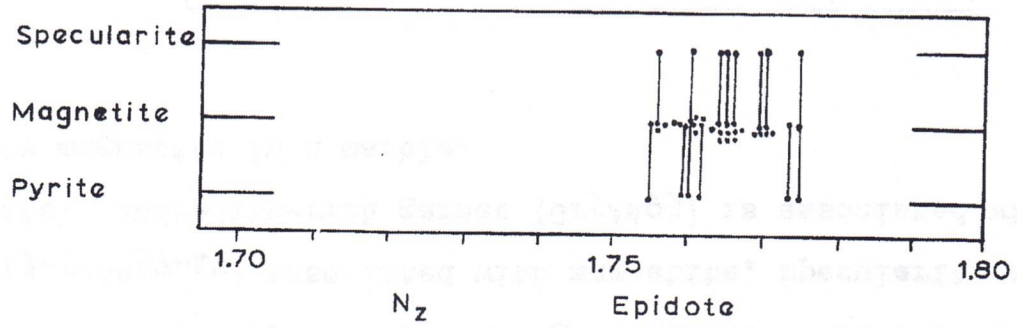

Figure 12: Diagram showing variation in epidote when associated with specularite, magnetite, or pyrite.

Garnet

Members of the grossularite-andradite series occur in the Craigmont skarn. Reddish brown and yellowish green; isotropic and anisotropic garnet occur in the same specimen. Refractive index has primarily been used to determine the composition of the garnets. Specific gravity determinations were unsuccessful owing to the presence of calcite and other impurities. Refractive index and 'a_o' when determinable from X-ray diffractometer patterns indicated compositions very close to the andradite-grossularite series. Determinative curves

used are those of Winchell and Winchell (1951) page 492, and Winchell (1958) page 595. All garnets in the Craigmont skarn rocks are lime garnets of the grossularite-andradite series with variations in the Al/Fe^{+++} ratio. It is possible that there may be small amounts of almandine molecule in these garnets.

Variation in composition of garnets which are associated with epidote and actinolite is shown in Figure 11, page 43 and Figure 8, page 41 respectively. Garnets range compositionally while the associated epidote and actinolite composition remains nearly constant. Garnet which is associated with specularite, magnetite and/or pyrite is compared in Figure 13. Join-lines represent specimens in which garnet occurs with more than one iron oxide and/or with pyrite. Three garnets (about $Gr_{78}An_{22}$) associated with pyrite are more grossularite-rich than garnets ($Gr_{43-53}An_{57-47}$) associated with magnetite, specularite and/or pyrite. Andradite-rich garnet (Gr_5An_{95}) is associated with platy magnetite in a marble.

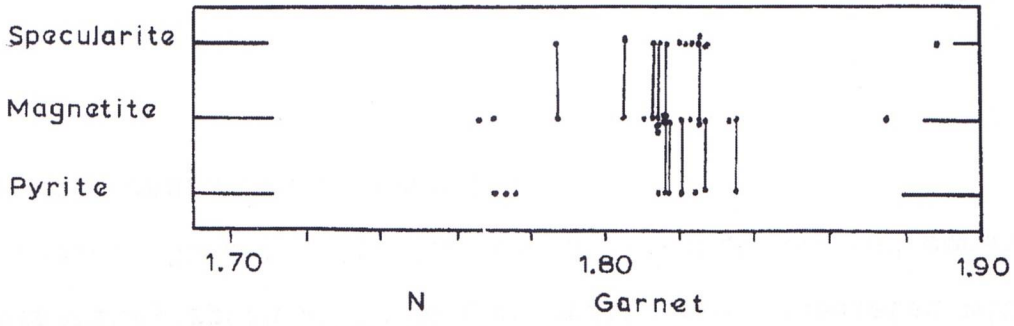

Figure 13: Diagram showing variation in garnet associated with specularite, magnetite, or pyrite.

Zoned garnets may have an isotropic core which is more grossularite-rich than the ansiotropic relatively andradite-rich rim. A few color zoned garnets have the same refractive index for core and rim. Rim garnet where present is usually colored red-brown.

Diopside

Colorless, cloudy diopside in a diopside-calcite-quartz-plagioclase rock has the following properties: optically positive with a moderate to high 2V; dispersion is r greater than v about Z; refractive indices are $n_z = 1.702 \pm 0.002$ and $n_x = 1.670 \pm 0.002$; $n_z - n_x$ is 0.032; and $Z \wedge c$ is about 43 (specimen 663-40). According to the optical data of Hess (1949) page 641, the diopside-hedenbergite ratio is $Di_{92}Hd_8$.

A diopside-hedenbergite pyroxene is a constituent of many skarn deposits but the occurrence of diopside in the Craigmont skarn rocks is scarce.

Chlorite

In thin section under crossed nicols, chlorite exhibits either an anomalous bluish-violet or brownish interference color. Those chlorites which show anomalous blue have positive elongation and are optically negative while those which show anomalous brown have negative elongation and are optically positive. To determine the elongation is sufficient to give the optic sign.

Refractive index of the varieties are as follows: abnormal brown, $n_y = 1.609 \pm 0.002$ (range 1.605 to 1.614); abnormal blue, $n_y = 1.625 \pm 0.002$ (range 1.620 to 1.630); normal optically negative, $n_y = 1.640 \pm 0.002$ (Specimens 663-79 to 90). In all cases, 2V is low and pleochroism is Z grass green and X colorless.

X-ray diffractometer patterns of these chlorites were not sufficiently distinctive to allow a reliable identification using the ASTM index. Differential thermal analysis of the three varieties was undertaken. Diffractometer and DTA patterns are reproduced in Appendix A. The results are summarized in Table 6. According to Grim (1953) and Brindley (1951), an exothermic peak between 800 - 850 C would indicate

Table 6

DTA Results of Craigmont Chlorite

Specimen	Exothermal Peak	Endothermal Peak	n_y
663-89 (Brown)	835 C	665 C	1.605
663-82 (Blue)	835	640	1.622
663-79 (Normal)	835	560	1.640

essentially complete dehydration. This would explain why the exothermic peak remains constant. Grim states that a distinct endothermic peak between 500 - 700 C indicates loss of the hydroxyl in the brucite-like layer. Chlorite with relatively higher iron content shows an endothermic peak at a lower temperature than chlorite with a relatively lower iron content (compare specimen 663-79 with specimen 663-89

in Table 6). This shows a distinct variation between composition and the temperature at which the hydroxyl is lost.

Significance of abnormal blue and brown interference colors is suggested by Albee (1962) whose conclusions are summarized below (Figure 14). Near the change from optically positive to negative, the birefringence crosses 0.00. Abnormal interference colors near the change point are the result of the mineral becoming isotropic for part of the spectrum and anisotropic for another part. According to Albee, the colors and optic sign indicate the relative change in Fe and Mg. Figure 15 agrees with the conclusions of Albee

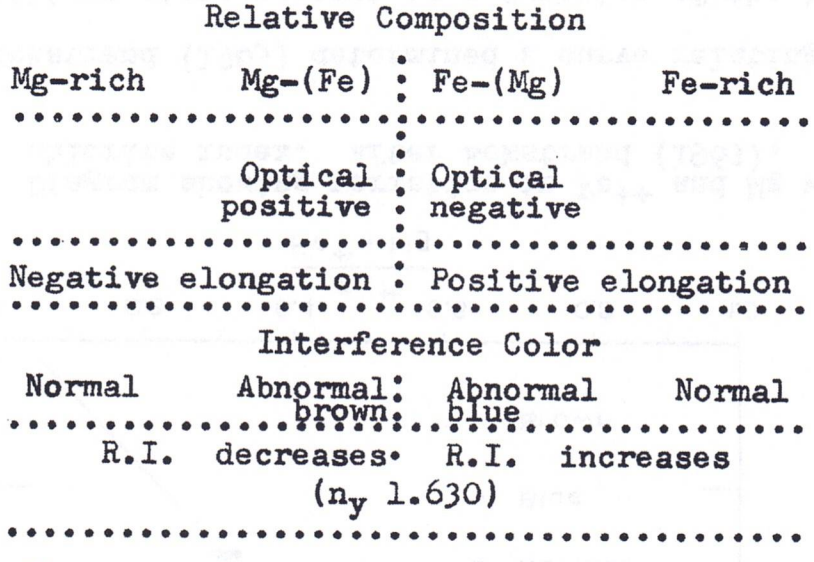

Figure 14: Diagrammatic summary of conclusion of Albee (1962) showing relation of interference color, index, and relative composition of chlorite.

and shows that the abnormal brown is relatively more Mg-rich than the abnormal blue variety.

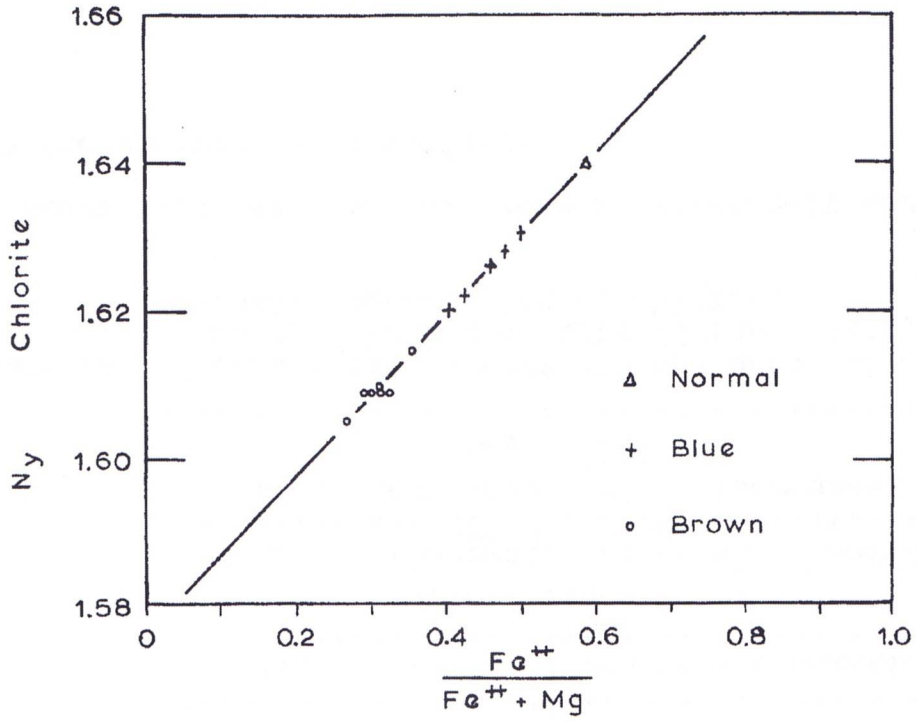

Figure 15: Diagram showing variation in Fe^{++} and Mg with chlorite index. After Eckstrand (1963).

Eckstrand (1963) determined a curve relating the number of silicon atoms present as a function of the basal spacing. Similarly, Brindley and Gillery (1956) used variation in basal spacing as a measure of the aluminum substitution for silicon in the formula $(Si, Al)_4$. Figure 16A indicates that the number of silicon atoms in each variety is about the same and Figure 16B shows that there is very little variation of the chlorites with respect to Al substitution for Si.

While the chlorites range in refractive

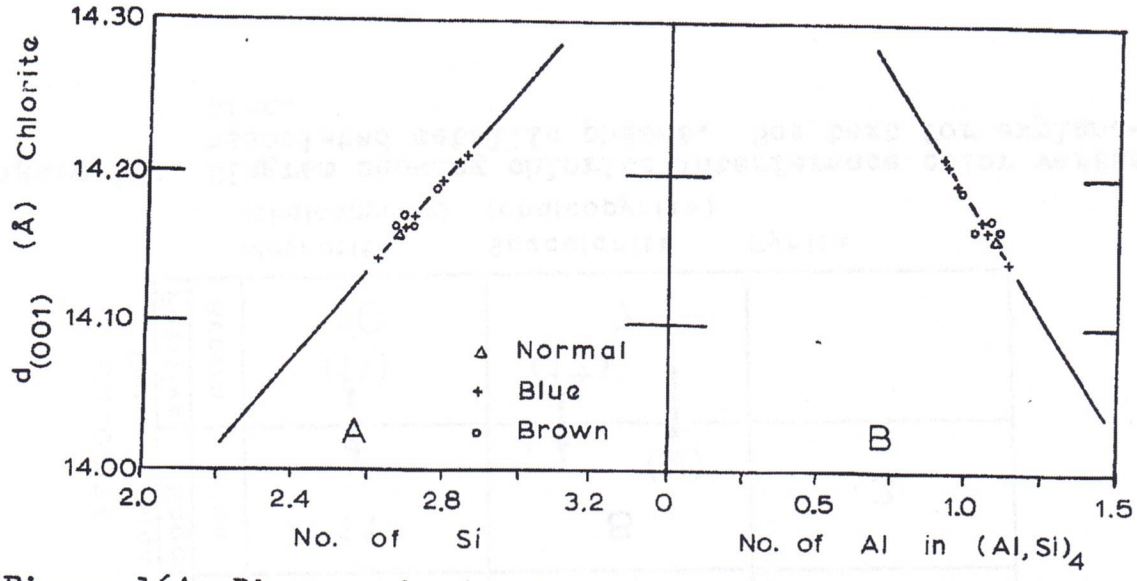

Figure 16A: Diagram showing Si content versus basal spacing. After Eckstrand (1963).
Figure 16B: Diagram showing Al substitution for Si versus basal spacing. After Brindley and Gillery (1956).

index, they are probably within a restricted compositional range (constant Al/Si ratio) with a variation in the Fe/Mg ratio. Possible compositions may range between aphrosiderite (ASTM 12-243)

$$Mg_{1.0}Fe^{++}_{3.2}Fe^{+++}_{0.4}Al_{1.2}(Al_{1.5}Si_{2.5})\ O_{10}(OH)_8$$

and repidolite (Deer, Howie and Zussman (1962) volume 3, page 141)

$$Mg_{2.5}Fe^{++}_{1.9}Fe^{+++}_{0.25}Al_{1.2}(Al_{1.2}Si_{2.8})\ O_{10}(OH)_8.$$

Hey (1954) states that aphrosiderite should be classed as a variety of repidolite (page 279).

Seventy-three chlorite-bearing assemblages were investigated to determine if composition changed with associated phases. The result is shown in Figure 17. Numbers within the squares refers to one type of chlorite associated with either magnetite, specularite, or pyrite. Numbers in brackets refer to that many chlorites with a rim of differing interference color. The arrow points toward the rimming variety. The significance of the variation in Fe/Mg ratio becomes difficult to assess when within one radical crystal abnormal brown changes to blue or, less often, abnormal blue changes to brown along the length of the crystal. Associated silicate and metallic phases do not show any specific correlation to chlorite composition with the possible exception of pyrite-bearing assemblages.

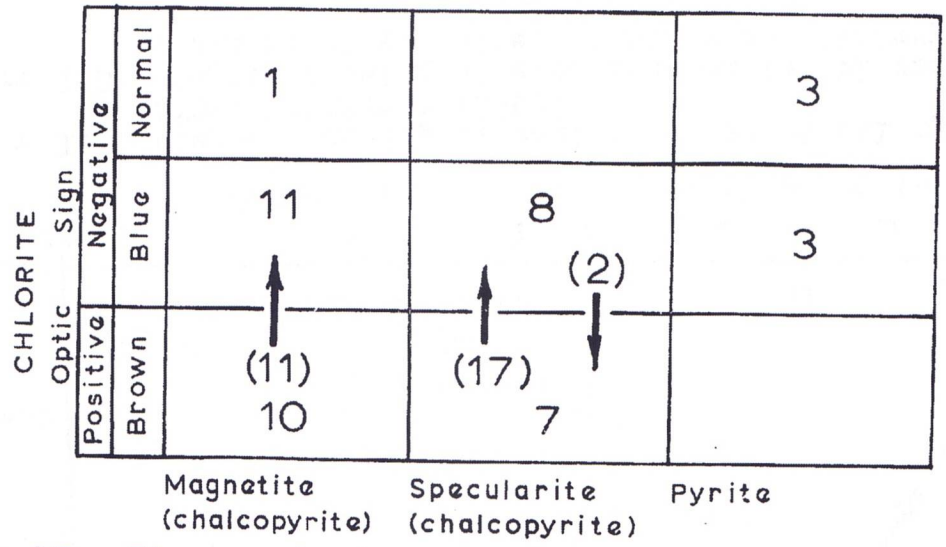

Figure 17: Diagram showing chlorite interference color versus associated metallic phases. See text for explanation.

Carbonate Minerals

Within the skarn rocks, the white and pinkish-tinged crystalline carbonate is calcite. Brownish yellow siderite is rarely present in the skarn rocks but is present in late fractures in the oxidized zone of the open pit.

Partial chemical analyses show that little Mn or Mg is present in the carbonates. The results are given in Table 7. The analyses indicate that calcite is quite pure

Table 7

Partial Analyses of Calcite and Siderite

	A	B	C	D	E
CaO	55.37	55.58	56.0	2.79	-
FeO	0.29	0.26	-	64.59	62.1
MnO	0.07	0.08	-	0.57	-
MgO	0.14	0.13	-	0.58	-
CO_2	-	-	44.0	-	37.9

A. White coarse-grained calcite (663-94).
B. Pale pink tinged calcite (663-95).
C. Theoretical calcite composition.
D. Brownish yellow siderite (663-96).
E. Theoretical siderite composition.
(Analysis by H. Sharples)

and that the light pink coloration is caused by something other than manganese. Siderite appears to contain more iron than it should (compare D and E in Table 7). Under high magnification, minute specks of pyrrhotite may be seen which would account for the excess iron.

Dolomite has not been recognized in thin section nor detected by X-ray.

Skarn Assemblages as Related to Iron Oxides

There is no recognizable range in compositions of actinolite and epidote when associated with each other, with garnet, nor with metallic phases. Garnet alone shows a recognizable change in composition. While the composition of the individual mineral phases of the skarn rocks remains relatively constant over the limits of the mine, a variation in the occurrence of these lime silicates with associated iron oxide is noted. Consequently, skarn assemblages are subdivided into three classes: (1) those associated with magnetite; (2) those with magnetite and specularite; and (3) those with specularite.

Skarn Assemblages With Magnetite

Skarn rocks which are associated with magnetite contain the following assemblages: (1) Actinolite-epidote-chlorite-calcite-quartz-apatite-sphene-magnetite-chalcopyrite (24/29*, Specimens 663-128, 129, 130, 132); (2) garnet-epidote-chlorite-calcite-quartz-apatite-sphene-magnetite-(chalcopyrite) (2/29); (3) garnet-epidote-actinolite-calcite-quartz-sphene-magnetite (1/29, 663-131); (4) garnet-actinolite-calcite-quartz-apatite-sphene-magnetite (1/29); and (5) epidote-diopside-actinolite-calicite-quartz-magnetite (1/29, 663-133).

A typical assemblage would contain epidote crystals in felted actinolite with interstitial calcite, quartz, magnetite, and chalcopyrite. Apatite and sphene are scattered

* The number of 24/29 refers to the number of that particular assemblage out of a total of 29 examples.

accessory minerals. Euhedral magnetite grains appear to replace actinolite but chalcopyrite is interstitial to the actinolite. This difference is shown in Plate 3. Chalcopyrite may locally replace actinolite as minute irregular chalcopyrite blebs can be found along the cleavage planes in the actinolite. Small acicular crystals of actinolite have developed within and across grain boundaries of quartz and calcite which suggests that actinolite formation continued until late in the sequence (Plate 4). Coexisting garnet is minor in this type of skarn.

The uncommon diopside-bearing rocks, in thin section, show crystals of diopside in a poikiloblastic texture with epidote (663-133). Diopside is also found with actinolite interstitial to the diopside-epidote crystals. This texture is shown in Plate 5.

Skarn Assemblages With Magnetite and Specularite

Skarn rocks which are associated with both magnetite and specularite have the following assemblages: (1) actinolite-epidote-calcite-quartz-apatite-magnetite-specularite-chalcopyrite (16/25*, 663-123, 124, 125); (2) garnet-epidote-actinolite-calcite-quartz-apatite-sphene-magnetite-specularite-chalcopyrite-(pyrite) (4/25, 663-121, 122); (3) garnet-epidote-calcite-quartz-magnetite-specularite-chalcopyrite (2/25); (4)

* The number 16/25 refers to the number of that particular assemblage out of a total of 25 examples.

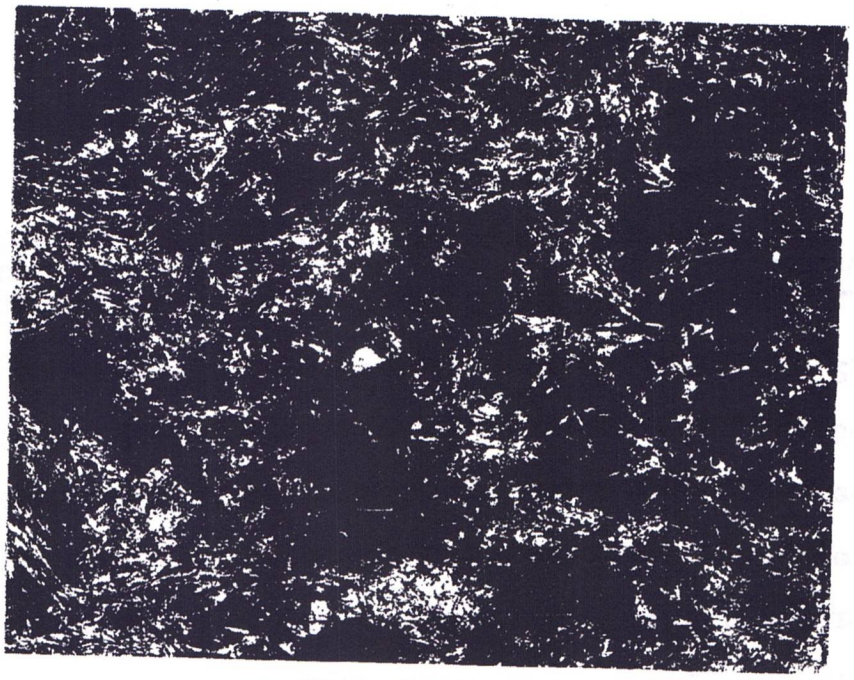

1 mm.

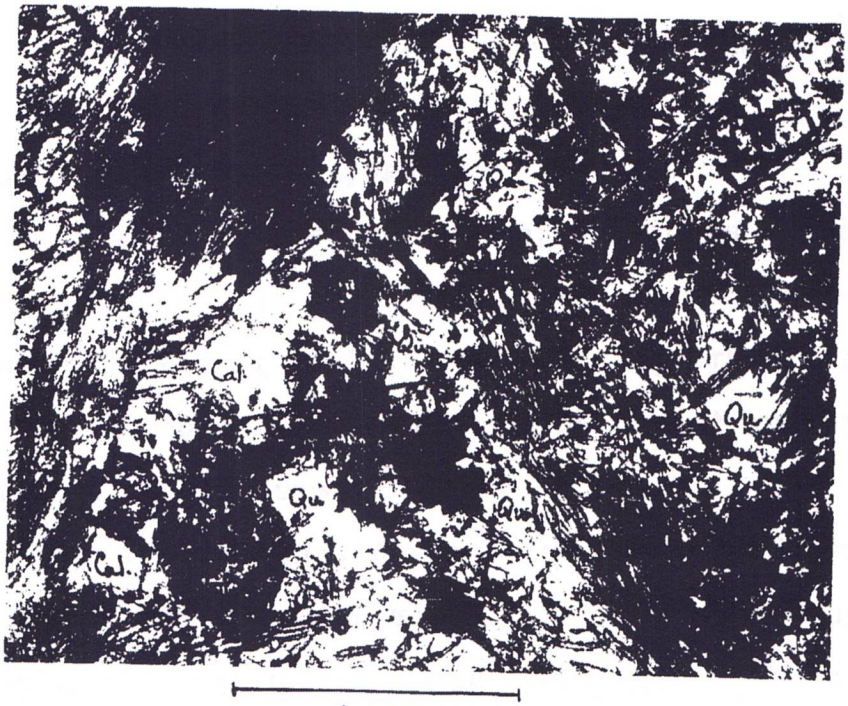

1 mm.

Plate 3 Photomicrograph showing euhedral magnetite and irregular interstitial chalcopyrite grains in felted actinolite. Plain light. (Specimen 663-128).

Plate 4 Photomicrograph showing actinolite needles in calcite and quartz. Rectangular crystals are epidote. Plain light. (Specimen 663-130).

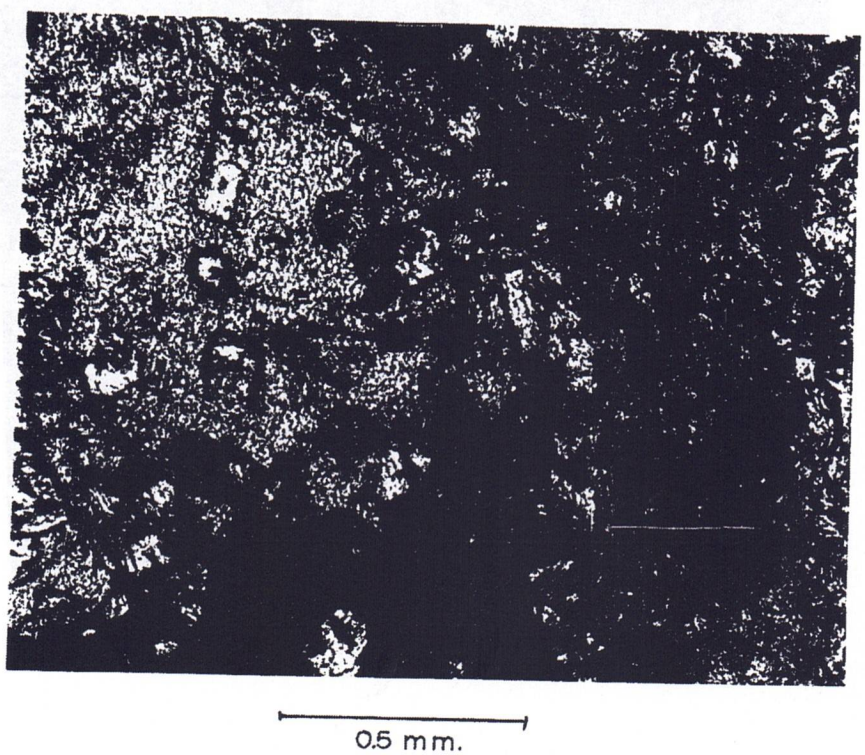

Plate 5 Photomicrograph showing diopside crystals within large epidote crystals and with actinolite interstitial to epidote. (Dark areas are magnetite). Plain light. (Specimen 663-133).

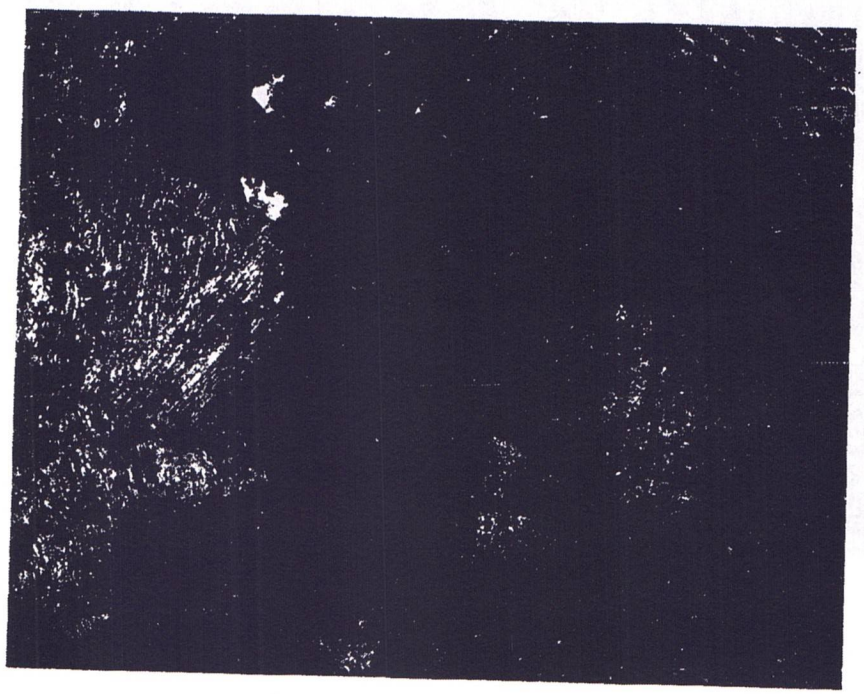

1 mm.

Plate 6 Photomicrograph of zoned garnet in calcite (Smaller grains in calcite are diopside). Crossed Nicols. (Specimen 663-127).

garnet-actinolite-calcite-quartz-magnetite-specularite-chalcopyrite (2/25); and (5) garnet-diopside-actinolite-calcite-magnetite-specularite (1/25, 663-127).

A typical association is actinolite, epidote, calcite, quartz, generally without coexisting garnet. Actinolite usually displays a felted texture between epidote grains. Quartz and calcite are interstitial. Euhedral sphene and apatite are scattered throughout the rock. Magnetite and specularite exhibit their crystal form but chalcopyrite is interstitial. Chalcopyrite is more abundant than pyrite and when in contact, chalcopyrite veins the pyrite.

Garnet crystals when present are characteristically birefringent and display zoning. A photomicrograph of zoned garnets with diopside, calcite, magnetite, and specularite is shown in Plate 6. Diopside may locally be replaced by calcite. Actinolite associated with garnet and epidote is usually fine-grained but in one section of the skarn rocks, actinolite crystals have a length of 6 to 7 inches (specimen 663-126). Very coarse-grained skarn rocks are not common at Craigmont.

Skarn Assemblages With Specularite

Skarn rocks which are associated with specularite contain the following assemblages: (1) garnet-epidote-calcite-quartz-(chlorite)-sphene-specularite-(pyrite) (4/9*, 663-119);

* The number 4/9 refers to the number of that particular assemblage out of a total of 9 examples.

(2) garnet-epidote-actinolite-calcite-quartz-sphene-specularite-(pyrite) (3/9, 663-118, 120); (3) garnet-actinolite-calcite-chlorite-specularite-pyrite-chalcopyrite (1/9); and (4) epidote-diopside-calcite-quartz-apatite-specularite (1/9). A mineral in brackets refers to its presence in minor amounts.

A typical association may include garnet, epidote, actinolite, calcite, quartz, (chlorite), specularite, pyrite, and (chalcopyrite). In thin section, quartz, calcite, and actinolite are interstitial to anisotropic garnet and epidote crystals. The typical texture is shown in Plate 7.

Magnetite

Magnetite in the skarn rocks is present either as euhedral or granular crystals or as platy magnetite. Under the mineralographic microscope, both habits of magnetite show a bluish anisotropic and a brownish isotropic phase (Plate 8 and 9). This latter phase usually is present along edges of fractures and grain boundaries or around pits in the polished surface. In some cases, the bluish phase appears to stand in relief against the brownish phase but in other cases, the colors merge into one another (663-101). Determination of hardness using a Kentron Microhardness tester shows that the difference is minor and inconclusive (See Appendix B).

X-ray investigation indicated no differences between the two color phases in the platy magnetite. X-ray powder films, using a 114.59 mm. diameter camera with cobalt

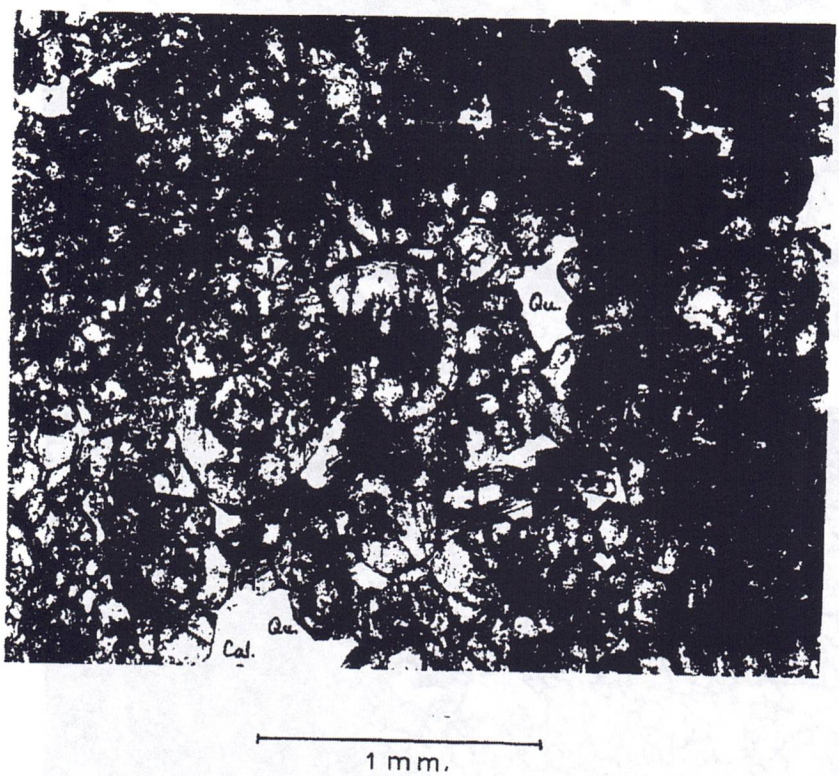

Plate 7 Photomicrograph showing actinolite, calcite and quartz interstitial to garnet crystals. Plain light. (Specimen 663-120).

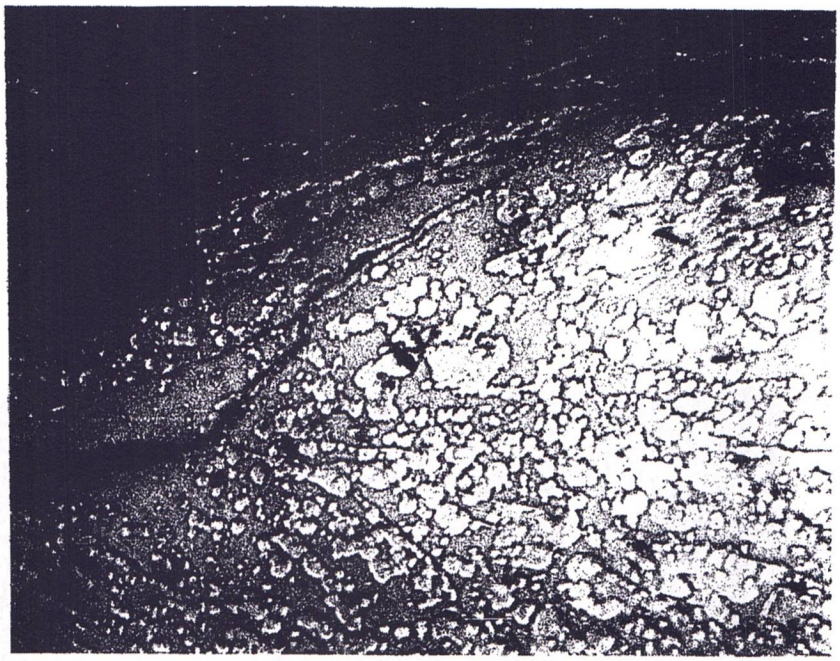

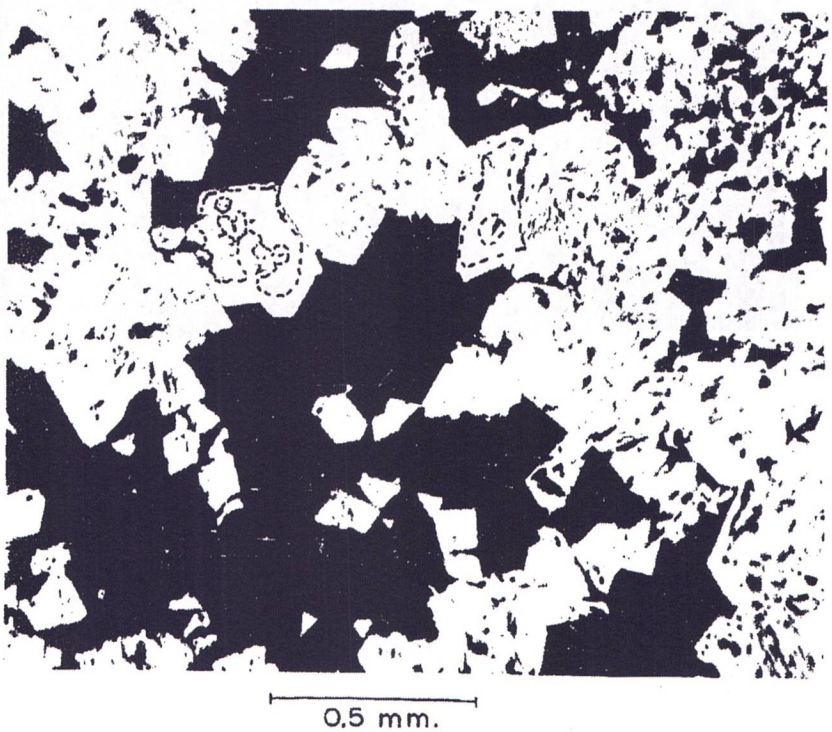

Plate 8 Photomicrograph showing two phases in platy magnetite (Note: lighter color is brownish isotropic phase and darker color is bluish anisotropic phase). Plain light. (Specimen 663-98).

Plate 9 Photomicrograph showing two phases in euhedral magnetite (Note: lighter color around holes and grain boundaries). Plain light. (Specimen 663-102).

radiation and iron filter show agreement with magnetite (ASTM 11-614). A few non magnetite lines could be assigned to either quartz, chlorite, or hematite. X-ray diffractometer patterns using cobalt radiation and an iron filter show sharp symmetrical peaks with no distortion. X-ray data and patterns are reproduced in Appendix C. The width of the half height of the three major peaks is the same for that peak in each specimen examined. Precession photographs of a single platy magnetite crystal show only one phase, magnetite. These photographs are reproduced in Appendix C. The cell dimension is that of magnetite. The octahedral (111) plane in the magnetite is parallel to the basal plane (0001) of the original specularite(?). There is no X-ray agreement for maghemite.

Scanning the bluish and brownish colored areas with the electron microprobe indicates only trace amounts of vanadium and/or titanium. The scans when compared with a scan of analyzed magnetite from Mineville, New York indicate that V_2O_3 is less than 0.1% and TiO_2 is less than 0.2%. A trace of MnO_2 is present in one scan. Results are given in Appendix D. Scans used in this study are reproduced in Appendix D. A continuous microprobe scan by Davidson and Wyllie (1965) across a platy magnetite crystal with a lighter colored core from the Cornwall iron deposit, Pennsylvania is reproduced in Figure 18. They concluded that the lighter colored core is magnetite which is slightly more pure than the magnetite of the rim.

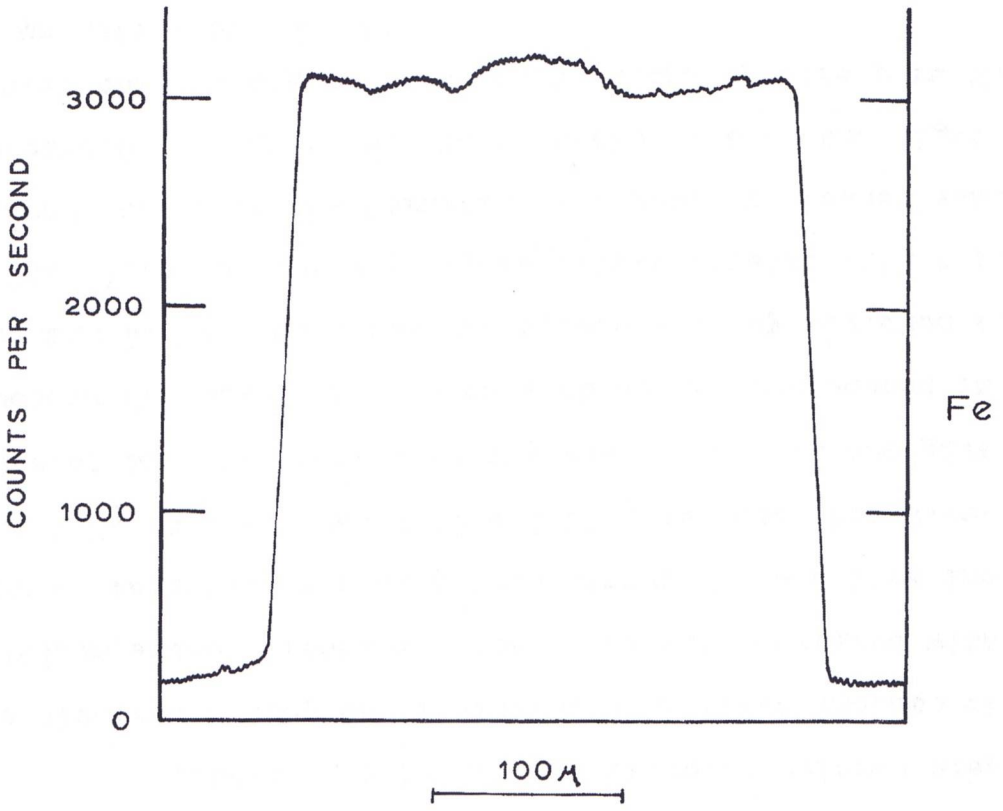

Figure 18: Continuous microprobe scanning traverse for Fe across platy magnetite from Cornwall, Pennsylvania. After Davidson and Wyllie (1965) Figure 6, p. 769.

As the above indicates only the presence of one phase, the answer to the presence of two colors in the magnetite may lie in the effects of polishing. Polishing procedure is outlined in Appendix E. All specimens were cold mounted. Hand and machine polished specimens from the same sample were compared. Hand polished platy magnetite shows only one phase while machine polished specimen shows two distinct colors. Photomicrographs illustrating this effect are shown in Plate 10 and 11. Similarly, anisotropic

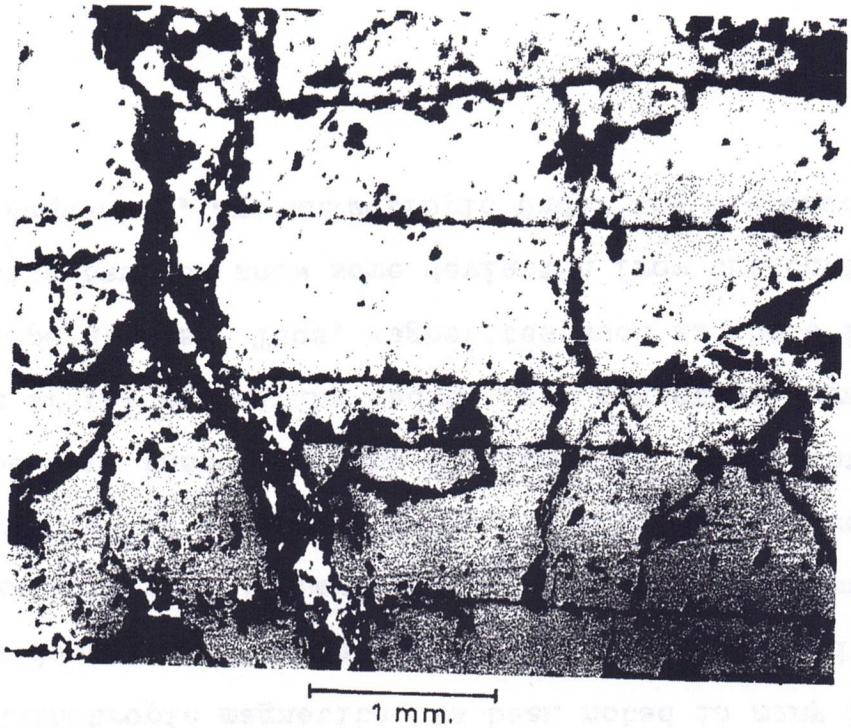

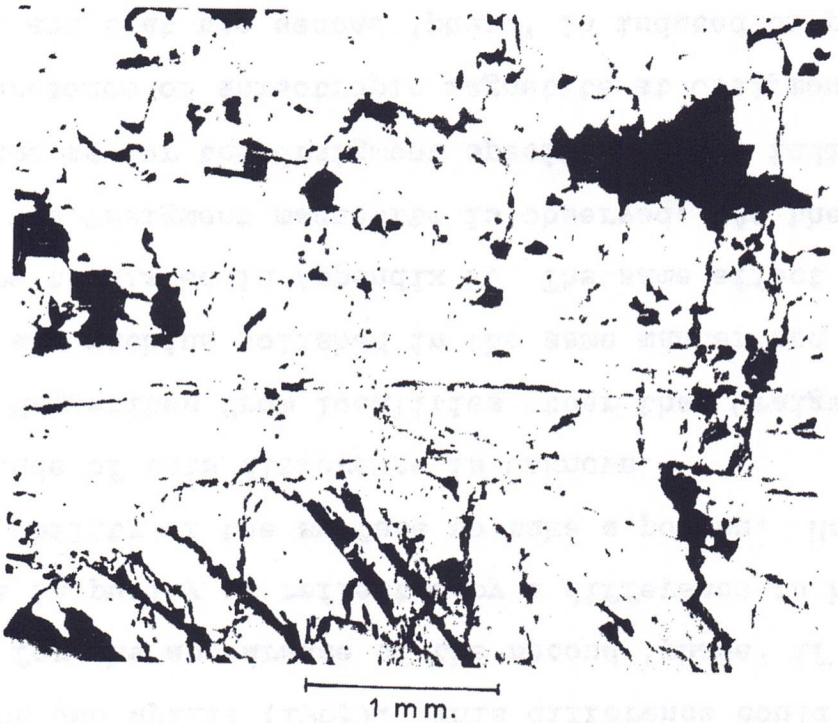

Plate 10 Photomicrograph of hand polished platy magnetite. Plain light. (Specimen 663-111).

Plate 11 Photomicrograph of machine polished platy magnetite. Plain light. (Specimen 663-111).

effect in hand polished samples is indistinct but present. In the machine polished samples, anisotropic effect is more readily observed. This suggests that anisotropism in magnetite is accentuated by machine polishing. A slight difference in magnetite purity between the two 'phases' is suggested by Davidson and Wyllie (1965). This difference could be responsible for the appearance of the second 'phase' if a difference in purity is reflected by a difference in hardness or in the ability of the surface to take a polish. However, the magnitude of this difference is unknown.

Magnetites from localities other than Craigmont were hand and machine polished in the same manner and compared. Results are tabulated in Appendix F. The same effect as that seen with the Craigmont magnetite is observed. As the results are the same as for the Craigmont specimens, this indicates that the presence of anisotropic magnetite at Craigmont is not unique and that the second 'phase' is induced by polishing.

Anisotropic magnetite has been noted in many high temperature deposits. A discussion of the presence and causes of anisotropism in magnetite is presented in Appendix G. The formation of magnetite at high temperature is concluded to be more susceptible to fluctuations in the internal equilibrium of the depositing medium than magnetite formed at lower temperatures. Thus, magnetites such as those in skarn deposits tend to show some deviation from the cubic system and consequently, are anisotropic under the microscope.

Specularite

Thin crystalline plates of micaceous hematite or specularite are locally associated with magnetite or found in veinlets without magnetite. Under the mineralographic microscope, blades are strongly anisotropic, show a deep red internal reflection, and display lamellar twinning. Warped blades tend to show well developed twinning which suggests a causal relationship between twinning and strain (W. Uytenbogaardt (1951) page 196).

Composition is probably near the theoretical for alpha-Fe_2O_3. Scans on the electron microprobe indicate only the presence of iron and a trace of vanadium (Appendix D, Run no. 4). Powder X-ray photographs agree with hematite, ASTM 13-534.

Textural relationships of early specularite and magnetite have been discussed above. Late hematite or martitization is noted along grain boundaries and fractures in magnetite (Plate 12). This suggests that some late stage oxidation of magnetite has occurred.

Sulphides

The most abundant sulphide within the skarn is chalcopyrite. Under the microscope, chalcopyrite is commonly interstitial and locally tends to vein iron oxides. Pyrite is present throughout the mine in small amounts. Pyrite can occur in contact with iron oxides and chalcopyrite. Small

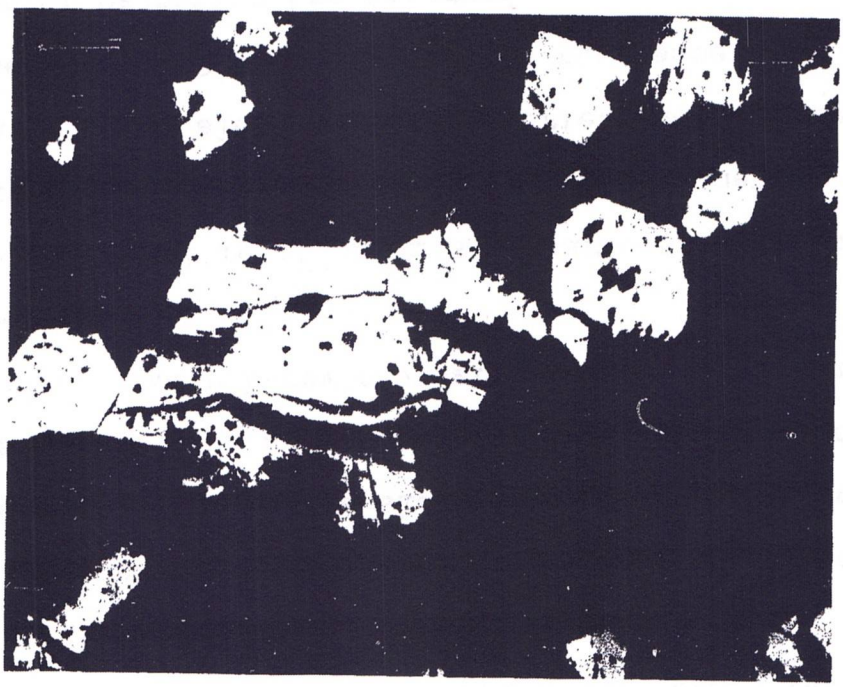

Plate 12 Photomicrograph showing secondary hematite along fractures and grain boundaries of magnetite (White is hematite). Plain light. (Specimen 663-117).

irregular crystals are found in and are veined by chalcopyrite. These two sulphides are the most important in the mine.

All other sulphides are present in scant amounts. Minute blebs of bornite are locally found in chalcopyrite. Pyrrhotite, pyrite, and chalcopyrite are in contact in specimen 663-96 with pyrite replacing the pyrrhotite. This assemblage is associated with siderite in an epidote-calcite skarn. Minute bluish flakes of molybdenite were noted in two specimens of altered dioritic rock. Arsenopyrite was identified in a late quartz vein.

Summary of Associations

Mineral association of the above skarn types may be summarized as follows: (1) garnet-epidote-(actinolite)-calcite-quartz-specularite-(pyrite); (2) epidote-actinolite-(garnet)-calcite-quartz-magnetite-specularite-chalcopyrite; (3) actinolite-epidote-(chlorite)-calcite-quartz-magnetite-chalcopyrite. These associations are diagrammatically presented in Figure 19. Epidote is present in all the skarn assemblages whether associated with garnet-specularite or actinolite-magnetite. Thus, epidote is associated with two distinct assemblages each of which indicates a different partial pressure of oxygen. Figure 19 also shows that chalcopyrite is more abundant in the reduced actinolite-magnetite assemblage relative to the oxidized garnet-specularite assemblage.

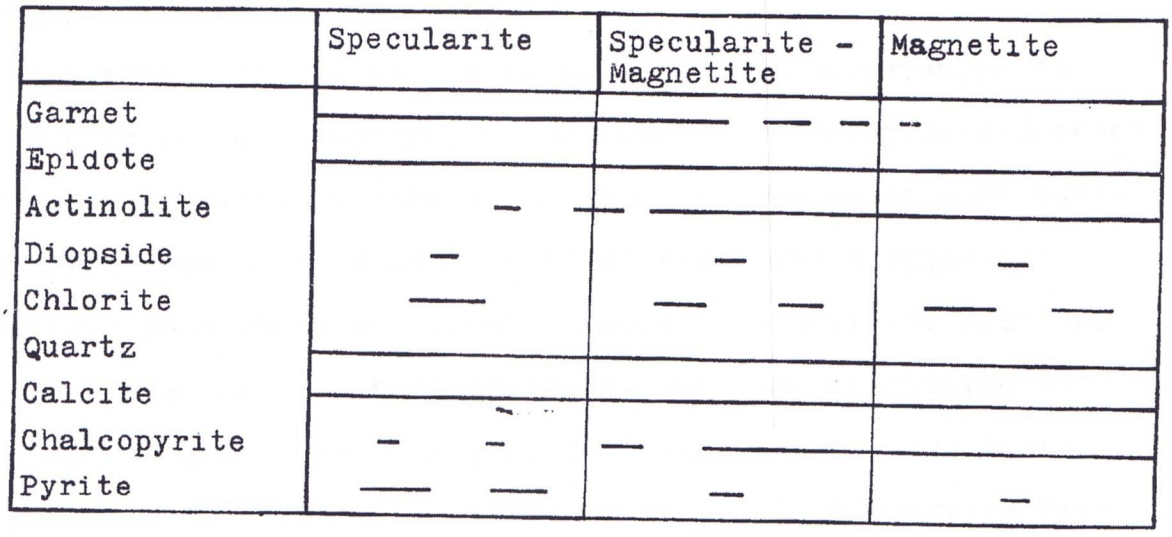

Figure 19: Diagrammatic presentation of skarn rocks with associated iron oxide phase.

Textural relations of the silicates indicate that they all formed at about the same time. Diopside-bearing associations are scarce and do not constitute a mapable unit. Chalcopyrite is present in portions of the actinolite-epidote skarn rocks in sufficient quantity to make ore. Garnet-bearing assemblages may contain trace amounts of chalcopyrite.

Distribution of Skarn Rocks

Skarn assemblages are restricted to a narrow steeply south dipping zone which approximately parallels the east-west contact of the Guichon diorite (see 2400, 3060, and 3500 level geological plans, in pocket). Hornfelses separate the skarn rocks from the main diorite mass but apophyses of diorite intrude the skarn zone. This is seen in geological

sections 9315, 8915, 8515, 8115, and 7715. Distribution of garnet-epidote and/or actinolite and actinolite-epidote associations are outlined in all plans and sections. Distribution of magnetite-specularite and chalcopyrite-potash feldspar are outlined on individual iron oxide and copper overlays for each section.

In sections 7415 and 7715, there is a downward change from marble to actinolite-epidote rocks to garnet rocks between about the 3060 level to below the 2400 level. Garnet assemblages are on the north or diorite side of the skarn area in these sections. Superficially, this suggests a garnet-actinolite-marble zonation outward from the diorite. A sketch illustrating this zonation is shown in Figure 20. In other sections, this sequence is not as readily seen. On section 8115, there is only a minor amount of marble remaining as garnet-epidote rock surrounds a diorite apophysis

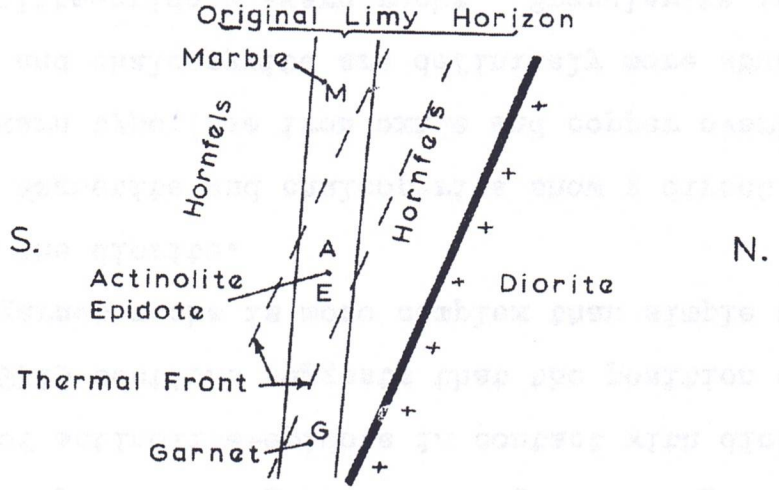

Figure 20: Sketch illustrating apparent skarn zonation at Craigmont.

between the 3060 and 3500 levels. Sections 8515, 8915, 9315, and 9715 shows that diorite can be in contact with both actinolite-epidote and garnet-bearing assemblages. The presence of actinolite-epidote in contact with diorite on 9715 and 9315 sections suggests that the position of actinolite and garnet rocks is more complex than simple zoning outward from the diorite.

Magnetite and chalcopyrite show a direct correlation to skarn type (see iron oxide and copper overlays). Magnetite and chalcopyrite are definitely more abundant in the actinolite-epidote skarn rocks. Specularite is generally present with garnet-epidote rocks. An area of 'high' magnetite is shown in sections 9315 and 9715. Around this 'core' is the association actinolite-epidote which changes downward to a garnet-bearing assemblage.

Discussion of the Skarn Assemblages

Craigmont skarn assemblages show simplicity and regularity. The following associations represent nearly all of the rocks at Craigmont: (1) garnet-epidote-actinolite; (2) actinolite-epidote-chlorite; (3) garnet-diopside-calcite; and (4) garnet-actinolite-diopside. These are shown in an ACF diagram (Figure 21, B) and are compared with ACF diagrams for the albite-epidote-hornfels and the hornblende-hornfels facies (Figure 21, A and C).

Chemical analyses of bulk samples representing the

garnet-epidote-actinolite and actinolite-epidote associations are given in Table 8. Analysis of a bulk sample of marble with argillaceous bands is also given (Table 8). These analyses when plotted on the ACF diagram fall within their expected areas of the diagram. This is shown in Figure 22. Argillaceous marble is plotted in the calcareous corner of the diagram.

It is significant that these associations can be shown on an ACF diagram. Such regularity and simplicity of a metamorphic assemblage suggests that the assemblage may be in equilibrium. Turner and Verhoogen (1960) discuss equilibrium associations and metamorphic facies. A brief summary is presented here. The following conditions must be considered: (1) some or all of the assemblages are commonly associated in space and time; (2) mineral composition of each assemblage is strictly a function of the bulk chemical composition as it now exists; (3) total number of essential mineral phases is relatively small; and (4) there is no textural or other evidence of mutual replacement by minerals of the same facies. These conditions are met in the Craigmont rocks by the following: (1) assemblages occur in a contact aureole; (2) chemical composition when plotted on an ACF diagram agrees with the mineralogical composition; (3) the total number of essential phases is small (usually three or four); and (4) essential minerals do not replace each other. As the above conditions are met, it is suggested

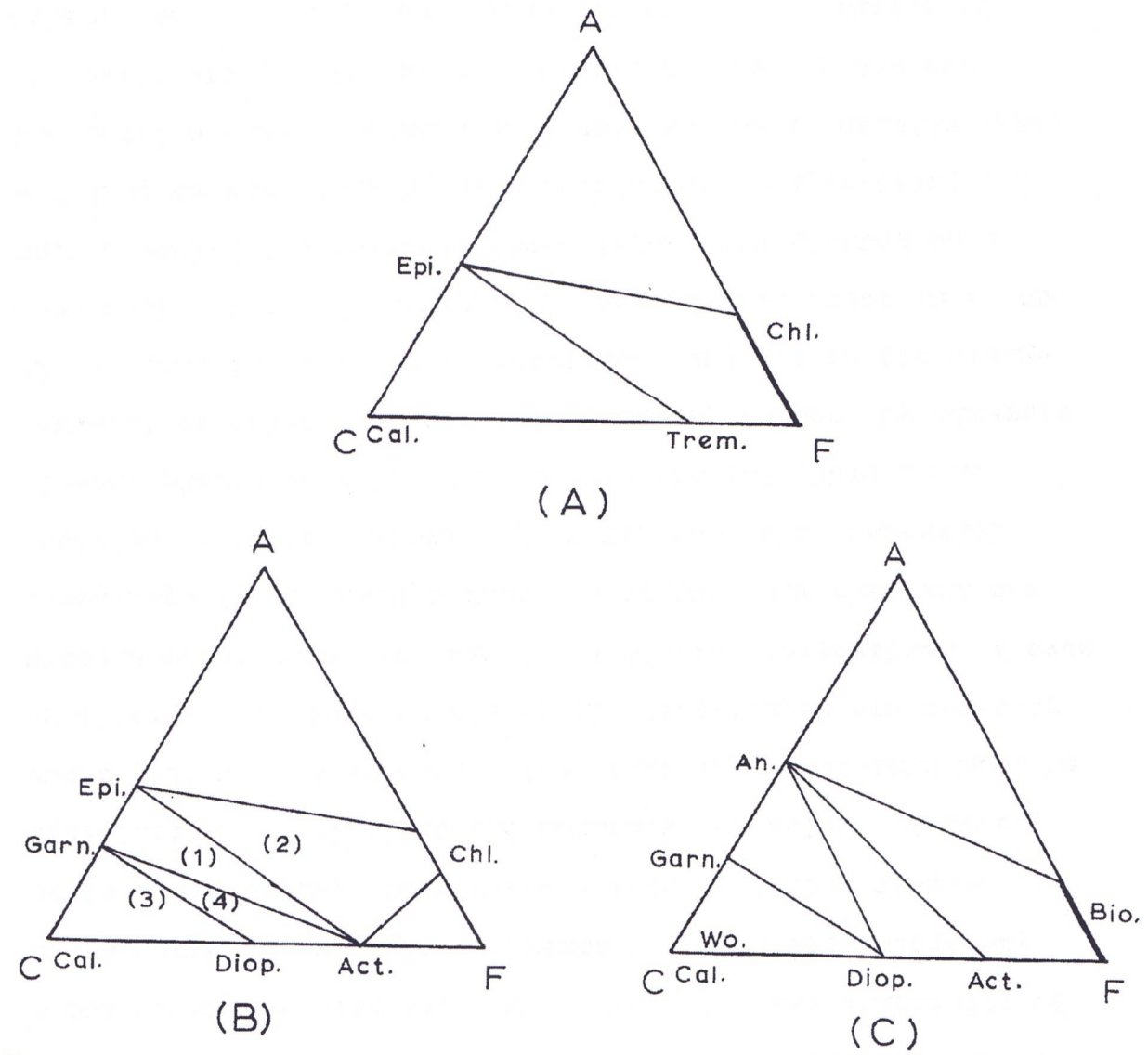

Figure 21: Diagrams showing mineral assemblages;
A. ACF diagram of the albite-epidote-hornfels facies, excess SiO_2, (After Fyfe, Turner and Verhoogen (1958) Figure 83, p. 204).
B. ACF diagram of the Craigmont skarn rocks, excess SiO_2, (for numbers, see text).
C. ACF diagram of the hornblende-hornfels facies, excess SiO_2 and K_2O, (After Fyfe, Turner and Verhoogen (1958) Figure 85, p. 206.

Table 8

Chemical Analyses Of Skarn Rocks and Impure Limestone

	A	B	C
SiO_2	16.56	35.66	41.32
TiO_2	0.16	0.18	0.41
Al_2O_3	3.49	4.09	7.16
Fe_2O_3	1.33	19.58	13.51
FeO	1.28	20.06	3.08
MnO	0.13	0.13	0.41
MgO	1.49	6.00	1.76
CaO	43.30	8.96	28.58
Na_2O	0.22	0.17	0.27
K_2O	0.42	0.35	0.07
P_2O_5	0.10	0.20	0.18
CO_2	30.59	1.25	2.41
H_2O+	0.04	0.03	0.13
H_2O-	0.71	1.20	0.78
S	-	1.92	-
Total	100.07	99.78	99.82

A. Impure marble, bulk sample, 663-153.
B. Actinolite-epidote skarn, bulk sample, 663-151.
C. Garnet-epidote-actinolite skarn, bulk sample, 663-149.
Analyses by E. Waren.

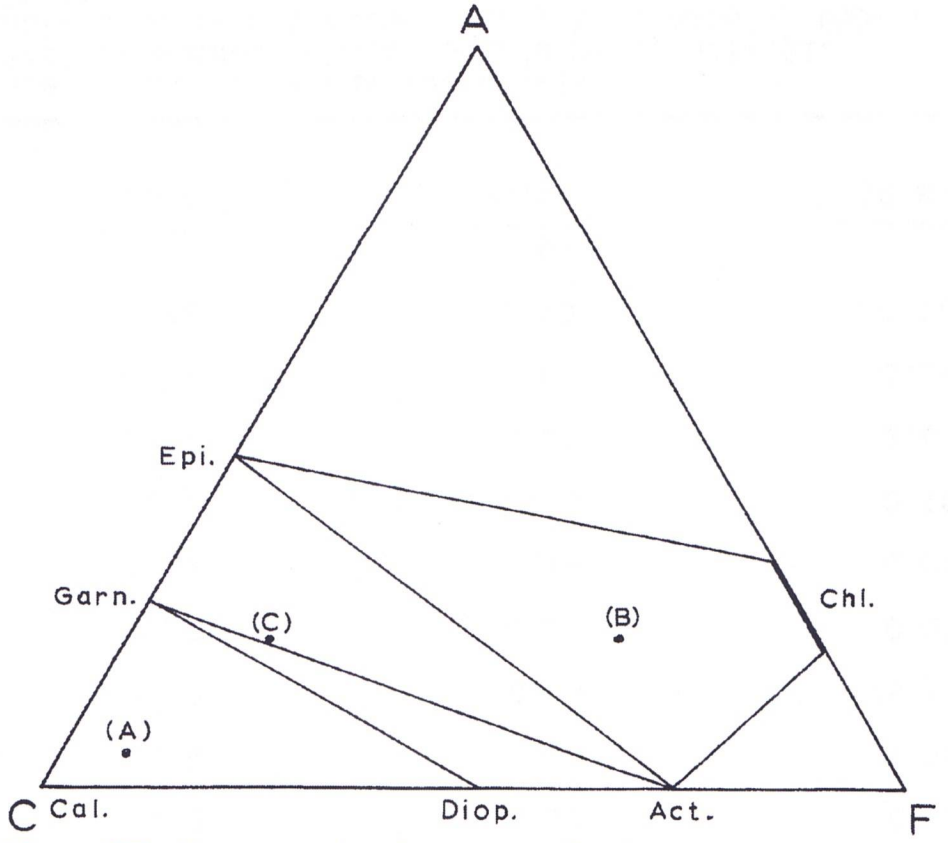

Figure 22: ACF diagram showing correlation between mineralogical and bulk composition for actinolite-epidote skarn (B) and garnet-epidote-actinolite skarn (C). Impure marble plots at (A).

that the skarn associations are equilibrium assemblages.

In cases of isochemical thermal or regional metamorphism, the plotted position of the unmetamorphosed rock on an ACF diagram would indicate the mineral phases to be expected during progressive metamorphism of that initial material. In the case of the Craigmont rocks, the shift in the plotted position of the various associations from the plotted position of the presumed initial material, that is, the impure argillaceous limestone, indicates that the resultant rocks are a product of allochemical thermal metamorphism or of Fe, Mg, and Si metasomatism. Comparison of analyses for impure limestone and actinolite-epidote skarn (A and B on Table 8) show that Si, Fe, Mg, and S were added to the limestone with a resultant loss in CaO and CO_2. This shift could be explained by isochemical metamorphism if the original rocks were of differing bulk compositions. However, this is unlikely as iron formation or iron-magnesium rich rocks are not found in the surrounding area which is composed predominantly of arenites, wackes, impure limestone and minor volcanic rocks.

The metamorphic environment under which these skarn assemblages formed is suggested by comparison with equilibrium associations from calcareous rocks in the albite-epidote- and hornblende-hornfels facies (Figure 21, A and C). Hornblende-hornfels facies is distinguished from the albite-epidote-hornfels facies by the presence of diopside- and grossularite-

bearing assemblages in calcareous rocks (Turner and Verhoogen (1960) p. 513). Presence of grossularite-andradite garnet and diopside in the Craigmont skarn rocks suggests that the pressure and temperature conditions were those of the hornblende-hornfels facies.

Lower limit of the hornblende-hornfels facies is considered by Ramberg (1952) p. 150 "to be the lowermost stability border of diopside in calcite". The following reaction is considered critical:

$$\underset{\text{tremolite}}{Ca_2Mg_5Si_8O_{22}(OH)_2} + 2SiO_2 + 3CaCO_3 = 5CaMgSi_2O_6 + 3CO_2 + H_2O.$$
$$\text{quartz} \quad \text{calcite} \quad \text{diopside}$$

The presence of diopside, even in minor amounts, suggests that pressure-temperature conditions were either transitional to or within the hornblende-hornfels facies.

Turner and Verhoogen (1960) correlate the hornblende-hornfels facies with temperatures of about 550-700 C in a pressure range of P_{H_2O} between 1000-3000 bars but "at water pressures about 500 bars, temperatures would be perhaps 50 C lower" (p. 520). This temperature may be somewhat high. The reaction of calcite and quartz to give wollastonite and carbon dioxide has been investigated by Goldschmidt (1912) and revised by Danielsson (1950). According to Danielsson, the temperature of wollastonite formation at P_{CO_2} = 1 atm. is about 300 C (Figure 23). Barth (1962) shows that if carbon dioxide escapes, the temperature of wollastonite formation will decrease with increasing pressure (Figure 23, curve C).

At Craigmont, calcite and quartz are everywhere present in contact with each other and interstitial to lime silicates (Plate 4, page 55 and Plate 7, page 60). Wollastonite is nowhere present. This indicates that P_{CO_2} could lie somewhere between $P_{CO_2} = 0$ and $P_{CO_2} = P_T$ in a system that is open to carbon dioxide. Thus, the absence of wollastonite would tend to indicate relatively low temperatures during skarn formation.

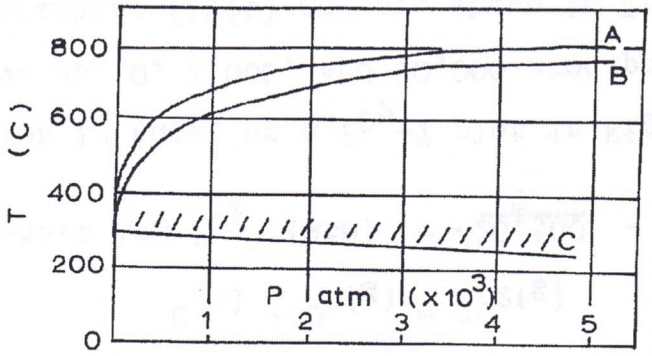

Figure 23: Pressure-temperature curve for reaction $CaCO_3 + SiO_2 = CaSiO_3 + CO_2$. (A. curve of Goldschmidt (1912); B. curve of Danielsson (1950); C. curve for wollastonite formation when system is open to CO_2, conditions will probably lie in the hatched area close to curve C).

Genesis of the Skarn Rocks

Skarn assemblages at Craigmont show that the original limestone horizon has undergone Fe, Mg, and Si metasomatism. The vapor phase in equilibrium with the skarn rocks would contain H_2O, CO_2, CO, O_2, S_2, HCl, etc. A discussion of the components of the vapor phase follows.

During contact metamorphism of lime-rich rocks, a system may be open to both water and carbon dioxide. At Craigmont, both components were present since calcite and hydrous silicate phases are found in all assemblages. The partial pressure of carbon dioxide could have remained relatively high throughout the development of the skarn.

Grey impure limestone on Promontory Hill, two miles west of the mine, contains organic material. If the composition of the limestone does not change drastically, there could have been some graphite in the original limestone in the mine area. Graphite is not now observed at the mine which suggests that the graphite must have been oxidized to carbon dioxide. The reaction is

$$C_{(c)} + O_{2(g)} = CO_{2(g)}$$

$$\text{where } \log P_{O_2} \text{ (atm)} = \frac{-20,500}{T} - 0.04.$$

This reaction is shown on a P_{O_2}-T plot in Figure 24. Position of the curve at 10, 1,000, and 10,000 atmospheres P_{CO_2} are given by Miyashiro (1964) and are shown in Figure 24 to indicate the effect of increased P_{CO_2}. The reactions $2C + O_2 = 2CO$ and $2CO + O_2 = 2CO_2$ are also shown in Figure 24. The magnetite-hematite reaction $4Fe_3O_4 + O_2 = 6Fe_2O_3$

$$\text{where } \log P_{O_2} \text{ (atm)} = \frac{-24,914}{T} - 14.400$$

is shown in the same figure. Any original graphite would control the partial pressure of oxygen by the reaction of carbon + oxygen = carbon dioxide and/or carbon + oxygen =

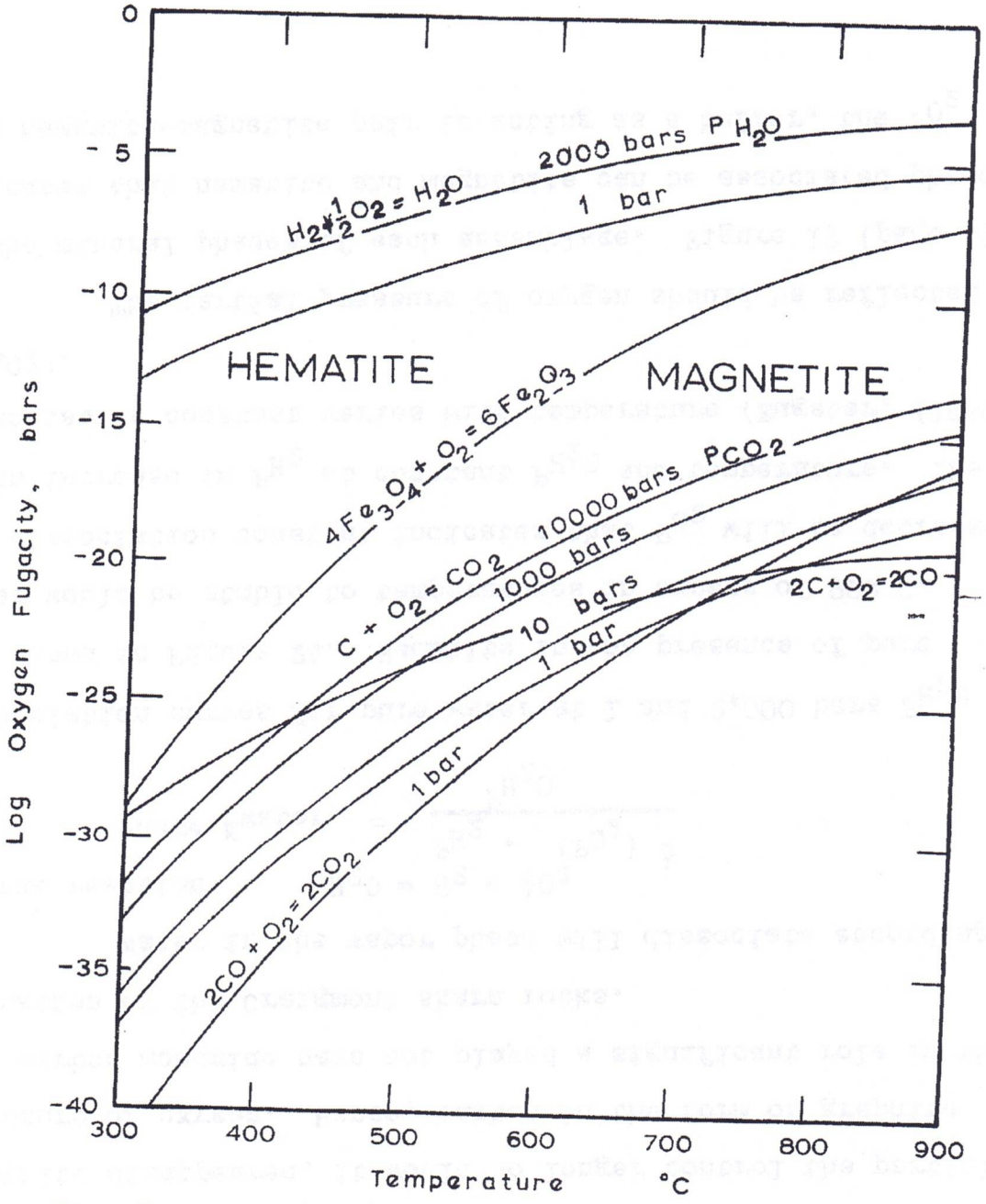

Figure 24: Log oxygen fugacity - temperature diagram showing hematite-magnetite stability fields with respect to water dissociation and oxidation of graphic and carbon monoxide to carbon dioxide. (Data compiled from Miyashiro (1964), Eugester (1959), Ward (1962), and Latimer (1952).

carbon monoxide. Ferric iron in the presence of graphite would tend to be reduced. Similarly, the partial pressure of oxygen in equilibrium with the reaction carbon monoxide + oxygen = carbon dioxide would tend to reduce ferric iron. However, the skarn assemblages contain both ferric iron-gearing silicates and oxides. Any graphite originally present must have been oxidized to carbon dioxide. Once graphite disappeared, it would no longer control the partial pressure of oxygen. Hence, carbon in the form of graphite and carbon monoxide have not played a significant role in the formation of the Craigmont skarn rocks.

Water in the vapor phase will dissociate according to the reaction $H_2O = H_2 + \frac{1}{2}O_2$

where $K_{water} = \dfrac{P_{H_2} \cdot (P_{O_2})^{\frac{1}{2}}}{P_{H_2O}}$

Dissociation curves for pure water at 1 and 2,000 bars P_{H_2O} are shown in Figure 24. Hematite in the presence of pure water would be stable to temperatures in excess of 900 C. The dissociation constant indicates that P_{O_2} will be decreased by an increase in P_{H_2} at constant P_{H_2O} and temperature. The dissociation constant varies with temperature (Eugster, (1959) p. 407).

The partial pressure of oxygen should be reflected in the mineral phases of each assemblage. Figure 19 (page 69) indicates that hematite and magnetite can be associated phases. If a hematite-magnetite pair is acting as a buffer, the P_{O_2}

in equilibrium must be in the order of 10^{-23} atmospheres at 400 C (Figure 24). This indicates that the hematite-magnetite reaction defines the P_{O_2} in rocks which contain both of these oxides in equilibrium with the gas. The magnitude of P_{O_2} will have an upper limit at 400 C if magnetite is the only phase in the rock. Similarly, P_{O_2} will have a lower limit in hematite-bearing rocks at the same temperature.

Eugster and Wones (1962) have outlined three possible cases in examining the magnitude of P_{O_2}. According to these authors (p. 115), P_{O_2} is either (1) internally defined and buffered, (2) internally defined and unbuffered, or (3) internally undefined. The assemblages of garnet-hematite and actinolite-magnetite would be examples of case 2, that is, the assemblage is not buffered but is defined in terms of P_{O_2}. Garnet-hematite indicates that P_{O_2} is within the stability field of hematite while actinolite-magnetite indicates the magnetic field. Between these assemblages is the association garnet-epidote-actinolite-hematite-magnetite which suggests that the assemblage is buffered and that P_{O_2} is defined. The three above mentioned assemblages indicate three conditions of P_{O_2} but the departure of P_{O_2} from that of the buffered assemblage may not necessarily be great.

Comparison of the associations garnet-epidote-hematite and actinolite-epidote-magnetite show the importance of P_{O_2}. A reaction of the following type appears to best illustrate the system:

$$2Ca_3(Al,Fe)Si_3O_{12} + 4Fe_2O_3 + Ca_2(Al_2Fe)Si_3O_{12}(OH) + 3H_2O +$$
(garnet) (hematite) (epidote)

$$21SiO_2 + 2CaO + 9MgO =$$

$$3Ca_2(Mg_3Fe_2)Si_8O_{22}(OH)_2 + Fe_3O_4 + 2Ca_2(Al_2Fe)Si_3O_{12}(OH) + \frac{3}{2}O_2.$$
(actinolite) (magnetite) (epidote)

Garnet composition is that for assemblages with only associated hematite (Figure 13, page 45). Composition of actinolite and epidote is taken from Figure 6 (page 40) and 10 (page 43). The above reaction indicates that epidote may be a stable phase on both sides of a reaction in which one side may be characterized by P_{O_2} in the hematite field and the other side, by P_{O_2} in the magnetite field. A possible mechanism for dehydration by oxidation at constant temperature and water pressure is suggested by the reaction. This mechanism is illustrated in Figure 25. Differences in bulk composition between the assemblages can be caused by the composition of the metasomatic fluid. The above reaction also suggests that rocks formed under the same conditions of temperature and total pressure can have differing mineralogical and bulk compositions depending on the magnitude of P_{O_2} in equilibrium with a particular assemblage.

A relationship between composition of the fluid and P_{O_2} is indicated. If P_{O_2} is within the hematite field, introduced iron will be fixed in the ferric state in garnet and hematite; if P_{O_2} is within the magnetite field, iron will be fixed as ferrous in actinolite and magnetite. Magnesium

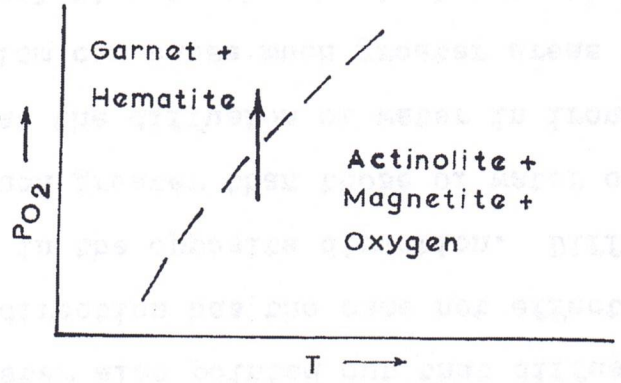

Figure 25: Diagram illustrating dehydration mechanism by increasing P_{O_2}, at constant P_{H_2O} and temperature.

followed ferrous iron and is fixed in actinolite. Silica has been introduced in excess, as quartz is present in all assemblages. Aluminum is present in all rocks but its mobility is unknown as the aluminum content of the original limestone could have ranged between wide limits. The ACF diagram (Figure 22) showed that Al_2O_3 content is similar for the garnet-epidote-actinolite and actinolite-epidote assemblages.

The MgO/FeO ratio in actinolite should vary under differing P_{O_2} conditions, if the temperature, P_{H_2O}, and P_{CO_2} are held constant. However, actinolite composition does not vary, that is, the MgO/FeO ratio is fairly constant regardless of associated silicate or iron oxide phase. If the MgO/FeO ratio in actinolite in the garnet-epidote-actinolite-hematite-

magnetite assemblage, a hematite-magnetite buffer would not explain the consistent actinolite composition between these two assemblages because each assemblage could be at a different partial pressure of oxygen. A similar argument would hold for the consistency of the epidote composition.

According to Wones and Eugster (1959), if a metamorphic system is permeated by a vapor phase, this should tend to bring all units to the same partial pressure of oxygen. In regional metamorphic terrains, adjacent assemblages may define differing partial pressures of oxygen if the system is closed to oxygen (James (1955), Chinner (1960), Miyashiro (1964)). Existence of distinct but closely associated hematite and magnetite layers indicate an absence of vapor phase in the system. Eugster (1959) mentioned that hematite and magnetite appear to coexist in a definite zone between hematite-chert and magnetite-chert bands. According to Eugster (p. 422), "this region which can be inches to feet wide, indicates exchange of oxygen during metamorphism, probably sparked by the presence of water (diffusion of hydrogen)". Eugster also pointed out that diffusion of hydrogen in one direction has the same net effect as diffusion of oxygen in the opposite direction. Diffusion rate of hydrogen is much greater than those of water or oxygen. This suggests that the diffusion of water in iron-rich rocks during metamorphism can cause much greater areas to "be equilibrated in relation to the chemical potential of oxygen"

(Eugster, (1959) p. 411). At Craigmont, the consistency of silicate composition suggests that the area of influence of a hematite-magnetite buffer system could be large if the chemical potential of oxygen approaches uniformity by diffusion in a circulating vapor phase. Thus, the magnitude of P_{O_2} in the vapor phase could be similar for all the skarn assemblages. This is diagrammatically presented in Figure 26. This would explain the consistency of actinolite and epidote composition because the partial pressure of oxygen in equilibrium with these phases would be fairly constant during skarn formation.

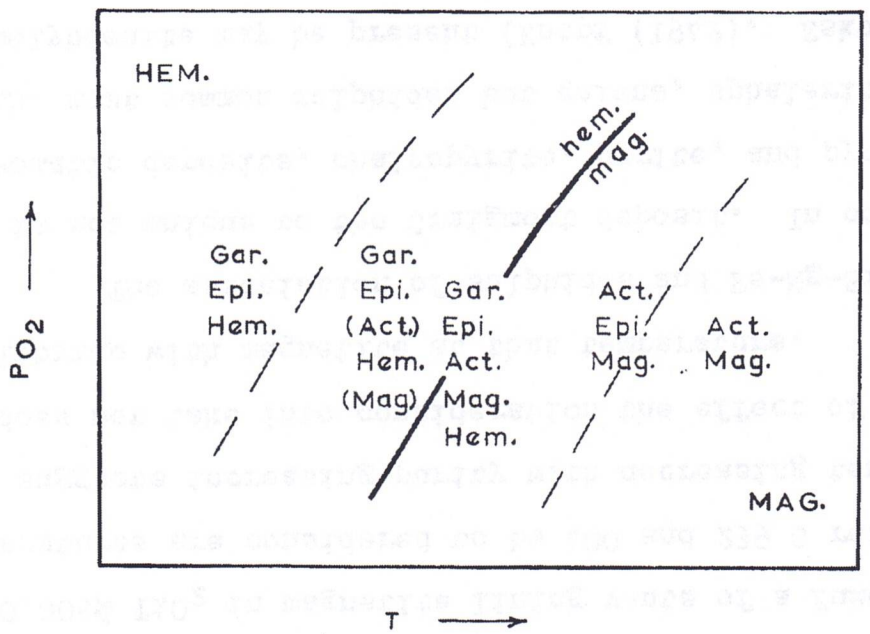

Figure 26: Diagram illustrating the area of influence of a hematite-magnetite buffer system in terms of the Craigmont skarn assemblages.

The purity of magnetite and hematite should be noted. Titanium, absent in the iron oxides, is present in sphene.

This is in agreement with Verhoogen (1962) who stated that magnetite and sphene are more likely at low temperature and high P_{O_2} than the mineral pair, diopside and ilmenite. Abdullah and Atherton (1964) suggested a correlation of TiO_2 content in magnetite and temperature. They report 1.09 to 1.56% TiO_2 in magnetite from the almandine amphibolite facies and 0.005% TiO_2 in magnetite lining vents of a fumerole. Temperatures are considered to be 400 and 239 C respectively. This suggests increasing purity with decreasing temperature but does not take into consideration the effect of P_{O_2} in equilibrium with magnetite at that temperature.

The association of sulphides and Fe-Mg-Si metasomatism is not unique to the Craigmont deposit. In contact metasomatic deposits, chalcopyrite, pyrite, and pyrrhotite are the most common sulphides but galena, sphalerite, bornite, and molybdenite may be present (Knopf (1942). Eskola (1914) describes 'tremolite' skarn rocks associated with chalcopyrite in the Orijarvi region of Finland. Titley (1961) p. 715 found magnesium minerals ("cummingtonite(?) and chlorites") closely associated with lead and zinc sulphides at the Linchburg orebody, New Mexico. Chalcopyrite and magnetite are found in the 'actinolite' zone of the Cornwall, Pennsylvania iron deposit (Hickok (1933)). Actinolite and epidote are associated with magnetite and chalcopyrite at the Pewabic mine, New Mexico (Schmitt (1939)). Reference to other examples is given by Knopf (1933, 1942) and Turner (1948). Lindgren (1905) noted

that "sulphides are not later introductions, but contemporaneous with the other contact minerals". The position of sulphides is generally on the outer or 'limestone side' of the metamorphosed contact rocks (Umpleby (1916)).

Zonation of the silicate assemblages in a thermal aureole is generally related to a decline in temperature outward from the intrusive body. As sulphides form simultaneously with silicates, the same control must also apply to sulphides. At Craigmont, the temperature and total pressure remained constant during skarn formation. Therefore, if the sulphides were deposited with the silicates, the control of sulphide precipitation must be some process other than temperature.

Metallic phases within the actinolite-epidote rocks at Craigmont are magnetite, chalcopyrite, and pyrite. The Cu-Fe-S-O system has been investigated by Gustafson (1963) whose diagram for the high-iron portion of the system is reproduced in Figure 27. Figure 27 indicates that chalcopyrite-magnetite-pyrite may coexist under several values of oxygen and sulphur fugacity (along the line between the two fields, chalcopyrite-pyrite and chalcopyrite-magnetite (point A to B)). This diagram also suggests that the sulphur vapor pressure in equilibrium with magnetite-chalcopyrite-pyrite must be higher than that in equilibrium with the reaction $2FeS + S_2 = 2FeS_2$. Consequently, pyrrhotite is not a stable phase in the Craigmont deposit. Pyrrhotite occurrence is

scarce but in one specimen (663-96) containing pyrrhotite, chalcopyrite, pyrite, and magnetite, the pyrrhotite is replaced by pyrite. This assemblage indicates a lower limit for sulphur and oxygen fugacity in the skarn rocks (see point A in Figure 27). At about 350 C, the magnitude of f_{O_2} and f_{S_2} would be in the order of 10^{-12} and 10^{-35} respectively (Holland (1959) p. 191). If chalcopyrite-magnetite-pyrite control the fugacity of oxygen and sulphur in the depositing medium, then the bornite field would not be reached (Figure 27). Thus, the presence of abundant bornite would not be expected.

Control of sulphide deposition is essentially the same as that for the silicate minerals. The partial pressure of sulphur and oxygen in the vapor phase in equilibrium with the skarn rocks would control the deposition of the sulphide phases. As a consequence, bornite and pyrrhotite are scarce while chalcopyrite and pyrite are abundant. In an environment of high iron and low copper, ferrous iron would be present in excess of that which can be accommodated by actinolite. Thus, the excess ferrous iron would be taken up by magnetite and chalcopyrite.

Potassium Feldspar-Specularite Veins

Specularite veins are found throughout the contact aureole. Presence of K-feldspar has been plotted on overlays for geological sections (in pocket). From these sections,

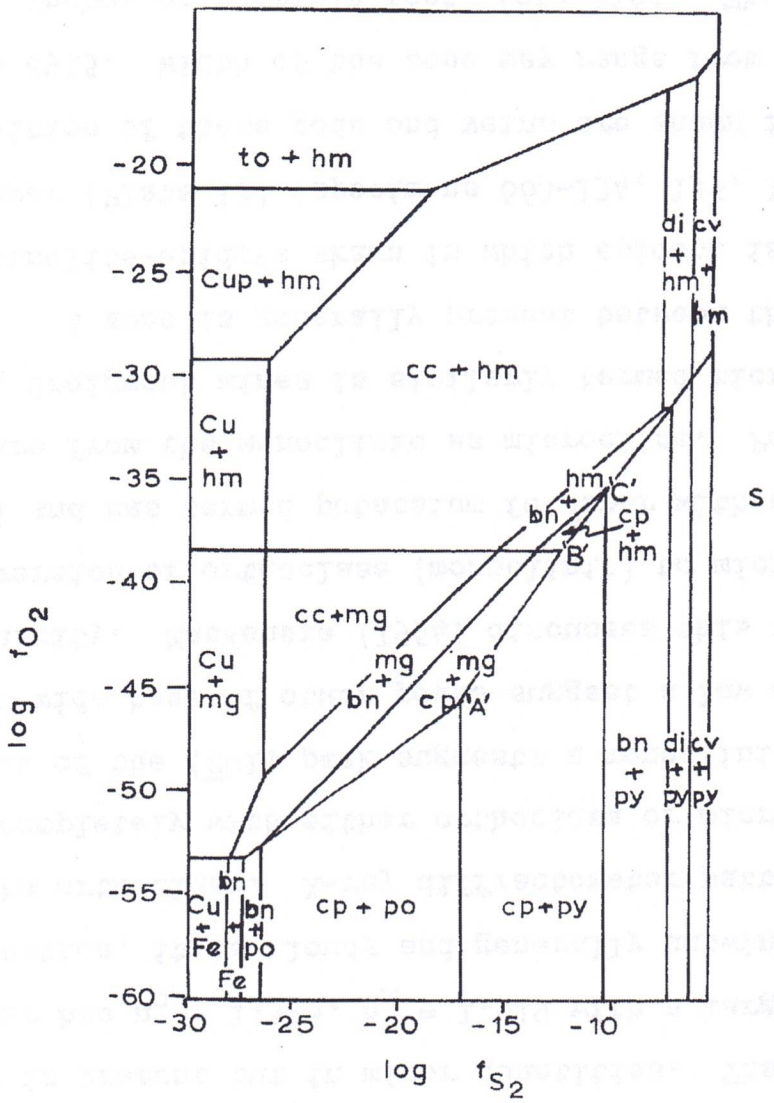

Figure 27: Phase relations in the high-iron portion of the Cu-Fe-S-O system at 200 C and low pressure; $0 < Cu/(Cu + Fe) < \frac{1}{2}$. After Gustafson (1963) p. 671. Abbreviations are as follows: bn-bornite, cc-chalcocite, cp-chalcopyrite, Cu-copper, cup-cuprite, cv-covellite, di-digenite, Fe-iron, hm-hematite, mg-magnetite, po-pyrrhotite, py-pyrite, S-sulphur.

K-feldspar-specularite veins are seen to be imposed not only upon the skarn rocks but also upon the adjacent wall rocks.

Veins in Skarn Rocks

Skarn assemblages have been veined and locally altered. Veins and irregular pods contain the following phases: K-feldspar, quartz, calcite, chlorite, hematite, (magnetite), and chalcopyrite. Brackets indicate that magnetite is present but in minor quantities. The salmon pink feldspar has $n_z = 1.525$, $n_x = 1.519$ with a large $2V_x$. In thin section, it is cloudy and generally untwinned which suggests orthoclase. X-ray diffractometer patterns do not agree completely with either orthoclase or microcline. The position of the $(\bar{2}01)$ peak suggests a monoclinic feldspar but the wide base of other peaks suggest a low degree of triclinicity. MacKenzie (1954) discusses this variation in the inversion of orthoclase (monoclinic) to microcline (triclinic) and has termed potassium feldspar with a low triclinic departure from the monoclinic as microcline. Potassium feldspar at Craigmont mines is similarly termed microcline.

A zone is generally present between the vein and the actinolite-epidote skarn in which epidote is replaced by K-feldspar (Plate 13) (specimens 663-134, 135, 136, 137). The position of these pods and veins are shown in geological section 8915. Width of the zone may range from 3 mm. to several inches or possibly feet, (663-136). The zonal arrangement is diagrammatically summarized in Figure 28.

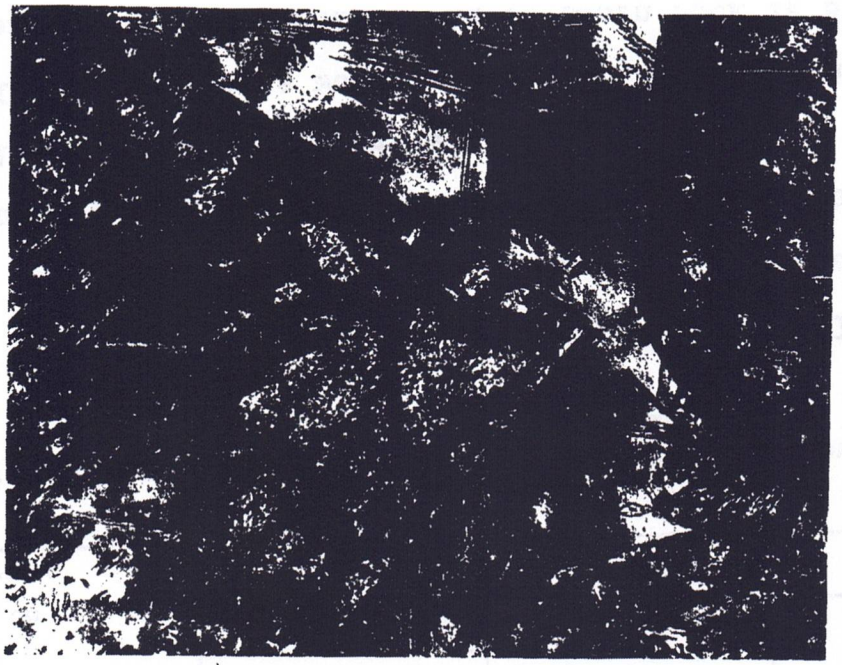

Plate 13 Photomicrograph showing potassium feldspar replacement of epidote crystals. Plain light. (Specimen 663-134).

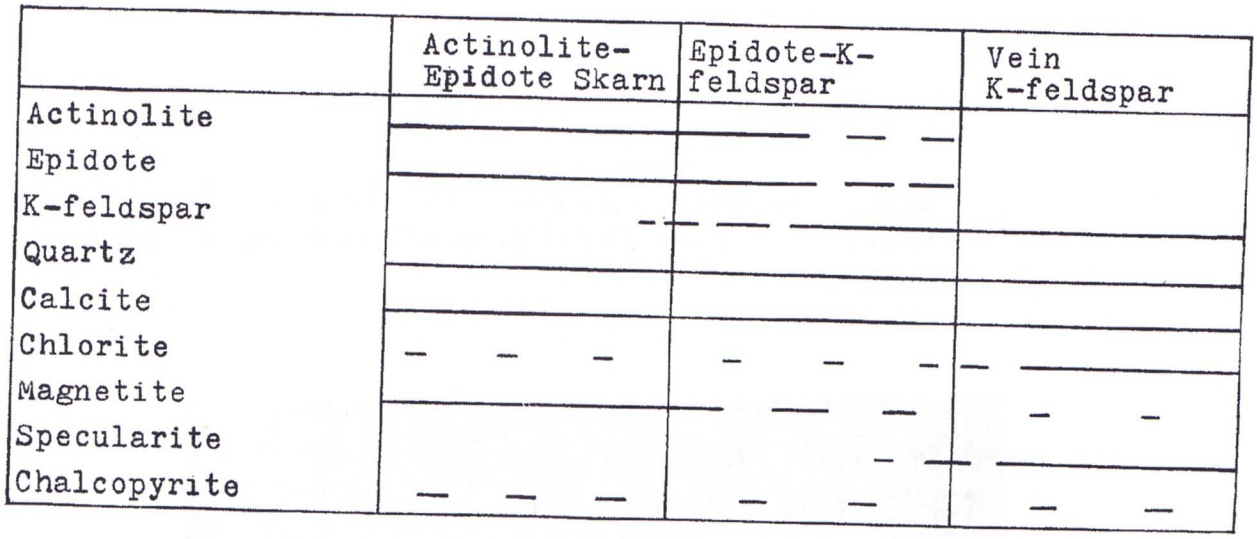

Figure 28: Diagrammatic representation of zoning about an irregular potassium feldspar-rich vein.

A chemical analysis of a sample from a K-feldspar rich area is given in Table 9, B. This sample included platy magnetite and some actinolite-epidote skarn so the Fe_2O_3 would be lower and FeO + MgO would be higher if only hematite-K-feldspar veins were represented. For comparison, the analysis of the actinolite-epidote skarn rock is shown. The analysis does show the notable increase in K_2O, Al_2O_3 and SiO_2.

In some veins, platy magnetite is found rather than hematite. The K-feldspar-specularite veins have the same mineralogy as the K-feldspar-specularite veins in the adjacent non skarn wall rocks. This suggests that the two assemblages are related to the same stage of veining and that chemical

Table 9

Chemical Analysis of Actinolite-Epidote and K-feldspar Altered Skarn Rocks

	A	B
SiO_2	35.66	45.54
TiO_2	0.18	0.20
Al_2O_3	4.09	9.05
Fe_2O_3	19.58	8.45
FeO	20.06	13.50
MnO	0.13	0.13
MgO	6.00	4.79
CaO	8.96	6.40
Na_2O	0.17	0.24
K_2O	0.35	5.40
P_2O_5	0.20	0.21
CO_2	1.25	1.74
H_2O+	0.03	0.09
H_2O-	1.20	1.02
S	1.92	3.00
Total	99.78	99.76

A. Actinolite-Epidote Skarn, Composite Sample (663-151).
B. K-feldspar Alteration of Actinolite-Epidote Skarn, Composite Sample (663-150).
Analyses by E. Waren.

variations have occurred in the veins at one place and not at another.

Association of actinolite and K-feldspar without epidote is found in specimen 663-138. Thin bands of aligned actinolite crystals with interstitial K-feldspar-calcite-quartz-apatite-sphene-magnetite are cut by a 3 mm. wide vein of coarse-grained K-feldspar, in the core of which is calcite-quartz-sphene-magnetite (663-138).

Veins Within the Hornfelsic Wall Rocks

These veins are generally thin, sharply defined, and show a definite cross-cutting relationship to the host rock. The most common assemblage contains K-feldspar, quartz, calcite, chlorite, tourmaline, specularite and chalcopyrite. The sharpness of a 2-3 mm. wide K-feldspar-quartz-calcite-(chlorite)-specularite-chalcopyrite vein which cuts a meta-andesite is shown in specimen 663-140. In the same specimen (663-140), separate veinlets of K-feldspar-quartz and K-feldspar-quartz-specularite-chalcopyrite are intersected by a massive specularite-chalcopyrite vein without K-feldspar. This suggests that several periods of movement have occurred and that K-feldspar-bearing veins are of an earlier age than specularite-chalcopyrite veins.

Specularite-rich 'Brecciated' Area

An assemblage of specularite, chalcopyrite, calcite, quartz, chlorite, and tourmaline with or without K-feldspar is found as veins and as a matrix in brecciated rock (see

geological sections and overlays for 8515 and 8115, above the 3500 level). Specimen 663-141 shows fragments of quartzfeldspathic hornfels surrounded and veined by specularite-chalcopyrite-quartz-calcite-tourmaline-(chlorite). Another brecciated rock has a similar matrix but contains K-feldspar (663-142).

An abrupt change in the size of the specularite crystals occurs in specimen 663-144. A thin section shows that the finer grained portion contains the assemblage K-feldspar-quartz-chlorite-tourmaline-specularite-chalcopyrite and that the coarser portion contains chlorite-calcite-tourmaline-specularite-chalcopyrite. This assemblage is the same as that composing the matrix of the breccia but the small fragments were not observed. The variation in the size of the specularite plates away from the coarse-grained part is given in Table 10.

Table 10

Variation In Specularite Plate Size

'Vein'		Distance From 'Vein' 0.4 cm.	1 cm.	1.75 cm.
All sizes present. Max. 5 mm. Min. 0.1 mm. (length) (Many bent plates)	Maximum Size			
	Length	1.5 mm.	0.7 mm.	0.3 mm.
	Width	0.25 mm.	0.25 mm.	0.05 mm.
	Average Size			
	Length	0.4 mm.	0.35 mm.	0.2 mm.
	Width	0.05 mm.	0.05 mm.	0.05 mm.

Specimen 663-144. (See text for explanation)

A similar texture to that noted in thin section can be observed in hand specimen. Laminated appearing rocks with

bands of fine-grained specularite-chalcopyrite-chlorite-quartz alternate with bands of coarser specularite-chalcopyrite-chlorite-quartz which contains broken pinkish and grey rock fragments (specimen 663-145). Adjacent to this fine-grained banded core, coarse specularite and chalcopyrite blebs occur with blocks (up to 4 inches across) of coarsely crystalline calcite (663-146).

The above texture suggests that there is some replacement of the fragments by specularite after or during deposition of hematite and chalcopyrite in the breccia matrix. Crystal size would then depend on the distance from the original fragment edge.

Relation of Platy Magnetite and Specularite

Textural evidence on the development of platy magnetite suggests two possibilities: (1) magnetite replaces specularite plates; and (2) magnetite crystals developed on specularite with their octahedral surface parallel to the basal plane of specularite. Evidence is presented in the form of several photomicrographs. Chemical significance of platy magnetite will be discussed later.

Magnetite pseudomorphous after specularite is suggested in Plate 14. An individual originally continuous specularite plate within chalcopyrite shows magnetite in the central portion of the plate. Plate 15 shows irregular laths of specularite within magnetite. Plate 16 shows the same

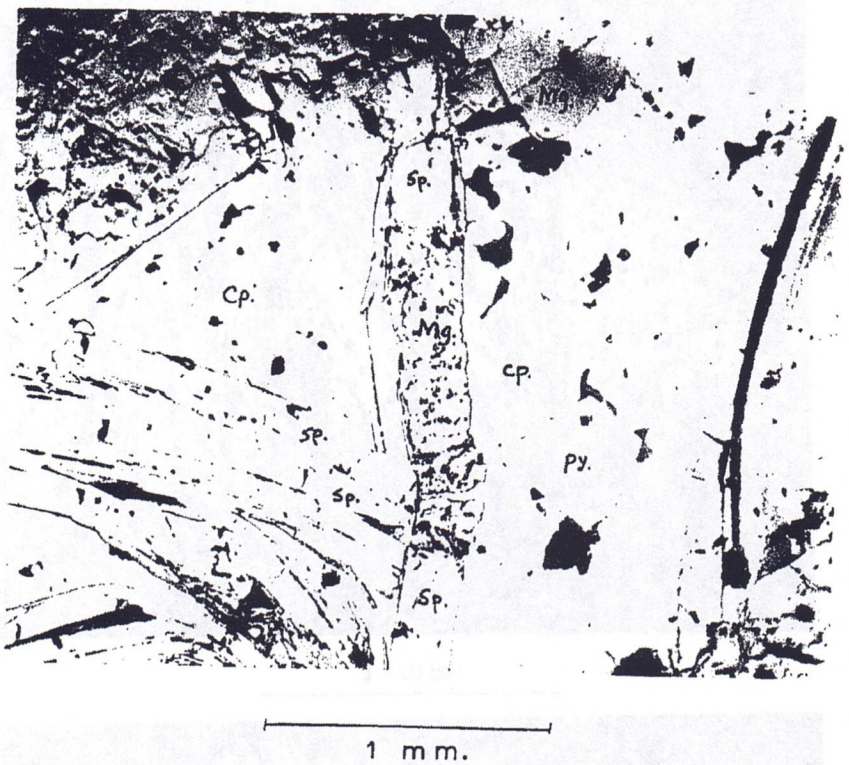

Plate 14 Photomicrograph showing partial replacement of a specularite plate. Plain light. (Specimen 663-112).

1 mm.

1 mm.

Plate 15 Photomicrograph of specularite replace by magnetite. (Whiter color is specularite). Plain light. (Specimen 663-113).

Plate 16 Photomicrograph of magnetite showing specularite habit. Plain light. (Specimen 663-109).

platy habit but only minute specks of specularite remain in a field of magnetite. The thin outline of the original specularite plates can be seen. This suggests that a replacement mechanism could produce some apparently thick magnetite plates. Under crossed nicols, these thick plates may show many thin parallel aligned plates which originally were specularite.

The thickness of some magnetite plates suggests that some process other than simple replacement has occurred. Specularite habit is micaceous with a high length to width ratio. Some plates of magnetite are very thick by comparison. Development of thick magnetite plates is suggested in Plates 17, 18, and 19. These photomicrographs suggest that magnetite crystals nucleated on the specularite plates, grew and coalesced into a relatively wide rim about a core of specularite. Some replacement of the core has occurred but the thickness is apparently caused by the growth of magnetite rather than by the replacement of specularite in these cases.

Late Veins

Tourmaline-quartz-calcite veins without K-feldspar, iron oxides or chalcopyrite are found as a matrix to broken hornfelsic sediments (specimen 663-73). Tourmaline is optically negative, uniaxial with $n_o = 1.671 \pm 0.002$ and $n_e = 1.642 \pm 0.002$, $n_o - n_e = 0.029$. Pleochroism is strong with O > E (O is dark bluish green and E is colorless to pale

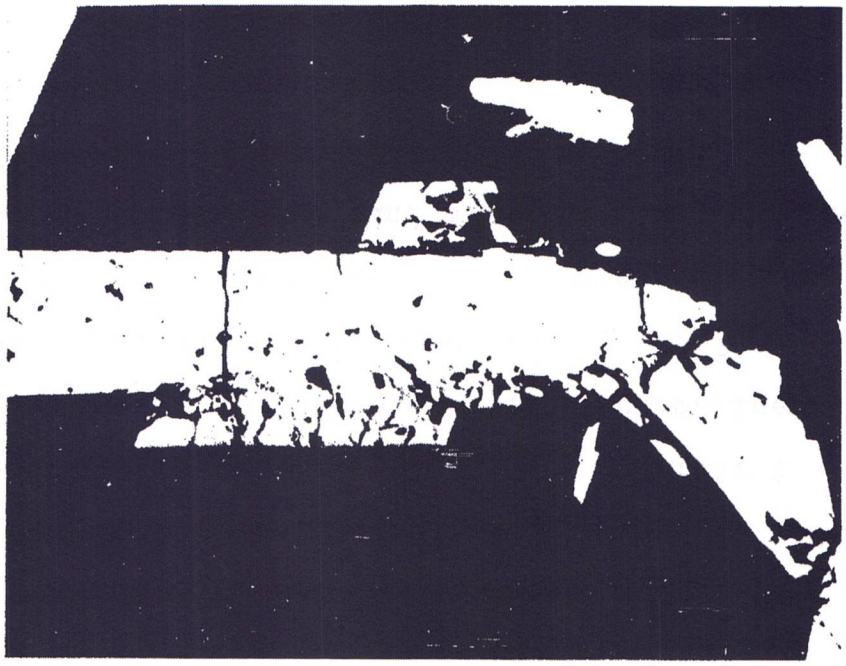

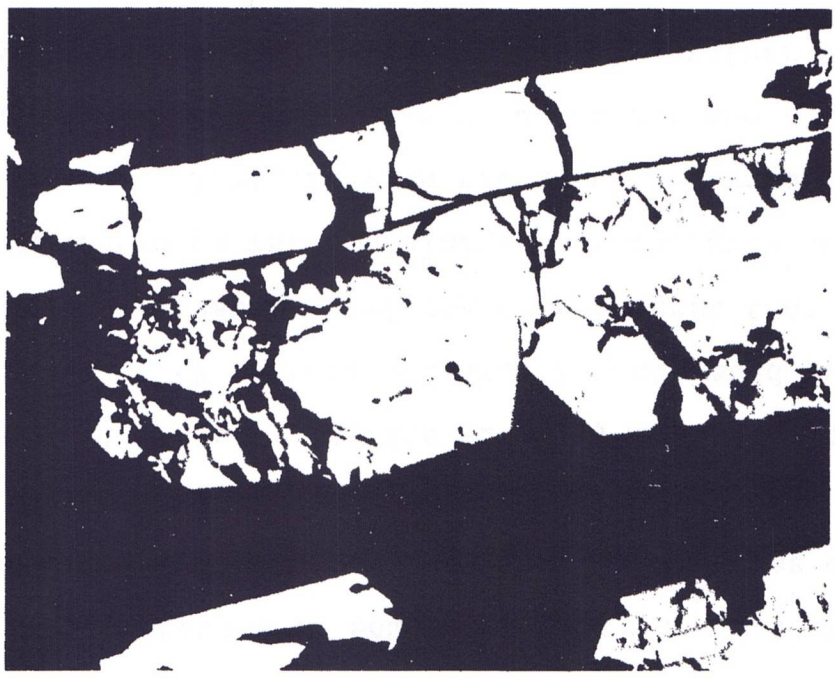

Plate 17 Photomicrograph of euhedral magnetite in contact with a specularite plate. Plain light. (Specimen 663-110).

Plate 18 Photomicrograph of several magnetite crystals in contact with a specularite plate (Note: magnetite replacement of specularite plate). Plain light. (Specimen 663-110).

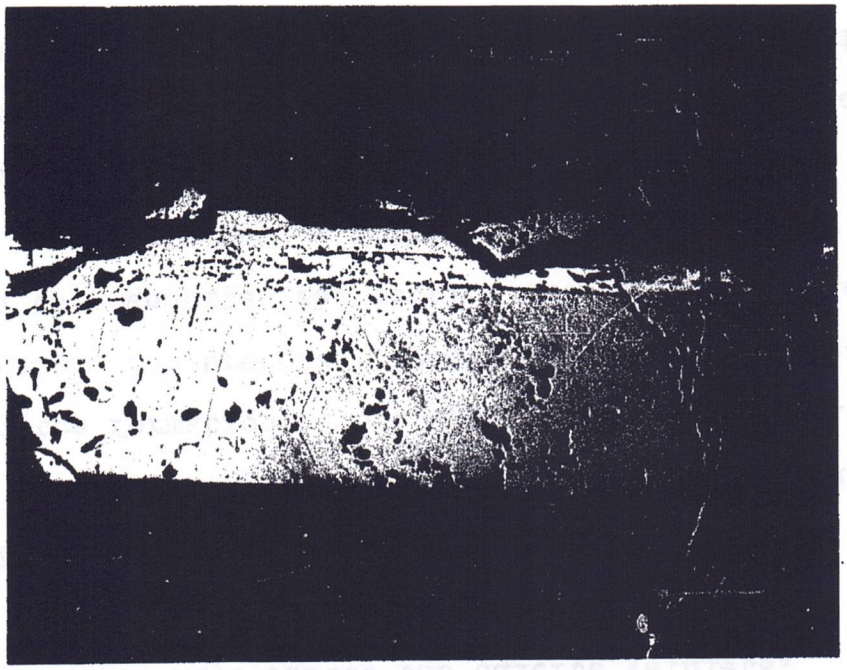

Plate 19 Photomicrograph of large euhedral magnetite crystal around a specularite plate. Plain light. (Specimen 663-100).

yellow). According to Winchell and Winchell (1951) Pt. II, page 468, the mineral is schorlite with about ten percent dravite. The relative age of the tourmaline-bearing veins is not known as they have not been observed to cut other veins. It is assumed that they are related to and possibly later than the K-feldspar-specularite veins.

Late calcite and calcite-quartz veins intersect and offset all previously mentioned veins and rocks. Some late fractures have offset the calcite veinlets.

Chemistry of the Veins

Fracturing of the rocks in the thermal aureole has allowed the formation of specularite and chalcopyrite-bearing pods, veins, and breccia. Specularite in some cases has been reduced to magnetite (see section on relation of platy magnetite to specularite). Within skarns rocks, platy magnetite is found predominantly as veins with, and sometimes without, K-feldspar (663-98, 99, 106, 109). Small crystals of specularite, chalcopyrite, and chlorite are found interstitially to large plates of platy magnetite in specimen 663-155. Platy magnetite crystals are found with thin hematite plates within a calcite vein-like pod in a garnet-epidote-actinolite rock (663-100, 156). Pods of K-feldspar-platy magnetite indicate reduction of ferric iron. Specimen 663-154 shows a platy magnetite vein intersected by a specularite vein which in turn is offset by a calcite vein. The latter example indicates

that at one period in time, hematite was deposited, reduced to form magnetite and at some later period, this reduced hematite was veined by specularite. The above examples reflect changes in the depositing medium of the veins.

The association of hematite and magnetite or the presence of platy magnetite indicates a change of P_{O_2} within the specularite-chalcopyrite vein system. Introduction of potassium into the actinolite-epidote skarn has produced a reaction of the following type:

$$\underset{\text{(epidote)}}{2Ca_2(Al_2Fe)Si_3O_{12}(OH)} + 6SiO_2 + 4CO_2 + H_2O + 4K^+ =$$

$$\underset{\text{(K-feldspar)}}{4KAlSi_3O_8} + \underset{\text{(hematite)}}{Fe_2O_3} + 4CaCO_3 + 4H^+$$

where the equilibrium constant is proportional to the activity ratio of K^+/H^+. Hemley (1959) investigated the K_2O-Al_2O_3-Si_2-H_2O system. He showed that the breakdown of wall rock minerals adjacent to a vein is controlled by the activity ratio of K^+/H^+. In the above reaction, potassium reacts with epidote with the attendant release of hydrogen ions. This reaction does not show reduction of iron, as iron in epidote and hematite is in the ferric state.

Sulphur fugacity in the veins must not be neglected, as chalcopyrite is present. Barnes and Kullerud (1961) p. 678 indicate that changes in pH (or activity in hydrogen ion) at constant oxygen partial pressure can cause changes in the sulphur partial pressure. The relationship of P_{O_2}, pH,

sulphur species, and metallic phases in the Fe-S-O system is presented in Figure 29. Unfortunately, this diagram is at 25 C but the authors (p. 680) show that with increasing temperature, the phase boundaries are shifted to lower pH. At constant P_{O_2}, Figure 29 indicates that at 'lower' pH, $SO_4^=$ is the dominant sulphur species with hematite and that $S^=$ is the sulphur species with magnetite at 'higher' pH. Thus, at constant P_{O_2}, changes in pH would cause changes in P_{S_2} and in the sulphur species present. Partial pressure of sulphur would be increased by lowering the Ph (Figure 29). Control for the reduction of hematite to magnetite in the veins is indicated by the reaction

$$8Fe^{+++} + 8e = 8Fe^{++}$$

$$S^= + 4H_2O = SO_4 = + 8H^+ + 8e$$

$$8Fe^{+++} + S^= + 4H_2O = 8Fe^{++} + SO_4^= + 8H^+$$

Thus, hematite is reduced to magnetite at constant P_{O_2} (P_{O_2} is fixed by the presence of magnetite and hematite) by a lowering of pH through reaction with the wall rock and by and increase in P_{S_2}.

Changes in the hydrogen activity (pH) would not be expected in veins where there is no reaction with the wall rock. In these veins, the assemblage K-feldspar-specularite-chalcopyrite would be stable and would indicate the presence of high K^+/H^+ ratio, high P_{O_2} (relative to hematite associated with magnetite), and P_{S_2} in the veins. Hematite would remain

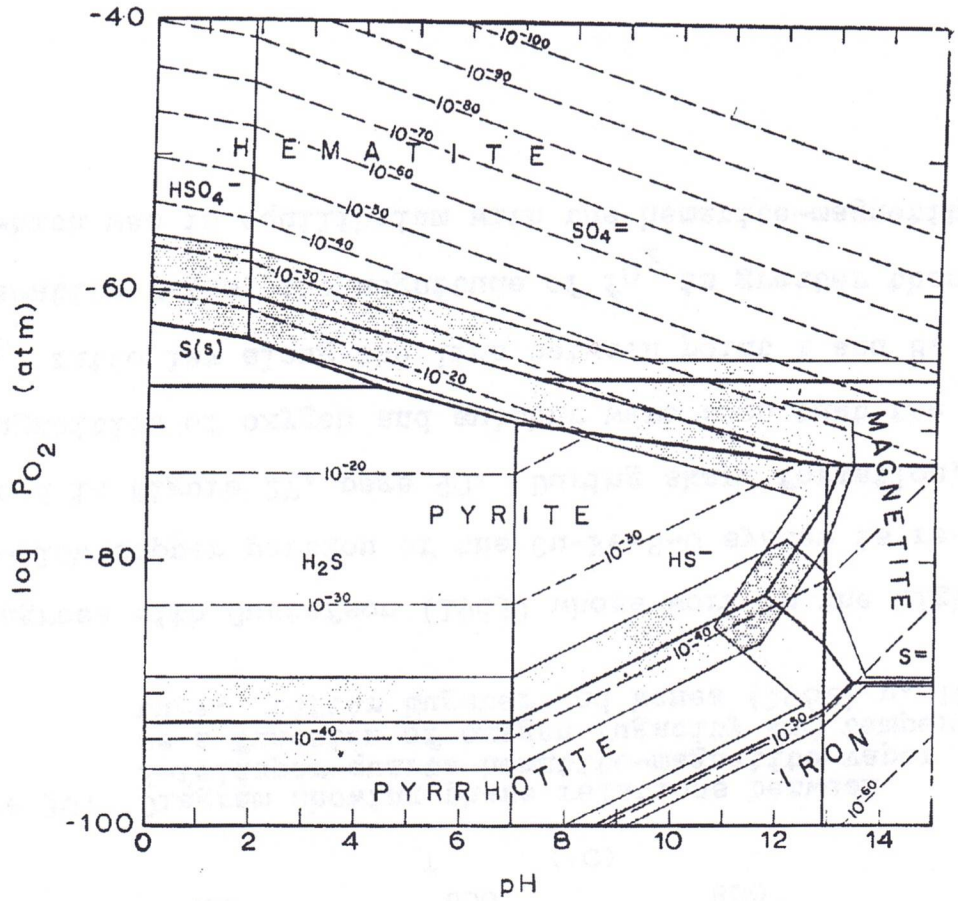

Figure 29: Equilibrium relations between iron oxides, iron sulphides, and aqueous solutions at (ΣS) = 0.001 m and 25 C. After Barnes and Kullerud (1961) p. 677. Dashed lines are contours of P_{S_2} in atmospheres. Heavy lines bound the areas of predominance of each ion or molecule. Shaded zones indicate the uncertainty in the limits to the fields of stabilities of the various minerals.

a stable phase with falling temperature. This is consistent with the work of Eugster and Wones (1962) who found that K-feldspar-quartz-hematite were stable phases at high P_{O_2} and low temperature (see Figure 30).

The vein assemblages platy magnetite-hematite-chalcopyrite and hematite-chalcopyrite suggest an increase in the partial pressure of sulphur over that which was in equilibrium with magnetite-chalcopyrite during skarn formation.

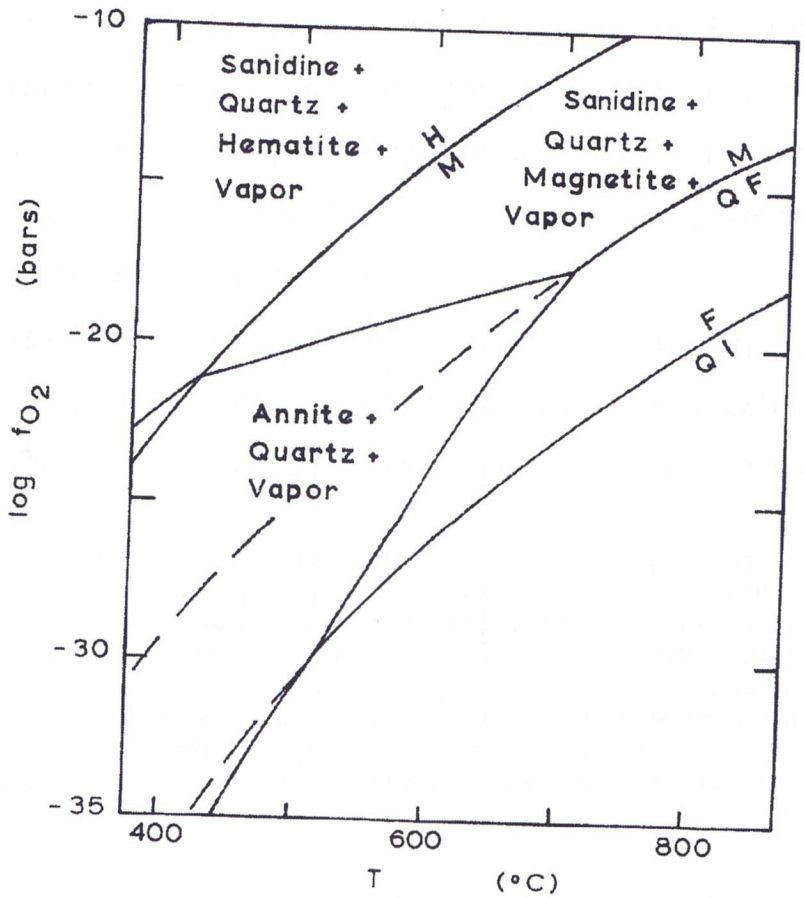

Figure 30: Diagram showing phase relations between K-feldspar-quartz-hematite-magnetite-vapor as a function of oxygen fugacity and temperature. (After Eugster and Wones (1962) p. 105).

This agrees with Gustafson (1963) whose work on the high iron - low copper portion of the Cu-Fe-S-O system is reproduced in Figure 27, page 90. During skarn formation, the fugacities of oxygen and sulphur were such that the f_{O_2}/f_{S_2} ratio lay along the line between point A and B. In the hematite veins, the magnitude of f_{O_2} is greater than that which was in equilibrium with the hematite-magnetite

skarn. This suggests an increase in the partial pressure of oxygen with time. Sulphur partial pressure has also increased with time. In Figure 27, page 90, the assemblage hematite-chalcopyrite indicates that during skarn formation, the f_{O_2}/f_{S_2} ratio has moved along line A-B toward point C. This indicates that chalcopyrite can be a stable phase under conditions of high partial pressure of oxygen.

Secondary Copper Minerals

Exposed on the upper benches of the open pit, an oxidized limonite-stained area contains secondary copper-bearing minerals. Steel blue chalcocite is found with native copper, siderite, and calcite in limonite-stained fractures. Malachite and azurite are present. Chrysocolla and cuprite were identified during the early stages of pit production.

Structure of Craigmont Mine

Introduction

Structural data in the present study is based on geological mapping in the open pit, underground workings, and on correlation of rocks intersected by diamond drilling.

A structural analysis at Craigmont must consider the following limitations. Lithologic correlations from drill holes in the Nicola group in the mine area could be hazardous as the stratigraphic succession is unknown. On

Promontory Hill, two miles west of the mine, the nearest exposed Nicola group rocks were studied by Carr (1960) but he was unable to establish the stratigraphic succession.

An attempt to subdivide the wall rocks has been made. This work was done in conjunction with Mr. W. S. Pentland of the Craigmont mine staff. Correlation of a relatively coarse-grained quartz-bearing metawacke (specimens 663-60, 61, 62, 63) on section 7415 has outlined an antiform structure in the south wall rocks. North and south wall rocks are respectively those rocks found to the north and south of the skarn zone. This relatively distinctive rock has been found on 7715 and 8115 sections. However, elsewhere the subdivision and correlation on either grain-size or rock sequence has been unsuccessful. This is partly a result of a lack of long drill holes into the wall rocks. Consequently, the area investigated is restricted to a relatively narrow zone between the 2400 level and the open pit.

Other limitations to be considered are the following: the lack of a marker horizon in the mine area; the obliteration of the structure in the ore zone through the action of hornfels development and metasomatic replacement; and the lack of outcrop of Nicola rocks outside the open pit area. Cretaceous Kingsvale volcanic rocks completely cover the Nicola rocks in the mine vicinity. All of the limitations outlined above must be considered in any proposed structural interpretation.

Structure

Rennie et al (1961) reports that the following hypotheses have been postulated for the Craigmont structure: (1) a simple calcareous bed of variable thickness has been offset by faulting down dip; (2) a calcareous bed has been folded into an anticline; (3) a calcareous bed has been folded not only into anticlinal but also into a parallel synclinal fold; and (4) there has been large scale drag folding of one calcareous horizon (see drag fold definition below). The present study supports the drag fold hypothesis.

The Craigmont orebody is restricted to an east-west trending, steeply south dipping zone which approximately parallels the Guichon diorite contact. Within this zone, the configuration of those areas in which skarn and marble occurs, is suggestive of a drag fold (see geological sections and plans). The term drag fold is used here to mean a fold that has formed in an incompetent bed when the competent beds on either side has moved in such a way as to subject it to a couple (A.G.I. Glossary of Geology, 2nd Ed., 1960). A configuration of this type is suggested in sections 8115 and 8515 where the upper part (above the 3500 level) has been brecciated and where diorite has intruded along the trough or synform portion of the structure. A similar pattern is suggested on section 7715. Eastward from 8515, the pattern on 8915 section is similar except that the synform portion is almost obliterated. The upper part has not been as

intensely shattered as on 8515 but the skarn rocks have been broken as seen by the distribution of K-feldspar-specularite veins. Further eastward, sections 9315 and 9715 show the calcareous or skarn horizon cut off by the diorite.

There are some consistent features of the structure within the area investigated. The antiform structure outlined on section 7415 and correlated to sections 7715 and 8115 appears to plunge about 40 degrees east. Small folds in the 30-783 service drift west on the 3060 level indicate plunges of 36 to 45 degrees east. This suggests that the fold structure must plunge to the east at about 40 degrees.

— A second feature is a persistent foliation which strikes east-west and dips steeply south. In specimen 663-157, small rock fragments have been elongated to lense-like shapes (1 cm. long and 4 mm. wide) which have their greatest dimension in the direction of the foliation. Argillite bands have been broken, pulled apart, and aligned parallel to the foliation in a recrystallized limestone (specimen 663-158). Calcite has recrystallized in the pressure shadows of the broken argillite band. Plate 20 shows the same relationship in which bands several inches wide have been broken and pulled apart. Specimen 663-159 shows small broken folds of very thin argillite bands in recrystallized limestone. Plate 21 illustrates the same relation on a larger scale.

The presence of this foliation is also suggested

from diamond drilling. The angle between banding in the rock and the core centerline when observed in several drill holes on the same section indicates a consistent steep south dipping banding or foliation. This can be observed from section to section.

Parallelism of rock banding with the direction of elongation or stretching, i.e., the foliation plane, suggests the possibility of transposed bedding. Turner and Weiss (1963) discuss transposition of bedding as "transposition of an initial layering from one dominant orientation to another, with the appearance of what is effectively a new foliation ...." (p. 92). Such a foliation may also be termed 'transposition foliation'. At Craigmont, information is not available to allow ready distinction between this secondary foliation and the original bedding.

The direction of elongation in both metamorphosed elastic and calcareous rocks is parallel to the foliation which is present throughout the mine along a zone more or less defined by the relatively incompetent original calcareous bed. Calcareous rocks are susceptible to flow at low temperatures and confining pressures depending upon water pressure. The rocks in the foliated zone have undergone displacement along planes of shear as seen in the examples of flowage and stretching. Hornfelsed sedimentary rocks within the calcareous horizon are also folded or elongated along this direction. In this sense, the term 'shear' may be applied to the entire zone

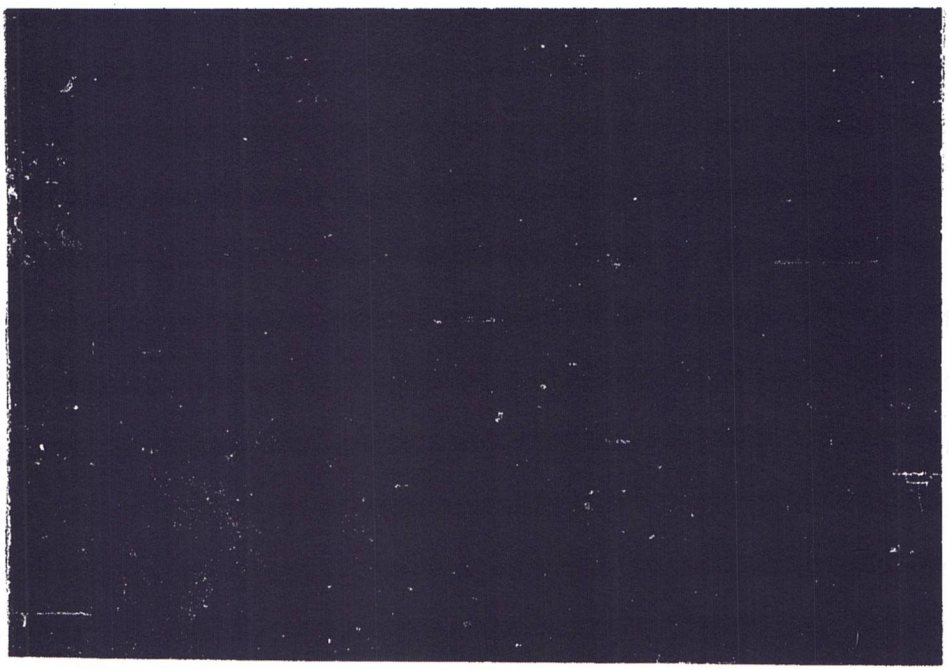

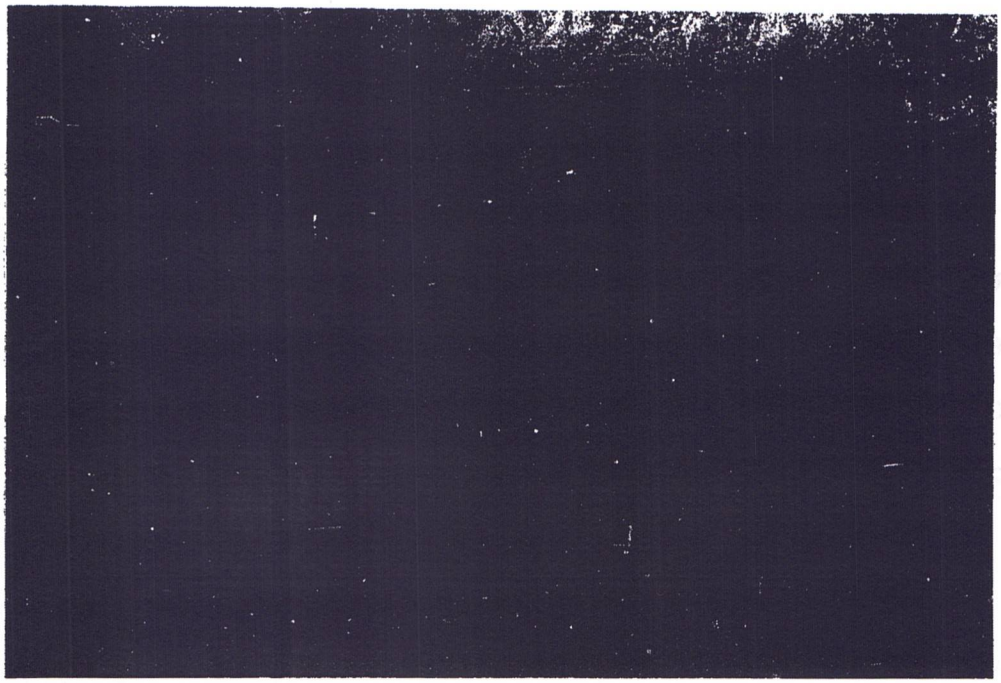

Plate 20 Photograph showing broken argillitic bands in recrystallized limestone. (3060 level).

Plate 21 Photograph showing elongated and folded argillitic bands in recrystallized limestone. (3060 level).

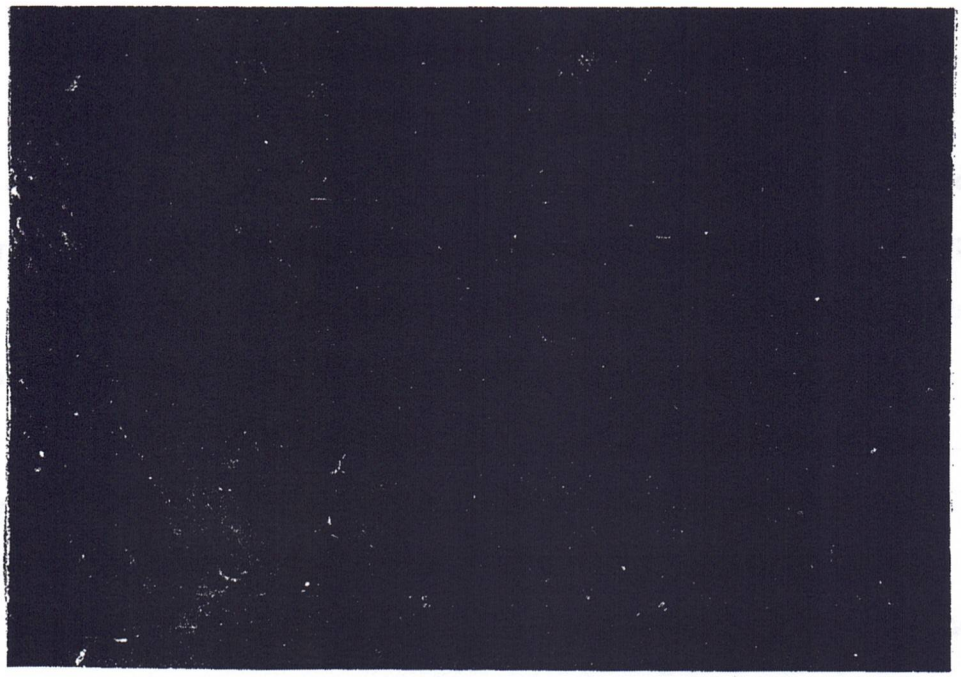

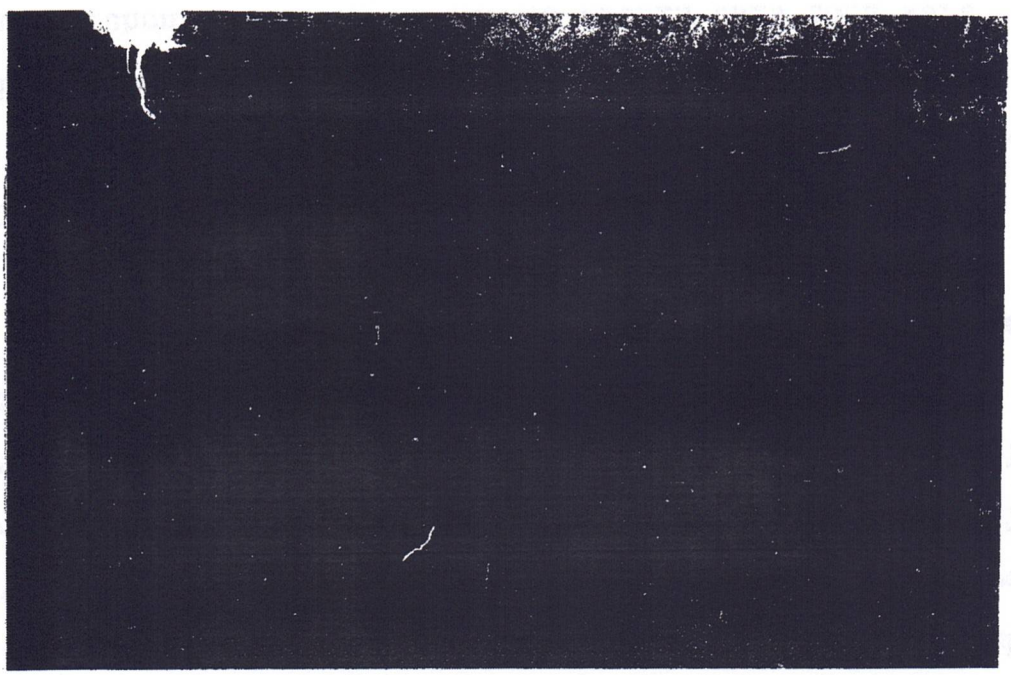

Plate 20 Photograph showing broken argillitic bands in recrystallized limestone. (3060 level).

Plate 21 Photograph showing elongated and folded argillitic bands in recrystallized limestone. (3060 level).

in which the drag fold structure occurs. This shear zone would include not only the present skarn-marble horizon but also the adjacent wall rocks.

Four distinct sets of faults are noted on the open pit composite plan: (1) N 80 E/steep S; (2) N 80 W/vertical to steep S or N; (3) N 30 W/65E; and (4) N 30 E/65E. Sets (1) and (2) are the most prominent and are present throughout the mine. These faults are more easily seen and correlated in the open pit than in the underground workings. The two main sets are important as they approximately parallel the foliation.

Any structural hypothesis must take into consideration the above mentioned features. The writer interprets the Craigmont structure to be a large scale east plunging drag fold formed in a shear zone which is more or less defined by a relatively incompetent calcareous horizon adjacent to the Guichon diorite. Movements within this zone were initiated by a water pressure and temperature sufficient to induce flowage. There is a possibility that the structure outlined in the mine is part of a much larger structure. Information on this is not available at present.

Relation of the Diorite and Andesite to Structure

Diorite apophyses are aligned along the east plunging synform portion of the drag fold. The lower termination of the eastern diorite dyke rises from east to west at about

the same angle that the drag fold plunges east. Their position in the mine appears to have been controlled by the structure which must have formed prior to the diorite intrusion. Similarly, the structure has guided the intrusion of the pre-diorite andesite. Detailed information is lacking, but the andesite appears to be present along the trace of the axial plane of the south wall antiform structure as shown in 7415 section (see 3060 level plan). The writer considers that the andesite is controlled by the presence of the antiform west of 8815 section. As the antiform plunges east, the structure pinches east such that on the 3060 level, east of 8815 section the structure becomes isoclinal and the andesite transects the drag fold structure into the more open limy horizon.

Relation of Skarn Type to Structure

The distribution of actinolite-epidote- and garnet-bearing assemblages has been discussed. In sections 7715 and 8115, actinolite-epidote rocks are found more or less along a line from the attenuated lobe of the drag fold down along the dip of the foliation. Section 8515 shows less actinolite-epidote rocks but the attenuation is also less. On both 8515 and 8915 sections, actinolite-bearing rocks are found along the upper stretched part of the structure. This pattern is not readily seen in 9315 and 9715 as diorite intersects the structure. The above appears to suggest that

actinolite-epidote rocks are found in areas of the structure that have undergone movements during the skarn formation. Replacement of the calcareous horizon by calc-silicates has obliterated the effect within the skarn zone.

Relation of K-feldspar-Specularite Veins to Structure

Distribution of specularite veins may be correlated to post-skarn movements. These movements appear to be continuations along the same directions of movement that existed during the period of fold and skarn formation. This is seen in 7715 section where specularite veins cut the actinolite-epidote skarn of the attenuated 'wing' and by the presence of a tourmaline-bearing breccia along the upper extension of the attenuation. Similarly, in sections 8115, 8515 and 8915, the upper part of the drag fold between 3500 level and the open pit has undergone shattering. Specularite and K-feldspar veins are found not only in the broken skarn but also in the wall rocks. The east end of the mine has not undergone intense post-skarn deformation and consequently, sections 9315 and 9715 show a relatively small number of veins.

Late Movements

Post-specularite vein stage movements have occurred possibly along the same directions as those previously mentioned. These late movements are seen in the open pit where the specularite-chalcopyrite ore has been brecciated and

altered to specularite-native copper in a limonitic matrix (specimen 663-147). Late open space filling is seen in specimen 663-148 where crystals of siderite, chalcocite and calcite line vugs.

Summary of Geological History

The geological history in the Craigmont mine vicinity is outlined below:

A. Initial deformation of the Upper Triassic Nicola group rocks occurred during an early stage of the Coast Range orogeny.

B. An easterly plunging drag fold structure was developed in a calcareous incompetent horizon along a shear zone which parallels but is separated from the southern border of the Lower Jurassic Guichon batholith. A dynamic environment existed with folding occurring contemporaneous with intrusion.

C. Andesite and diorite intruded the folded calcareous horizon.

D. Within the thermal aureole of the diorite, sedimentary and volcanic rocks were metamorphosed under conditions of the hornblende-hornfels facies. Calcareous rocks were made into garnet-epidote-actinolite-iron oxide-chalcopyrite assemblages by Fe-Mg-Si-Cu-S metasomatism. The partial pressures of oxygen and sulphur controlled the mineralogy of these rocks and produced the actinolite-epidote-magnetite-chalcopyrite skarn ore.

E. Continuation of movements in the shear zone allowed shattering of the skarn and adjacent wall rocks, and allowed veining by specularite-chalcopyrite with or without K-feldspar. Reaction between the vein and skarn produced pods and veins in which K-feldspar is associated with platy magnetite. The specularite-chalcopyrite breccia orebody was formed at this time.

F. Late movements brecciated the specularite-chalcopyrite ore.

G. The batholith and Nicola group rocks were eroded to a level that exposed the orebody, and lower Cretaceous Kingsvale group volcanic rocks were deposited unconformably over the ore zone.

H. Pyroxene andesite dykes intruded the Buichon diorite.

I. Basalt dykes intruded the Nicola group rocks. These are probably related to Tertiary volcanism.

J. Pleistocene glaciation and Recent glacial drift deposition were the latest events to occur in the Craigmont mine area.

References Cited

Abdullah, M. I. and Atherton, M. P. (1964) The Thermometric Significance of Magnetite in Low Grade Metamorphic Rocks: Am. J. Sci., v. 262, pp. 904-917.

Albee, A. L. (1962) Relationships Between The Mineral Association, Chemical Composition and Physical Properties of the Chlorite Series: Am. Min., v. 47, p. 851-870.

Baadsgaard, H., Folinsbee, R. E., and Lipson, J. (1961) Potassium-Argon Dates of Biotites From Cordilleran Granites: Geol. Soc. Am. Bull., v. 72, pp. 689-702.

Barnes, H. L. and Kullerud, G. (1961) Equilibria in Sulphur-Containing Aqueous Solutions, in the System Fe-S-O, and Their Correlation During Ore Deposition: Ec. Geol., vol. 56, pp. 648-688.

Barth, T. F. W. (1962) Theoretical Petrology, 2nd. Ed.: J. Wiley and Sons, New York, 403 p.

Brindley, G. W. (1951) X-ray Identification and Crystal Structures of Clay Minerals: Mineralogical Society, London, 321 p.

Brindley, G. W. and Gillery, F. H. (1956) X-ray Indentification of Chlorite Species: Am. Min., v. 41, p. 169-186.

Cameron, E. N. (1961) Ore Microscopy: J. Wiley and Sons, New York, 248 p.

Carr, M. (1959) Report on Craigmont Mines: B. C. Minister of Mines Report, pp. 31-34.

_____(1960) Geology of Promontory Hills: B. C. Minister of Mines Report, p. 26-40.

Chinner, G. A. (1960) Pelitic Gneisses With Varying Ferrous/Ferric Ratios From Glen Clova, Angus, Scotland: Journal Petrology, v. 1, Pt. 2, pp. 178-217.

Cockfield, W. E. (1948) Geology and Mineral Deposits of Nicola Map-Area, B. C.: Geol, Surv. Can., Memoir 249.

Danielsson, A. (1950) Das Calcit-Wollastonitgleichgewicht: Geochim. et Cosmochim. Acta, vol. 1, pp. 55-69.

Davidson, A. and Wyllie, P. J. (1965) Zoned Magnetite and Platy Magnetite in Cornwall Type Ore Deposit: Ec. Geol., vol. 60, no. 4, pp. 766-771.

Deer, W. A., Howie, R. A., and Zussman, J. (1962) Rock Forming Mineral: vol. 1, 2, and 3, J. Wiley and Sons, New York.

Duffell, S. and McTaggart, K. C. (1952) Ashcroft Map-Area, B. C.: Geol. Surv. Can., Memoir 262.

Eastwood, G. E. P. (1965) Replacement Magnetite on Vancouver Island, B. C.: Ec. Geol., v. 60, pp. 124-148.

Eckstrand, O. R. (1963) Crystal Chemistry of Chlorite: unpublished Ph.D. thesis, Harvard University, Cambridge, Mass.

Eskola, P. (1914) On the Petrology of The Ori jarvi Region in Southwestern Finland: Comm. Geol. Finland, Bull., v. 40, 277 p.

Eugster, H. P. (1959) Reduction and Oxidation in Metamorphism: in Researches in Geochemistry, Ed. P. H. Abelson, J. Wiley and Sons, New York, pp. 397-426.

_____ and Wones, D. R. (1962) Stability Relations of The Ferruginous Biotite, Annite: Journal Petrology, v. 3, Pt. 1, pp. 82-125.

Fryklund, Jr., V. C. (1964) Ore Deposits of the Coeur d'Alene District, Shoshone Co., Idaho: U.S.G.S. Prof. Paper 445, 82 p.

Fyfe, W. S., Turner, F. J., and Verhoogen, J. (1958) Metamorphic Reactions and Metamorphic Facies: Geol. Soc. Amer., Memoir 73, 257 p.

Goldschmidt, V. M. (1912) Die Gesetze der Gesteinsmetamorphose mit Beispielen aus der Geologie des Sudlichen Norwegens: Kristiania Videnskˇ. Skr., I Math.-Naturv. Kl. 22.

Grim, R. E. (1953) Clay Mineralogy: McGraw-Hill Book Co., Inc., New York, 368 p.

Gruner, J. W. (1922) Paragenesis of the Martite Ore Bodies and Magnetites of The Mesabi Range: Ec. Geol., v. 17, no. 1, pp. 1-14.

Guild, F. N. (1934) Microscopic Relations of Magnetite, Hematite, Pyrite and Chalcopyrite: Ec. Geol., v. 29, No. 2, pp. 107-120.

Gustafson, L. B. (1963) Phase Equilibria in The System Cu-Fe-As-S: Ec. Geol., v. 58, no. 5, pp. 676-701.

Hemley, J. J. (1959) Some Mineralogical Equilibria in The System K_2O-Al_2O_3-SiO_2-H_2O: Am. J. Sci., vol. 257, pp. 241-270.

Hess, H. H. (1949) Chemical Composition and Optical Properties of Common Clinopyroxenes: Am. Min., v. 34, pp. 621-666.

Hey, M. H. (1954) A New Review of Chlorites: Min. Mag., vol. 30, no. 224, p. 277-292.

Hickok, W. O. (1933) The Iron Ore Deposits at Cornwall, Pennsylvania: Ec. Geol., v. 28, no. 3, pp. 193-255.

Holland, H. D. (1959) Some Applications of Thermochemical Data to Problems of Ore Deposits. I. Stability Relations Among the Oxides, Sulphides, Sulphates, and Carbonates of Ore and Gangue Metals: Ec. Geol., vol. 54, pp. 184-233.

James, H. L. (1955) Zones of Regional Metamorphism in The Pre-Cambrian of Northern Michigan: Geol. Soc. Amer. Bull., v. 66, pp. 1455-1488.

Klemm, D. D. (1962) Anistropieeffekte bei kubischen Erzmineralien: Neues Jahrbuch fur Mineralogie, Abhandlungen, Band 97, Heft 3, pp. 337-356.

Knopf, A. (1933) Pyrometasomatic Deposits: In AIME, Lindgren Volume, Ore Deposits of The Western States, pp. 537-557.

_____(1942) Ore Deposition in The Pyrometasomatic Deposits: In Ore Deposits as Related to Structural Features, Ed., W. H. Newhouse, pp. 63-72.

Latimer, W. M. (1952) The Oxidation States of the Elements and Their Potentials in Aqueous Solutions, 2nd. Ed.: Prentice-Hall, Inc., 239 p.

Leube, A. and Stumpfl, E. F. (1963) The Rooiberg and Leeuwpoort Tin Mines, Transvaal, South Africa, Pt. 2: Ec. Geol., v. 58, no. 4, pp. 527-557.

Lindgren, W. (1905) The Copper Deposits of The Clifton-Morenci District, Arizona: USGS Prof. Paper 43.

Lowden, J. A. (1963) Age Determinations and Geological Studies: Geol. Surv. Can., Paper 62-17, Pt. 1.

MacKenzie, W. S. (1954) The Orthoclase-Microcline Inversion: Min. Mag., v. 30, no. 225, pp. 354-366.

Miyashiro, A. (1964) Oxidation and Reduction in The Earth's Crust With Special Reference to the Role of Graphite: Geochim. et Cocmochim. Acta, v. 28, pp. 717-729.

Newhouse, W. H. (1936) Opague Oxides and Sulphides in Common Igneous Rocks: Geol. Soc. Am. Bull., v. 47, no. 1, pp. 1-52.

Ramberg, H. (1952) The Origin of Metamorphic and Metasomatic Rocks: Univ. of Chicago Press, Chicago, 317 p.

Ramdohr, P. (1960) Die Erzmineralien und Ihre Verwachsungen: Akademie Verlag, Berlin, 1023 p.

Rennie, C. C., Pentland, W. S., and Sheng, C. C. (1961) Geology of The Craigmont Mine: Can. Min. and Met. Bull., v. 54, pp. 297-301.

Renshaw, R. E. and Price, F. (1958) Soil Sampling and Magnetometer Surveying Finds Copper Ore: World Mining, v. 20, no. 8, pp. 44-48.

Rice, H. M. A. (1947) Geology and Mineral Deposits of The Princeton Map-Area, B. C.: Geol. Surv. Can., Memoir 243.

Ross, C. P. (1925) Geology and Ore Deposits of The Aravapia and Stanley Mining Districts, Graham Co., Arizona: U.S.G.S. Bull. 763.

Schmitt, H. (1939) The Pewabic Mine: Geol. Soc. Am. Bull., v. 50, pp. 777-818.

Schwart, G. M. and Ronbeck, A. C. (1940) Magnetite in Sulphide Ores: Ec. Geol., v. 35, no. 5, pp. 585-610.

Shido, F. and Miyashiro, A. (1959) Hornblendes of Basic Metamorphic Rocks: Hourn. Fac. Sci., Univ. of Tokyo, sec. 2, v. 12, Pt. 1, pp. 85-102.

Smith, J. R. (1956) The Powder Patterns and Lattice Parameters of Plagioclase Feldspar, I, The Na-Rich Plagioclases: Min. Mag., v. 31, no. 232, pp. 47-68.

_____and Yoder, H. S. (1956) Variation in X-ray Powder Diffractometer Patterns of Plagioclase Feldspars: Am. Min., v. 41, pp. 632-647.

Smitheringale, W. V. (1928) Mineral Associations at The George Gold-Copper Mine, Stewart, B. C.: Ec. Geol., v. 23, no. 2, pp. 193-208.

Titley, S. R. (1961) Genesis and Control of The Linchburg Orebody, Socorro Co., New Mexico: Ec. Geol., v. 56, no. 4, pp. 695-722.

Turner, F. J. (1948) Mineralogical and Structural Evolution of The Metamorphic Rocks: Geol. Soc. Am., Memoir 30, 317 p.

_____and Verhoogen, J. (1960) Igneous and Metamorphic Petrology: McGraw-Hill Book Co., New York, 672 p.

_____and Weiss, L. E. (1963) Structural Analysis of Metamorphic Tectonites: McGraw-Hill Book Co., New York, 525 p.

Umpleby, J. B. (1916) The Occurrence of Ore on The Limestone Side of Garnet Zones: Univ. of Calif. Publ., Bull. Dept. Geol., vol. 10, no. 3, pp. 25-37.

Uytenbogaardt, W. (1951) Microscopic Identification of Ore Minerals: Princeton Univ. Press, Princeton, New Jersey.

Verhoogen, J. (1962) Distribution of Titanium Between Silicates and Oxides in Igneous Rocks: Am. J. Sci., v. 260, pp. 211-220.

Vermaas, F. H. S. (1952) The Amphibole Asbestos of South Africa: Trans. Geol. Soc. of South Africa, v. 55, pp. 199-229.

Ward, R. G. (1962) An Introduction to The Physical Chemistry of Iron and Steel Making: E. Arnold Publishers, London, 238 p.

White, W. H., Thompson, R. M., and McTaggart, K. C. (1957) The Geology and Mineral Deposits of Highland Valley, British Columbia: Can. Min. and Met. Bull., Trans., vol. 60, pp. 273-289.

Williams, H., Turner, F. J. and Gilbert, G. M. (1954) Petrography: Freeman and Co., San Francisco, 406 p.

Winchell, A. N. and Winchell, H. (1951) Elements of Optical Mineralogy, Pt. 2: J. Wiley and Sons, New York.

Winchell, H. (1958) The Composition and Physical Properties of Garnets: Am. Min., v. 43, pp. 595-600.

Wones, D. R. and Eugster, H. P. (1959) Biotites on The Join Phlogopite-Annite: Carnegie Inst. Washington, Geophys. Lab., Yearbook 58, pp. 127-132.

APPENDIX A

D.T.A. Patterns For Graigmont Chlorite

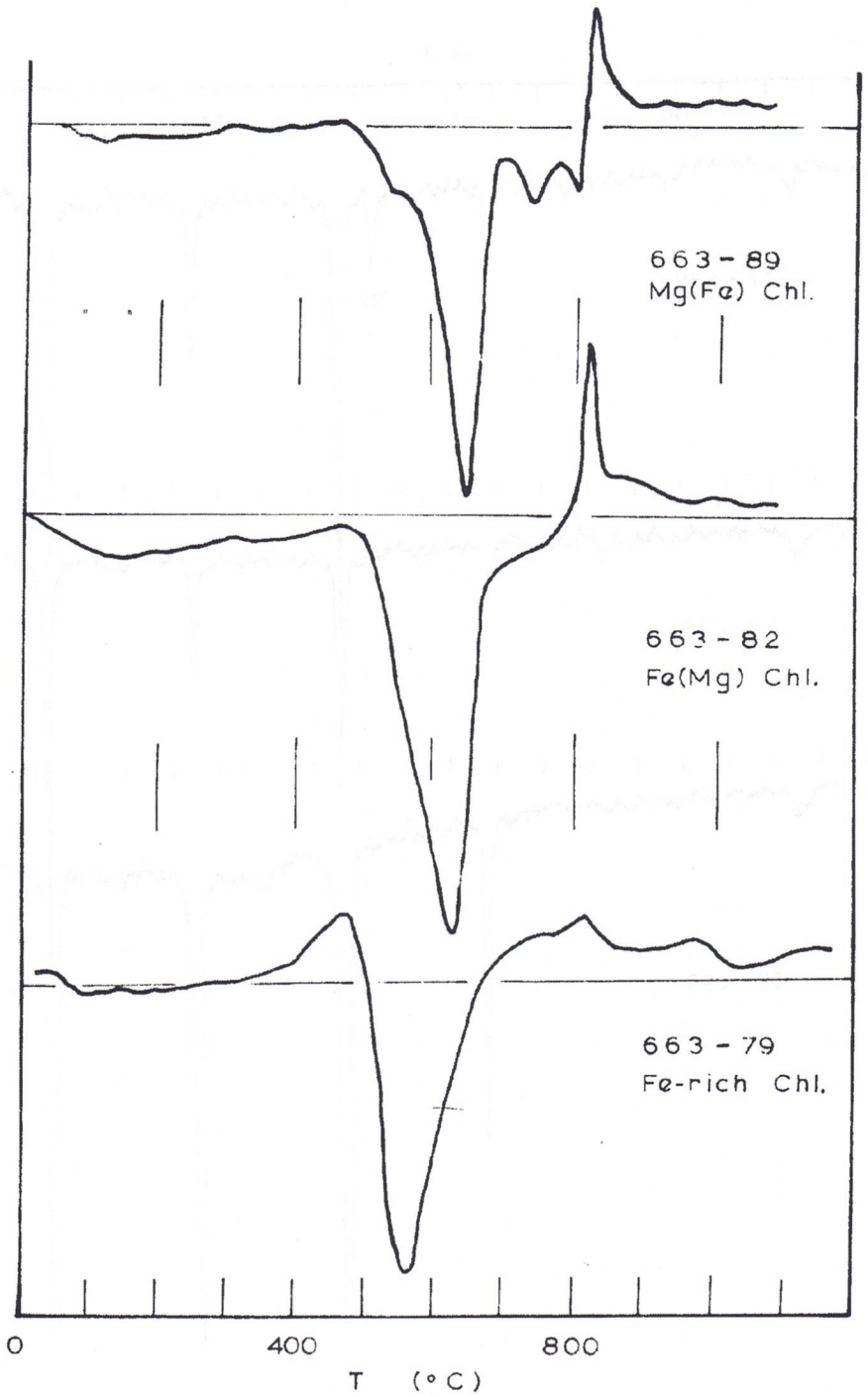

APPENDIX A

(continued)

X-ray Diffractometer Patterns of Craigmont Chlorite

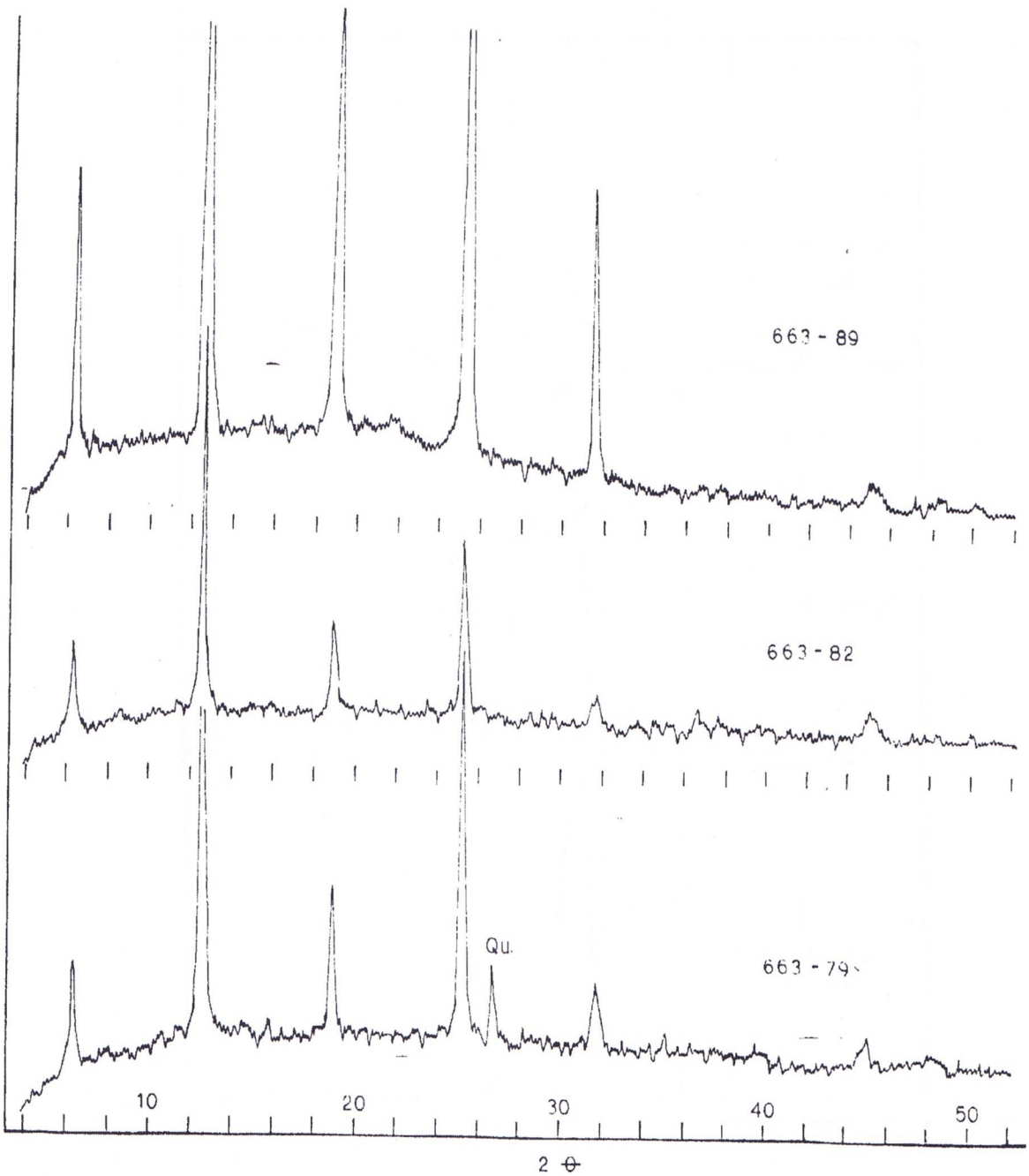

APPENDIX B

Hardness of Blue and Brown Magnetite Phases

Specimen	Phase	Knoop Hardness Numbers				
		A	B	Mean		
663-104	Brown	535	553	544	558	
663-105	Brown	547	597	572		
	Blue	606	597	601		541
663-99	Blue	532	546	539	524	
663-106	Blue	452	411	431		

Each reading represents the average of three or four determinations. Columns A and B are for the same mineral but A is oriented 90 degrees to B. A Kentron Microhardness tester was used. Knoop numbers for magnetite range from 380 to 600 and average 528.

APPENDIX C

X-ray Powder Data For Platy Magnetite

Specimen 663-98 (about 90% bluish and 10% brownish 'phase').

I.	Left	Right	4θ	2θ	$d_{meas.}$	M.*	H.**
1	74.3	117.0	42.7	21.35	4.84	4.85	
3	60.5	130.9	70.4	35.2	2.97	2.966	
1	56.9	134.6	77.7	38.85	2.69		2.69
10	54.1	137.2	83.1	41.55	2.523	2.530	
1	52.1	139.1	87.0	43.5	2.416	2.419	
3	45.0	146.3	101.3	50.65	2.092	2.096	
1	32.4	158.7	126.3	63.15	1.711	1.712	
3	28.2	163.0	134.8	67.4	1.613	1.614	
6	21.3	170.0	148.7	74.35	1.481	1.483	

* Magnetite ASTM 11-614.
** Hematite ASTM 13-534.
U.C. Film no. 2678; Radiation Co K-alpha; Filter Fe.

APPENDIX C (continued)

Specimen 663-107 (about 95% bluish and 5% brownish 'phase').

I.	Left	Right	4θ	2θ	$d_{meas.}$	M.*	C.**
1	81.9	111.0	29.1	14.55	7.07		7.05
3	75.2	117.7	42.5	21.3	4.86	4.85	
1	67.1	125.7	58.6	29.3	3.54		3.52
4	61.3	131.5	70.2	35.1	2.97	2.966	
10	54.9	137.8	82.9	41.45	2.529	2.530	
1	53.1	139.8	86.7	43.35	2.423	2.419	
5	45.9	146.9	101.0	50.5	2.098	2.096	
2	33.4	159.4	126.0	63.0	1.713	1.712	
5	29.1	163.7	134.6	67.3	1.615	1.614	
7	22.2	170.6	148.4	74.2	1.484	1.483	

* Magnetite ASTM 11-614.
** Chlorite ASTM 12-243.
U.C. Film no. 2677; Radiation Co K-alpha; Filter Fe.

APPENDIX C (continued)

Specimen 663-108 (about 50% bluish and 50% brownish 'phase').

I.	Left	Right	4θ	2θ	$d_{meas.}$	M.*
3	75.2	117.7	42.5	21.25	4.86	4.85
1	65.4	127.3	61.9	30.95	3.35	Q.** 3.34
4	61.3	131.5	70.2	35.1	2.97	2.966
½	59.4	133.5	74.1	37.05	2.82	(?)
1	57.7	135.0	77.3	38.65	2.71	H.***2.69
10	54.9	137.8	82.9	41.45	2.529	2.530
1	53.1	139.8	86.7	43.35	2.423	2.419
½	48.6	144.3	95.7	47.85	2.211	(?)
4	45.9	146.9	101.0	50.5	2.098	2.096
½	38.2	154.7	116.5	58.25	1.839	Q.** 1.82
2	33.4	159.4	126.0	63.0	1.713	1.712
4	29.1	163.7	134.6	67.3	1.615	1.614
6	22.2	170.6	148.4	74.2	1.484	1.483

* Magnetite ASTM 11-614.
** Quartz ASTM 5-0490.
*** Hematite ASTM 13-534.
U.C. Film no. 2676; Radiation Co K-alpha; Filter Fe.

X-ray Diffractometer Patterns of Platy Magnetite

Patterns were run at 1 degree per minute using Co radiation and an iron filter (30Kv. and 10 m.a.). The three peaks are: $d_{(226)}$ 2.96 A; $d_{(311)}$ 2.53 A; $d_{(400)}$ 2.093 A.

A. Specimen 663-98 (about 90% bluish and 10% brownish 'phase').
B. Specimen 663-107 (about 95% bluish and 5% brownish 'phase').
C. Specimen 663-108 (about 50% bluish and 50% brownish 'phase').
D. Specimen 663-109 (about 95% bluish, 2 - 3% brownish 'phase' and 1 - 2% hematite).

APPENDIX C (continued)

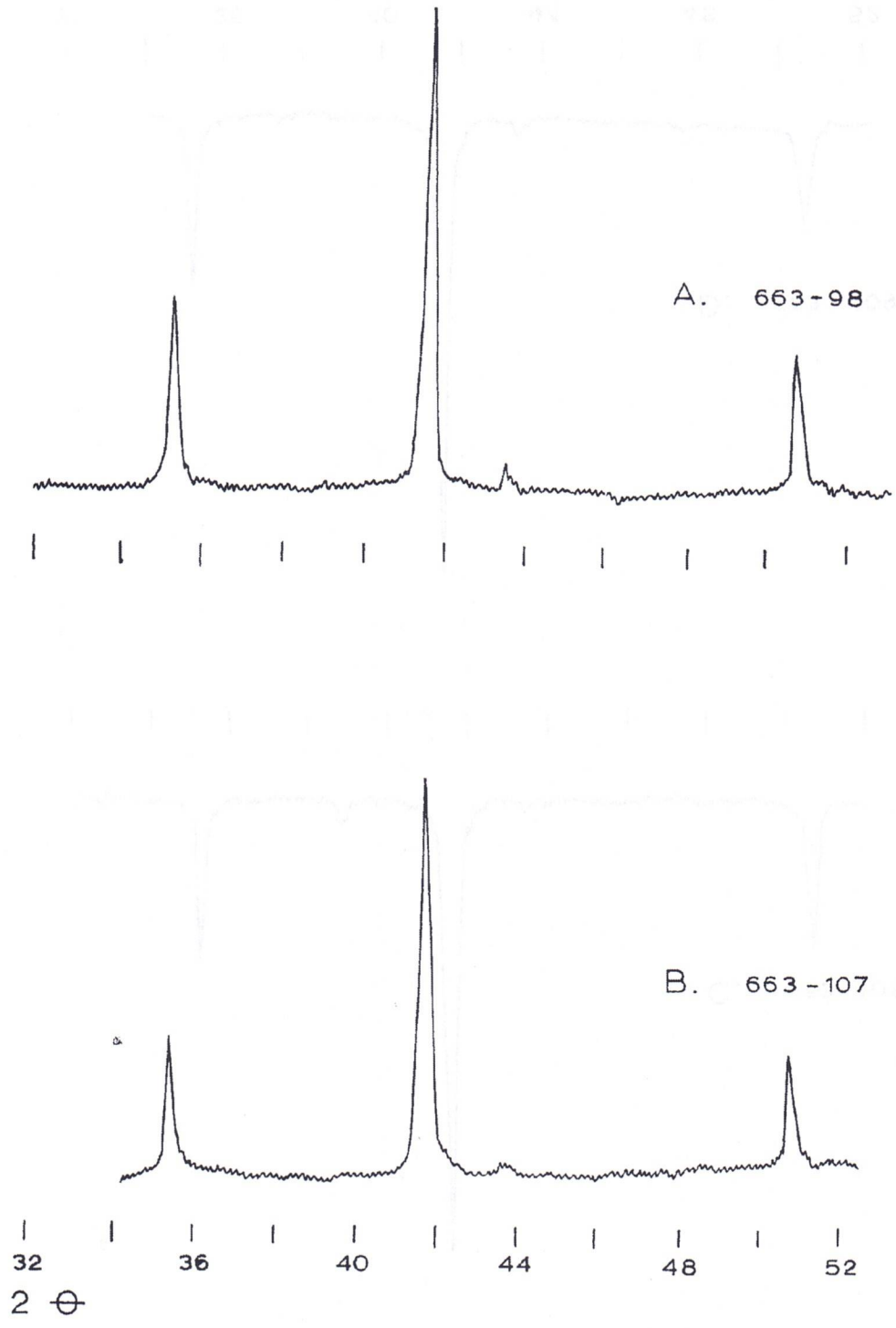

APPENDIX C (continued)

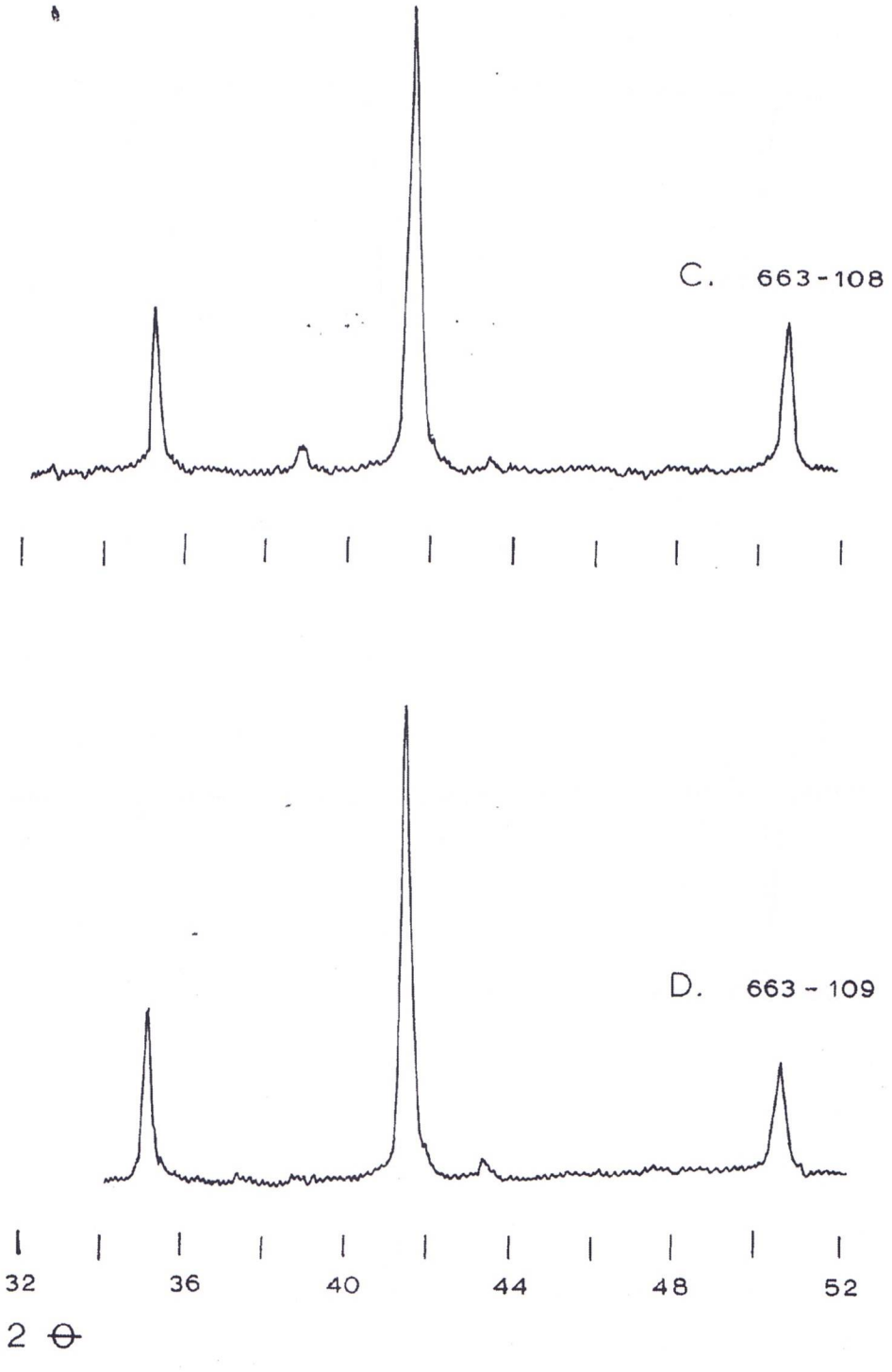

APPENDIX C (continued)

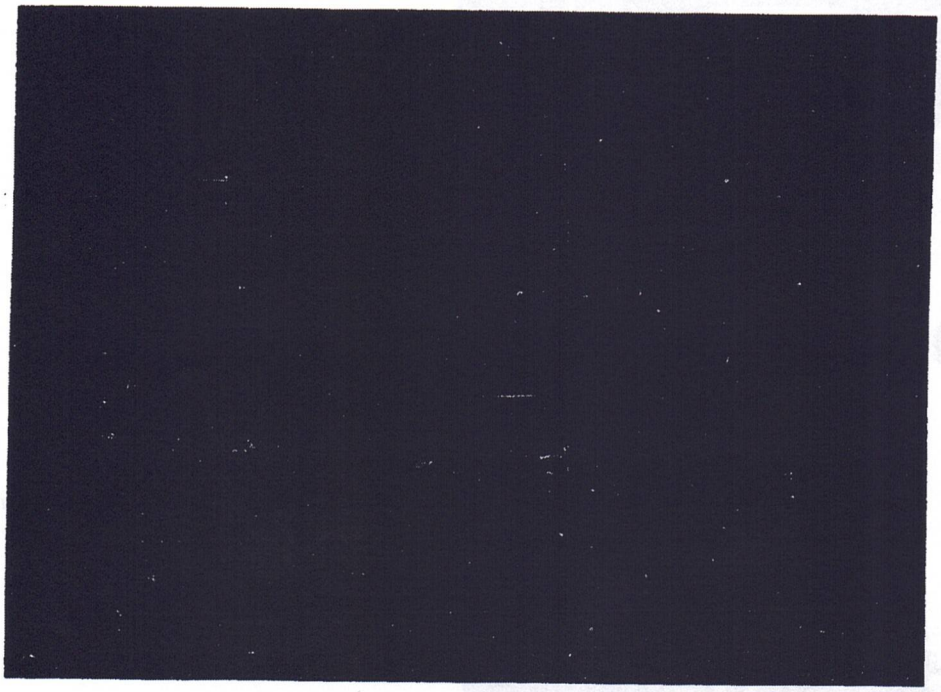

[111] precession pattern showing only spots of one platy magnetite crystal. UC no. S-4815.

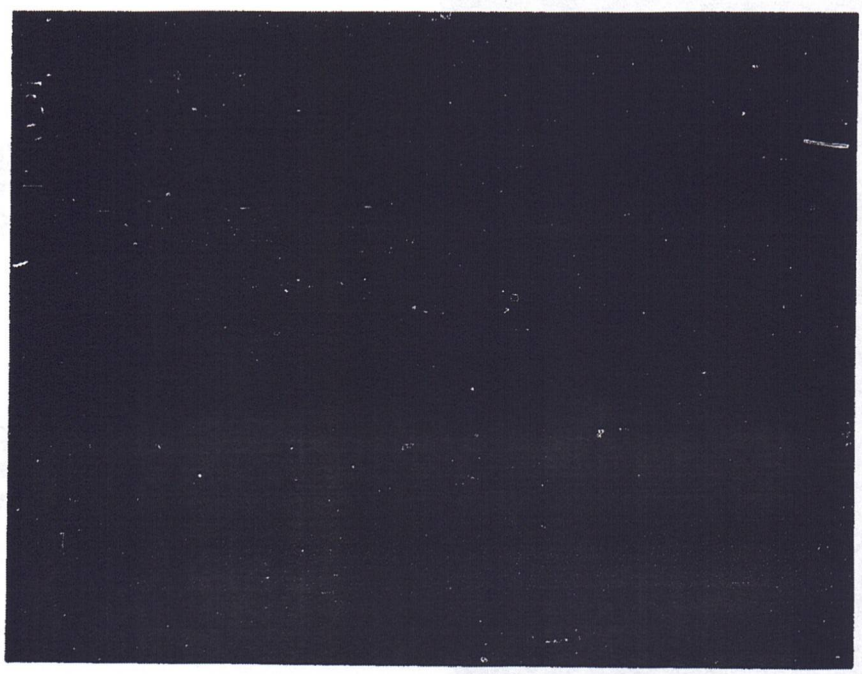

[1$\bar{1}$0] precession pattern for platy magnetite crystal. UC no. S-4817

APPENDIX C (continued)

UC 2676, Specimen 663-108, magnetite with 50% bluish and 50% brownish phase.

UC 2677, Specimen 663-107, magnetite with 95% bluish and 5% brownish phase.

UC 2678, Specimen 663-98, magnetite with 90% bluish and 10% brownish phase.

Radiation Co K-alpha; filter, Fe.

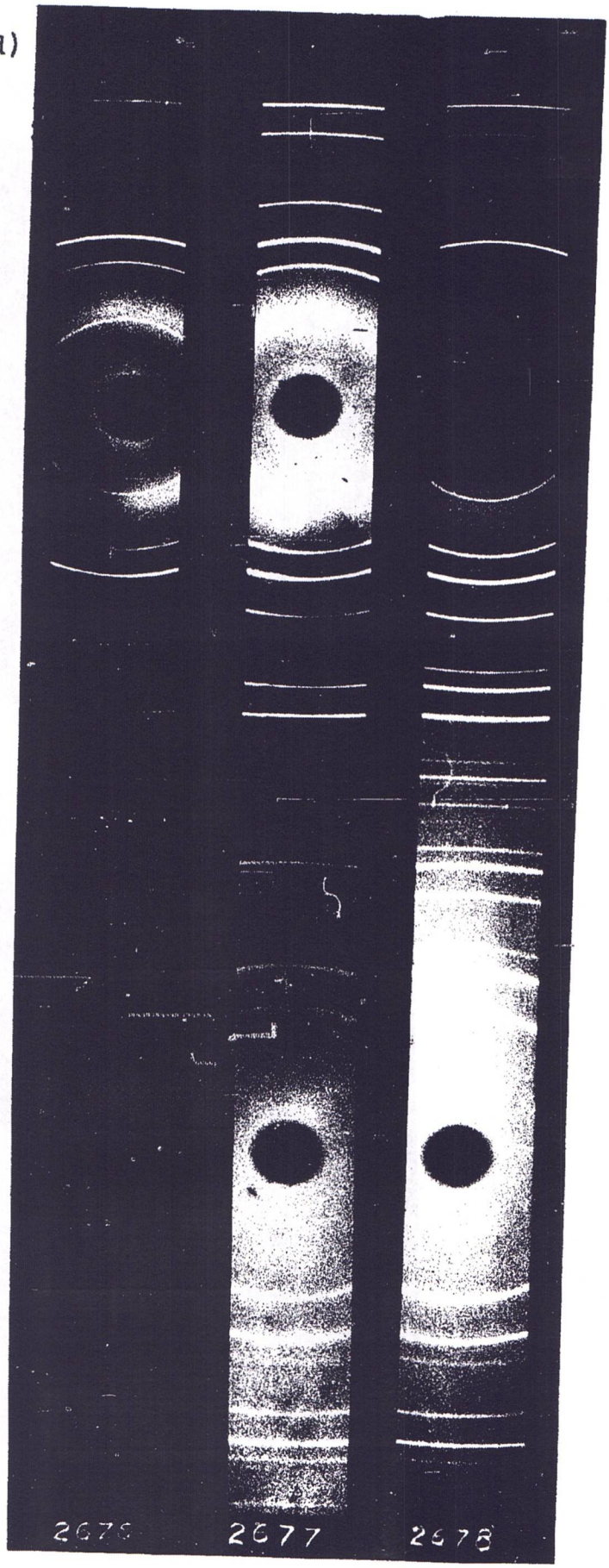

APPENDIX D

Magnetite Scan With Electron Microprobe

Run No.	Specimen No.	Phase	Elements Present**
1.	663-98	Magnetite blue	Fe
2.	663-98	Magnetite blue	Fe
3.	663-110	Magnetite blue in hematite crystal	Fe
4.	663-110	Specularite	Fe, V (tr.?)
5.	663-110	Magnetite brown	Fe, V (tr.), Mc (tr.)
6.	663-98	Magnetite brown	Fe, V (tr.?)
7.	663-98	Magnetite blue	Fe, V (tr.), Ti(?)
8.	Mineville Magnetite*		Fe, Ti, Mn, V

* Mineville magnetite standard contains 1.99% TiO_2, 0.08% MnO, and 0.2% V_2O_3.
** The following elements were not observed: Cr, Co, Ni, Cu, Zn, Mo, Ag.

The traces of the electron microprobe scans are reproduced on the following page.

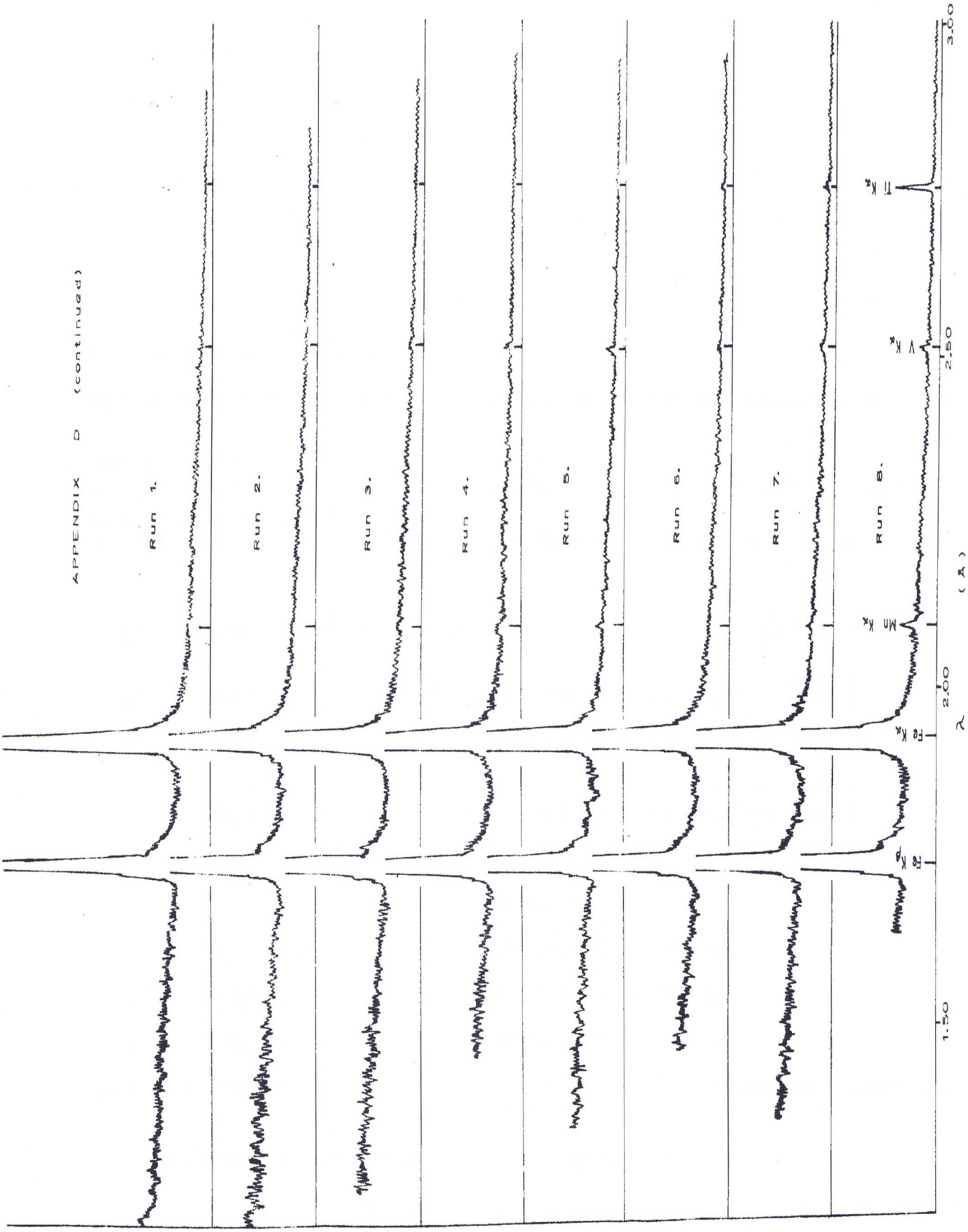

APPENDIX E

Polish Procedure

Hand polishing involved the following steps: (1) diamond saw marks were removed by light touch on a bronze lap with American Optical aluminum oxide abrasive number 303½; (2) initial grinding was accomplished on a glass plate with the same abrasive until the surface was flat; (3) grinding was continued on glass with aluminum oxide (number F-1232); (4) specimen was polished with magnesium oxides F-1234 and F-1235 successively. The latter three abrasives are manufactured by Mico Instrument Co., Cambridge, Massachusetts.

A Graton-Vanderwilt polishing machine with lead laps is used in preparing the polished sections. Specimens are cold mounted and are ground on a glass plate with abrasive 303½ and F-1232 until the surface is flat. Initial machine polishing is with abrasive F-1234 for about twenty minutes. Several runs are necessary before the surface is prepared for the final polishing. A second lead lap and abrasive F-1235 are used in the final polishing.

APPENDIX F

Comparison of Hand and Machine Polished Magnetites

Specimen	Hand	Machine	Results
576-15(1)	X		One anisotropic phase.
		X	Two phases, no distinct boundary between phases; anisotropic.
576-15(2)	X		One anisotropic phase.
		X	Two phases, anisotropic blue and isotropic brown with a distinct boundary.
541-2	X		One anisotropic phase.
		X	Two phases, anisotropic blue and isotropic brown around holes and along fractures.
8441*		X	One(?) anisotropic phase, some color change near holes and fractures.
3332*		X	Anisotropic blue color grades or merges to grey (isotropic(?)) near grain boundaries and holes.

---

* These samples were not polished on the final lap.
576-15(1) and (2): Kiruna Pit, Kurina, Sweden.
541-2: Boy Smith Mine, Ontario, Canada.
8441: Bergiesshubel, Saxony, Germany.
3332: Nevada County, California.

APPENDIX G

Causes of Anisotropism

Anistropism of isometric minerals could be caused by the presence of foreign elements, distortion of the lattice, or strain imposed during polishing. Craigmont magnetite is relatively pure and apparently free of foreign elements. X-ray studies indicate that the lattice is cubic and that the cell dimension is that of magnetite. Cameron (1961) page 92, states that "not all isometric minerals are fully isotropic". He gives an example of pyrite and bornite which "are often anisotropic, although many X-ray studies have shown that pyrite at least is invariably isometric". Strain imposed by conversion of specularite to magnetite cannot be suggest at Craigmont as both platy and regular magnetite crystals show anisotropic effects. Hickok (1933) page 220, correlated anisotropic magnetite with heavily blasted areas of the Cornwall iron mine. This source of strain could affect both 'platy' and regular magnetite. Its importance cannot be determined as the rate of strain is unknown. At Craigmont, anisotropic magnetite may be found in drill cores from areas which have not been 'heavily' blasted.

Pressure briquetting of polished sections is suggested by P. Ramdohr (1960) as a possible cause of anisotropism. Craigmont samples were cold mounted in epoxy plastic so there was a minimum of pressure involved in mounting. If strain was

imposed by polishing then the anisotropism should not be present in the hand polished samples where heat and pressure were a minimum. Deformation during and/or after magnetite crystallization may supply the necessary strain.

Anisotropism in magnetite is mentioned in most mineralogy books but references to actual localities are generally lacking. Hickok (1935) and Davidson and Wyllie (1965) describe anisotropic magnetite at the Cornwall skarn deposit. Newhouse (1936) reports that anisotropic magnetite is a common accessory in diabases. Ramdohn (1960) reports anisotropic magnetite from Kirunavarra, Sweden. Anisotropic euhedral zoned magnetite from Leeuwpoort tin mines, Transvaal, South Africa is described by Leube and Stumpfe (1963). Anisotropic magnetite is reported by Klemm (1963) to occur in 44 of 73 unnamed localities. Most of the deposits in which anisotropic magnetite is found are high temperature deposits. The deposits which contain platy magnetite (anisotropism unknown) are mostly skarn deposits. These latter occurrences are outlined in below.

According to Klemm (1962) p. 342, magnetites of pegmatitic, pneymatolytic, and contact metasomatic (skarn) origin, especially the latter, are always anisotropic; hydrothermal magnetites are rarely anisotropic; and magnetite in dynamic metamorphic occurrences are always isotropic. This suggests a direct correlation between anisotropism and temperature of formation. The presence of anisotropism in

magnetite must be caused by some departure from isometric symmetry. However, X-ray investigations indicate that the lattice is not distorted. The strain which may be caused by such factors as the rate of deposition and rate of supply of constituents, is only detected optically. Thus, any departure from the cubic system must be small. This suggests that variations in optical properties are a more sensitive measure of strain than X-ray analysis. The formation of magnetite at high temperature must be more susceptible to flucuations in the internal equilibrium of the depositing medium than magnetites formed at lower temperatures. Thus, magnetites with a high temperature of formation (such as those in skarn deposits) tend to show some deviation from the cubic system and consequently, are anisotropic under the microscope.

Platy Magnetite Occurrences

The presence of platy magnetite has been mentioned by several writers. The following is a brief description of the locality and any textural evidence. Ross (1925) described the Cobre Grande skarn deposit, arizona and stated that the ore (p. 66) "contains both specularite and magnetite but the visible crystal form is always that of specularite". Smitheringale (1928) on the George Gold copper skarn deposit at Stewart, British Columbia reported that hematite was of interest (p. 203) "due to its later alteration to magnetite which faithfully preserves the specularite crystal form".

Hickok (1933) described platy magnetite from the actinolite zone of the Cornwall, Pennsylvania iron deposit. Guild (1934) showed photographs of magnetite plates within chalcopyrite in his report on skarn zones near Tuscon, Arizona. Schwart and Ronbeck (1940) examined magnetite in sulphide ores from 130 deposits. They mention only one case of magnetite after hematite at the Granby copper skarn deposit, Phoenix, British Columbia. Fryklund, Jr. (1964) reported magnetite pseudomorphous after specular hematite in the Coeur d'Alene district, Idaho. Eastwood (1965) reported "lath-like aggregates of magnetite after hematite" at the Coast Copper skarn deposit on Vancouver Island, British Columbia. An example of a non skarn occurrence is given by Gruner (1922) who shows photographs of magnetite pseudomorphous after hematite in the Mesabi Range.